Fall 2017

Real-time diesel particulate matter monitoring in underground mine atmospheres, association with the standard method and related challenges

Muhammad Usman Khan

Department: Mining and Nuclear Engineering

REAL-TIME DIESEL PARTICULATE MATTER MONITORING IN UNDERGROUND MINE ATMOSPHERES, ASSOCIATION WITH THE STANDARD METHOD AND RELATED CHALLENGES

by

MUHAMMAD USMAN KHAN

A DISSERTATION

Presented to the Faculty of the Graduate School of the

MISSOURI UNIVERSITY OF SCIENCE AND TECHNOLOGY

In Partial Fulfillment of the Requirements for the Degree

DOCTOR OF PHILOSOPHY

in

MINING ENGINEERING

2017

Approved by

Kelly O. Homan, Advisor

Grzegorz Galecki

Nassib Aouad

David Rogers

Hsin Wei WU

ABSTRACT

Diesel-powered equipment is a significant component of underground mining operations. Miners' exposure to diesel exhaust is harmful. The standard Diesel Particulate Matter (DPM) monitoring method (NIOSH 5040 method) has limitations that preclude rapid DPM estimation and detailed understanding of DPM variations over time. However, real-time DPM monitors do not inherit these limitations. Biodiesel is often used as a substitute for regular petroleum-diesel because of its ability to emit less DPM. However, accuracy of available real-time DPM monitors has not been determined in mines using 70% to 99% (high-percent) biodiesel. The present research addresses this need by rigorous testing of a commercial real-time DPM monitor against the NIOSH 5040 method in active underground metal mines using high-percent biodiesel.

The real-time DPM monitor was used to collect transient DPM data at mines' work faces, in exhaust air and intake air drifts. The extensive amount of data is characterized by use of Frequency Distribution (FD) models. The collected data revels strong variations in local DPM levels and suggests that attention to DPM area concentrations would provide a valuable complement to the miners' personal DPM exposure determinations. The results also highlight the potential importance of monitoring miners' short term DPM exposure. The measured data also revels the significance of DPM recirculation by auxiliary fan and ventilation duct systems. This research uses a 2D CFD model to examine stope ventilation parameters for a dead-end mine entry and identifies improved ventilation practices for efficient ventilation. Lastly, good work practices for the real-time DPM monitor (FLIR Airtec) used in this research are suggested.

To my parents Mr. and Mrs. Zahid Khan who have always been a great source of inspiration for me

&

To my brother Engineer Muhammad Zaid Ullah Khan, my sister, my loving wife, and my children Rohaan Khan, Farheen Khan and Aahil Khan

ACKNOWLEDGEMENTS

All the praises and gratefulness are for the Almighty Allah, the most gracious and merciful, Who blessed me wisdom, knowledge and courage to accomplish my research.

I would like to express my gratitude to my research advisor, Dr. Kelly O. Homan, for his precious time, keen interest, and intellectual guidance, without him this dissertation would have been a difficult task to accomplish. I am also thankful to my previous PhD advisor Dr. Stewart Gillies, who provided me the opportunity to gather valuable research data from active underground mines. During my PhD, Dr. Stewart has been a great help. Unfortunately, he left due to some unavoidable circumstances during my research, I wish him best health. I am thankful to my respected committee members Drs. Grzegorz Galecki, Nassib Aouad, David Rogers, and Hsin Wei WU for their feedback and suggestions. I am obliged to Dr. James Noll from the NIOSH for his valuable research suggestions and help.

I am grateful to the United States based mining company that allowed me to gather my research data, purchased real-time DPM monitors for my research, and bore all testing and research expenses. I am also grateful for the support of mines' technical section manager and his subordinate staff for providing operational support during this project.

I owe my deepest thanks to my parents, my elder brother, my lovely and caring wife, and my three kids who have provided me the greatest happiness of my life.

I am thankful to the Mining and Nuclear Engineering Department of Missouri S&T for providing funding for my PhD. Thanks to the University of Engineering & Technology Lahore, Pakistan for providing me a platform and an opportunity to study from the United States.

TABLE OF CONTENTS

Page

LIST OF ILLUSTRATIONS

Page

LIST OF TABLES

Page

1. INTRODUCTION

Diesel equipment plays a vital role in the mining industry. Most surface and underground, Metal and Nonmetal (M/NM) mining operations utilize diesel-powered equipment to perform major mining activities. A harmful aspect of the use of diesel fuel is its resultant emissions. Exposure to Diesel Particulate Matter (DPM) has been identified as a major cause of a large number of occupational diseases (Safety, 2005b). DPM monitoring methods are relatively new in the mining industry and techniques that can determine real-time DPM in underground mines are still emerging. This research was conducted to understand and address the issues that are associated with DPM monitoring in underground mines. The study has examined the effect of using multiple diesel-powered machines on the quality of the mine air by direct measurements and quantified miners' personal exposure to DPM. In this Section, the background of current research is reviewed, the key problems are identified and their importance and impacts on the field of real-time DPM monitoring are discussed. This Section also describes the research methodology, objectives and scope of this study, expected industrial and scientific contributions, and the structure of the dissertation report.

1.1. RESEARCH BACKGROUND

The use of diesel equipment in mines is an attractive option due to its ability to convert a large fraction of available energy into useable work. Diesel engines are rugged, dependable, and fuel efficient (McKinnon, 1999). It is very common for diesel engines in heavy duty trucks to have a life of around 1,600,000 kilometers (McKinnon, 1999). In

underground mines, generally diesel equipment provides more flexibility and maneuverability as compared to electric-powered equipment. Despite the development of other energy alternatives, the underground mining industry appears likely to maintain its reliance on diesel-powered equipment (Anon, 2001).

Health concerns related to DPM are a relatively new development in mining that really began in the late 1970s to early 1980s (Ames, Attfield, Hankinson, Hearl, & Reger, 1982; Gamble, Jones, Hudak, & Merchant, 1978; Panel, 1981; Reger, Hancock, Hankinson, Hearl, & Merchant, 1982). DPM is a major cause of large number of occupational diseases (Safety, 2005b). Published studies (Control, 1988; Scott, Grayson, & Metz, 2004; Walsh, 1999) report severe effects of DPM exposure in which a particular concern is the reported chronic health effects of DPM exposure. These health effects include respiratory diseases, lung cancer, reduced lung capacity, pneumonia, and heart disease (Control, 1988; Scott et al., 2004; Walsh, 1999). The National Institute of Occupational Safety and Health (NIOSH) regards diesel exhaust as a potential carcinogen and states that reduction in workplace DPM exposure reduces cancer risks (Control, 1988). The International Agency for Research on Cancer (IARC) has declared that "diesel engine exhaust is carcinogenic to humans" (Cancer, 2011). Diesel particles are very small in size, generally less than a micron (D. B. Kittelson, 1998). Due to this small size, diesel particles reside in the mine air for a longer period of time as compared to the respirable dust particles (D. B. Kittelson, 1998) and DPM particles can penetrate deep into human lungs (A. D. Bugarski, Janisko, Cauda, Noll, & Mischler, 2012).

In underground mines, identification and control of DPM levels is a challenging task (S. Gillies & H. W. Wu, 2008). The NIOSH 5040 method is the accepted standard and is viewed as the most accurate method to determine miners' DPM exposure over a period of time. Mine Safety and Health Administration (MSHA) uses the NIOSH 5040 method for DPM compliance determinations in underground M/NM. The NIOSH 5040 method is widely used to measure DPM because its results are less likely to suffer from interferences by mineral sources or other combustibles and it differentiates carbon content into organic and elemental components. However, the NIOSH 5040 method is a shift-average based method and, like any other shift-average based measurement method, it inherits some limitations. One limitation of the NIOSH 5040 method is the time lag due to its requirement for processing results by a specialized remote laboratory. Another deficiency is its inability to detect elevated DPM levels over short but significant, time periods. The NIOSH 5040 method is fundamentally unable to determine DPM transients during measurement. The limitations of shift-average based DPM measurement methods are circumvented by real-time DPM monitoring. Use of and results from real-time DPM monitoring are relatively new in the mining industry since these devices have only been become available during the last ten years. Ongoing research continues to improve the accuracy of real-time DPM monitors and test their ability to measure DPM in various underground mining situations. At present, the Real-time DPM monitors can almost instantly quantify DPM concentrations, produce data that is required for engineering evaluation exercises, and highlight mine situations where DPM levels are relatively high for substantial time periods (ADS Gillies, B. Belle, H.W Wu, & Khan, 2014).

This research focuses on extensive measurements of DPM concentrations at active underground metal mines by employing two types of monitoring methods. The extensive DPM sampling at active work faces and in exhaust air drifts provides an identification of frequently encountered DPM levels in a work stope of an underground metal mine. This research provides a significant step forward in developing DPM frequency distribution models for active work zones. DPM recirculation from an auxiliary fan and ventilation duct system, and ventilation parameters for dead-end mine entry are also studied.

1.2. PROBLEM STATEMENT

Diesel is an efficient fossil fuel. The high energy efficiency of diesel makes it an attractive fuel choice for many industrial and domestic applications (Stephenson, Spear, & Lutte, 2006). Diesel engines are highly efficient, rugged, dependable, and offer more flexibility as compared to electric powered system. This makes diesel-powered equipment an attractive choice in large mining operations. In United States, it is estimated that diesel-powered equipment is used in approximately 14,000 mining operations (Stephenson et al., 2006). MSHA has estimated that approximately 230,000 mine workers are potentially exposed to DPM (MSHA, 2003). In view of the large population of workers that are exposed to DPM in underground mines, DPM has rightfully become a subject of increasing concern. Some studies indicates that underground miners' exposure to DPM can be ten times higher than other industries (R. A. Haney, Saseen, & Waytulonis, 1997).

The accepted method for compliance determination of DPM exposure in M/NM mines is the NIOSH 5040 method. This is a shift-average based measurement method that collects DPM from the mine air while sampler is being worn by a worker. The NIOSH

5040 DPM sample is collected at a filter cassette by a small pump that has a fixed flow rate. The exposure sample is then submitted to a laboratory for analysis after the miner has completed his work-shift. This process adds a significant time-lag between exposure and a determination of exposure level. During this time-lag, miners could be overexposed to airborne levels of DPM without even knowing the severity of DPM levels. In addition, by the time the mine operators receive results from the laboratory, the mining situation may have changed. Mine operators are therefore forced to judge the relevance of this old information are left unable to identify DPM concentration when it is needed.

Because of the lag-time and the inability of a shift-average based method to depict the DPM concentration over short time periods, the concept of real-time DPM monitoring has evolved. Real-time monitors can almost instantly quantify the level of DPM and can drastically reduce the cost of monitoring DPM. Several real-time monitors have been tested in mines and in the laboratory to measure DPM concentrations. However, all studies that have employed real-time DPM monitors have been limited to equipment using conventional petroleum diesel. However, a large number of mining companies use biodiesel to operate underground mine machinery. DPM generated from petroleum diesel differs significantly from the DPM that is produced by biodiesel. In underground mines, biodiesel is used as an alternative to petroleum diesel because biodiesel has been reported to decrease the DPM concentrations up to 60% as compared to the petroleum diesel (A. D. Bugarski, Cauda, Janisko, Hummer, & Patts, 2010). Until now, no real-time DPM monitor has been used to determine the characteristics of biodiesel DPM in the underground mine environment. Considering the benefits of using biodiesel in mines in the context of its resultant DPM emission, a critical need exists to test and calibrate a real-time DPM monitor

for biodiesel exhaust measurement. In the past, real-time DPM monitors used in the mining industry have been primarily tested and calibrated for regular diesel. The calibration of a real-time monitor for biodiesel exhaust will provide a means for instant biodiesel exhaust determination, thereby resolving the lag-time issue associated with the NIOSH 5040 method.

This study will seek to achieve desired research outcome by proposing a correlation between a real-time monitor and the NIOSH 5040 method for 70% to 99% (high-percent) biodiesel exhaust. The proposed correlation would assist mine operators in accurately estimating instantaneous DPM concentrations simply by employing a real-time DPM monitor. This research also collected extensive real-time monitoring results from the work faces and exhaust air drifts. DPM frequency distribution models for active work zones will be developed, DPM recirculation will be measured, and work stope ventilation parameters will be assessed.

1.3. OBJECTIVES AND SCOPE OF STUDY

The objective of this research is to investigate several significant aspects associated with the measurement and behavior of DPM concentrations in underground metal mines. The primary objective are as follows:

- Examine the correlation between shift-average based (the NIOSH 5040 method) and the FLIR Airtec (real-time DPM monitor) for high-percent biodiesel exhaust. The proposed correlations could be used for accurate estimation of DPM exposure.
- Measure commonly encountered DPM levels at mines work faces and in exhaust air drifts.

- Determine appropriate DPM frequency distribution models for work faces and exhaust air drifts based upon measured data. Highlighting the significance of DPM area sampling and the importance of determining DPM short term exposure limit.
- Measure the effects of using multiple diesel-powered equipment on DPM concentration levels at different mine locations and the determination of DPM recirculation by an auxiliary fan and ventilation duct system.
- Computationally examine the effects of different parameters that are involved in the ventilation of a dead-end mine entry.
- Suggest good work practices for the FLIR Airtec monitor.

This research is restricted in determining the DPM concentrations at active metal mine sites by adopting two different measuring methods. Measurement results are used to demonstrate DPM concentrations at active mines, and frequency distribution models are based on the real-time DPM measurements data. Fan recirculation is measured with real-time DPM monitors, and stope ventilation parameters are evaluated by a 2D CFD analysis. Finally, lessons learned by the extensive use of the FLIR Airtec real-time DPM monitors are used to suggest good work practices for the monitor.

1.4. RESEARCH METHODOLOGY

In order to accomplish the research objectives, extensive DPM area sampling was conducted at active underground metal mines in the United States. DPM concentrations were measured at various mine locations by two types of measurement methods. The FLIR Airtec monitor was used for real-time DPM monitoring, whereas the NIOSH 5040 method was used for shift-average DPM measurements. For this research, two FLIR Airtec real-

time DPM monitors have been purchased by the mining company involved, whereas shift-average based DPM monitors (NIOSH 5040 method) were rented from a commercial laboratory (GALSON). The correlation data was achieved by installing real-time and shift-average based monitors at same locations in the mine so that their results can be compared. The presence of correlation equation between DPM concentrations obtained from both monitors was investigated and statistical techniques were used to validate the established correlation.

During extended monitoring time periods, logs of all diesel equipment movement in the area under observation were maintained. DPM concentration results were analyzed for the work face and exhaust air drift measurements, and frequency distribution models were developed for both work face and exhaust air drift mine locations. Simultaneous real-time DPM measurement plots have also been plotted for different measurement locations and the effects of any diesel equipment movement on DPM concentration studied. Fan recirculation was estimated by installing DPM monitors at both upstream and downstream locations of the fan and ventilation duct system. Finally, a 2D CFD model was used to assess different work stope ventilation parameters.

1.5. BROADER RESEARCH IMPACTS

The broad research impacts are as follows:

- This research will assure the access of mining industry to a real-time DPM monitor that can be used in underground mines for accurate DPM determination of high-percent biodiesel exhaust.

- This study provides a significant data base about transient DPM concentrations at the work faces and in exhaust air drifts of underground metal mines. The information regarding transient DPM levels will help to understand and interpret most commonly encountered DPM levels in conventional underground metal mines.
- This project has been completed with the cooperation of a large mining company. Findings from this study will help similar mines to understand the extent of DPM levels at different locations in their mines and allow them to estimate DPM quickly, cost effectively, and accurately.
- This research is a pioneering effort to determine DPM frequency distribution models for active mining zones in underground mines. So far, no such effort has been made by any other researcher. The developed frequency distribution models allow for estimation of probable DPM exposure when a miner visits specific mine working areas.
- This study is the first attempt to specifically address DPM area sampling at the work faces and in exhaust air drifts of operational mines. This research provides evidence to support DPM short-term exposure limits.
- This research is a pioneering effort that highlights the impact of auxiliary fan recirculation in the context of DPM.
- Finally, this research determines the effect of stope ventilation parameters and suggests the best ventilation practices to control DPM concentrations in mines' dead-end entries.

1.6. STRUCTURE OF THE DISSERTATION

This dissertation is organized into ten sections for easy comprehension. Section 1 has provided research background and a problem statement with the expected scientific and industrial contributions. Section 2 gives a critical review of literature that pertains to this research. Section 3 discusses the correlation between the FLIR Airtec and the NIOSH 5040 method. Section 4 gives extensive work face and exhaust air drift measurement results. The DPM frequency distribution models for work faces and exhaust air drifts are given in Section 5. Section 6 examines case studies of work face and simultaneous DPM measurements. Section 7 discusses the recirculation of DPM from an auxiliary fan and ventilation duct system. Section 8 assesses the impact of stope ventilation parameters in a dead-end mine entry via a 2D CFD model. Section 9 provides good work practices for the FLIR Airtec real-time DPM monitor. Finally, Section 10 provides the conclusions drawn from this research along with research contributions and recommendations for future work.

2. LITERATURE REVIEW

This section includes a comprehensive review of literature that focuses on the various aspects of diesel equipment usage and its exhaust in underground M/NM mines. This section will present the DPM measurement method that is used for compliance purpose in M/NM mines of the United States. A review of the real-time DPM measurements in mines with special emphasis on the FLIR Airtec monitor will also be discussed in this section.

2.1. DIESEL EQUIPMENT IN MINING

Diesel is an efficient fossil fuel and the energy efficiency of diesel makes it an attractive choice for many industrial and domestic applications (Stephenson et al., 2006). The use of diesel equipment in the mining industry is an attractive option not only because of the ability to convert a large fraction of available energy into useable work, but also because diesel engines are fuel efficient, rugged, and dependable. It is very common for diesel engines in heavy duty (HD) trucks to have a life of 1,600,000 kilometers (McKinnon, 1999). Generally in underground mines diesel equipment provides more flexibility and maneuverability as compared to electric-powered systems. In the United States, it is estimated that diesel powered equipment is used in 14,000 mining operations (Stephenson et al., 2006). Even considering the pace of developments in other energy alternatives, it can be assumed that the underground mining industry will maintain its reliance on diesel powered equipment for the near future (Anon, 2001).

Because diesel vehicles are one of the primary components of underground mining systems, they are the main source of miners' exposure to diesel exhaust aerosols and gases (Spencer, 2009). In mine air, diesel engines emit sub-micrometer sized carbonaceous aerosols, respirable, and total particulate mass (Zielinska et al., 2002). Diesel equipment operators and other miners spend most of their working time within close proximity to this equipment causing their exposure to harmful diesel exhaust mixtures. In view of the large population of workers who are exposed to DPM in underground mines, DPM has become a subject of increased concern. Documents which support MSHA DPM regulations clearly demonstrate that underground miners and other personnel who work in confined spaces are exposed to higher DPM than any other occupation (Cohen, Borak, Hall, Sirianni, & Chemerynski, 2002; Pronk, Coble, & Stewart, 2009). Underground miners' exposure to diesel exhaust can be 100 times more than its normal environmental concentrations and 10 times more than concentrations present in other diesel engine work environments (B. K. Cantrell & Watts Jr, 1997; R. Haney, 1990).

2.2. DIESEL PARTICULATE MATTER

Nearly all mine workers are exposed to aerosols – both mechanically generated and from the combustion of diesel (B. Cantrell, 1987; B. K. Cantrell, Williams, Watts, & Jankowski, 1993; McDonald, Zielinska, Sagebiel, McDaniel, & Mousset-Jones, 2003; Mody & Jakhete, 1987). Diesel engine exhaust is a primary source of submicron (particles with diameter less than 1 μm) mine aerosols (Cantrel, Rubow, & Watts, 1993). DPM is a general term for sub-micrometer aerosols that are emitted by diesel engines as a product of incomplete combustion of fuel and lubricant hydrocarbons. The US Code of Federal

Regulations title 30 (Safety, 2001b) describes the composition of diesel engine exhaust as a complex mixture of several compounds that contains both particulate and gaseous fractions. The exact composition of diesel exhaust varies due to engine design, engine life, engine maintenance, engine tuning, equipment operator, type of fuel used, load cycle, and exhaust after-treatment devices. In addition to these factors, different environmental settings in which diesel engines are used also effect the gaseous and particulate matter composition of diesel engine exhaust. In a DPM mixture, the gaseous concentrations of diesel exhaust are oxides of nitrogen, carbon, and sulfur; alkenes and alkanes; aldehydes; and monocyclic and polycyclic aromatic hydrocarbons; whereas particulate constituents are diesel soot and other solid aerosols including metallic abrasion particles, ash particulates, silicates, and sulfates (Safety, 2001b).

The primary particulate fraction of diesel exhaust is very tiny individual particles with a solid Elemental Carbon (EC) core that absorbs many toxic substances. In general, DPM is primarily composed of an EC core and other organic and inorganic aerosols (A. D. Bugarski, Cauda, Janisko, Mischler, & Noll, 2011). The EC core is formed in the engine cylinder, within localized areas of the injection plume that lack the amount of oxygen required for complete combustion. The fuel is pyrolyzed within these regions, creating charred remains (EPA, 2001) known as EC or solid carbon soot. Once formed, most of the EC will combine with oxygen and burn during later stages of the combustion process, however, some amount is emitted from the engine exhaust as solid particulate matter (EPA, 2001; D. Kittelson, Pipho, Ambs, & Siegla, 1986; D. B. Kittelson, 1998). EC core particles are slowly covered by a thin layer of volatile material (Ålander, Leskinen, Raunemaa, & Rantanen, 2004; D. B. Kittelson, 1998; Konstandopoulos & Papaioannou, 2008). The

process of EC formation during combustion and expulsion is mainly governed by temperature, oxidant availability, and residence time (EPA, 2001). The Organic Carbon (OC) fraction of DPM forms compounds that are different from EC because it is composed of volatile and semi-volatile organic material. More than 1,800 different organic compounds have been known to adsorb on an EC core. Some of these organic fractions result from incomplete fuel combustion in the diesel engine and are formed when lubricating oil is not completely oxidized during the process of combustion (Heywood, 1988). Diesel particles also contain a fraction of non-organic absorbed compounds (Safety, 2001a). Figure 2.1 shows a simplified diagram of the DPM composition.

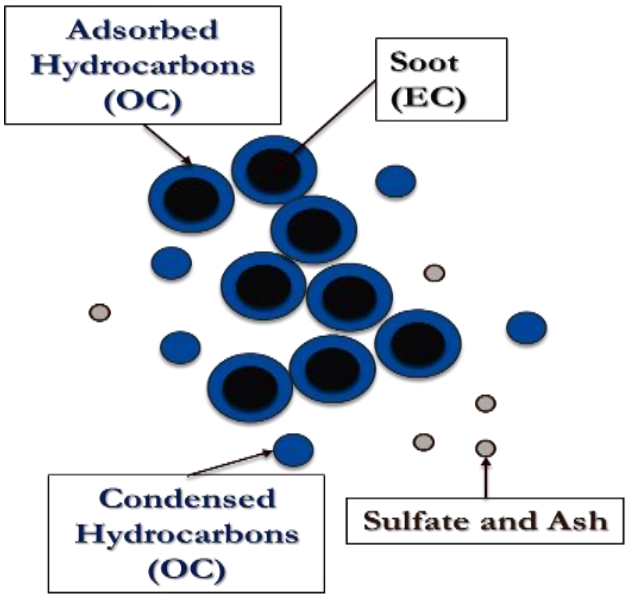

Figure 2.1 Diesel particulate matter composition

The diameter of diesel particles depends upon engine design and operating conditions. In terms of size, the aerosols emitted into the environment by diesel engines are typically poly-dispersed and log normally distributed in one, two, or even three

distinctive modes: (D. Kittelson et al., 2004; D. B. Kittelson, 1998) (a) nucleation mode (3-30 nm), (b) accumulation mode (30-500 nm), and (c) coarse mode (> 500 nm). Although the approximate geometric mean diameters are as given in the parentheses, all these modes are more appropriately defined by their distinct nature than by their fixed size boundaries (D. B. Kittelson, 1998). In most cases, the size distribution of diesel aerosols emitted by diesel engines lie between accumulation and nucleation mode (Biswas et al., 2008; A. D. Bugarski et al., 2009; Du & Yu, 2006; Guo, Xu, Laing, Hammerle, & Maricq, 2003; Mathis, Mohr, Kaegi, Bertola, & Boulouchos, 2005; Skillas, Qian, Baltensperger, Matter, & Burtscher, 2000; Voutilainen, Kaipio, Pekkanen, Timonen, & Ruuskanen, 2004; Warner, Johnson, Bagley, & Huynh, 2003). Particles in the accumulation mode contribute to the majority of the DPM mass. The chemical composition of accumulation mode particles is mainly a carbonaceous core and adsorbed volatile organic compounds. Particles in the nucleation mode are mainly composed of volatile organic compounds, sulfur compounds, and trace elements (A. D. Bugarski et al., 2011). The nucleation mode contains the majority of the particles based on numbers but do not contribute significantly to the total DPM mass (Schnakenberg & Bugarski, 2002).

In general diesel aerosols are one order of magnitude smaller than other respirable aerosols generated in mines (Joy et al., 2006). Since most aerosols emitted by diesel engines and other combustion aerosols are sub-micrometer in size (D. B. Kittelson, 1998), DPM aerosols behave in a manner which is similar to the mine gases. In underground mines, DPM will therefore have much longer residence times than larger mechanically-generated particles that are removed from the mine atmosphere quite quickly by gravitational settling. The residence time of diesel aerosols in the atmosphere depends on

the size and concentration of other particles present in the air. Aerosols between 100 nm and 10 μm have the longest residence time and are typically about 1-week (D. B. Kittelson, 1998). The typical residence time for 100 nm particles is about 15 minutes as these particles primarily coagulate with larger particles from accumulation, coarse modes, and dust (A. D. Bugarski et al., 2011).

2.3. HEALTH CONCERNS RELATED TO DPM EXPOSURE

A harmful aspect of the use of diesel as a fuel is its resultant emissions which are an adverse environmental agent. Health concerns related to DPM are a relatively new concept in mining, beginning in the late 1970s to early 1980s (Ames et al., 1982; Gamble et al., 1978; Panel, 1981; Reger et al., 1982). According to MSHA, all diesel aerosols can be classified as respirable aerosols (A. D. Bugarski et al., 2011). Particle size and distribution have a major impact on the transportation of diesel aerosols and ultimately on the health effects associated with DPM exposure. This is primarily because the deposition efficiency of the particles in the respiratory tract depends upon its size (ICRP & Protection, 1994; Jarvis, Birchall, James, Bailey, & Dorrian, 1996; Pietikäinen et al., 2009; Voutilainen et al., 2004). The nucleation and accumulation mode diesel aerosols readily penetrate in bronchial, bronchiolar, and alveolar regions of the human respiratory tract (Pietikäinen et al., 2009), whereas coarse mode aerosols are mainly deposited in the anterior nose and extrathoracic regions of the human respiratory tract.

DPM has been identified as a major cause of a large number of occupational diseases (Safety, 2005a). Diesel emissions contain various respiratory irritants in both the gas and particulate phases that can cause various acute effects. Published studies (Control,

1988; Scott et al., 2004; Walsh, 1999) report the severe effects of DPM exposure in which particular concern is the reported chronic health effects of DPM exposure. Diesel particles are very small in size and generally less than a micron (D. B. Kittelson, 1998). Long-term and continuous exposure to DPM can result in severe health issues which include respiratory diseases, lung cancer, reduced lung capacity, pneumonia, and heart disease (Control, 1988; Panel, 1981; Scott et al., 2004; Walsh, 1998). In occupational settings, human epidemiological studies have demonstrated an association between increased lung cancer rate and diesel exhaust exposure (Attfield et al., 2012; EPA, 2002; Silverman et al., 2012). The NIOSH regards diesel exhaust as a "potential carcinogen," and states that reduction in workplace DPM exposure reduces cancer risks (Control, 1988). The IARC has declared that "diesel engine exhaust is carcinogenic to humans" (Cancer, 2012). A reported study suggests that the risk of lung cancer among workers that are heavily exposed to respirable EC (between 640 and 1,280 $\mu g/m^3$) was five times more than the risk in the lowest exposure category (less than 20 $\mu g/m^3$). In addition, acute exposure to diesel exhaust can also cause eye and nose irritation, headaches, nausea, lightheadedness, vomiting, numbness, and asthma (Kahn, Orris, & Weeks, 1988; Ris, 2007). Other diesel exhaust exposure effects include bronchial irritation, cough, phlegm, and neurophysiologic symptoms (Lloyd & Cackette, 2001).

2.4. DPM REGULATORY IMPACT ON MINES DIESEL EQUIPMENT

MSHA regulates the usage of diesel equipment in US underground mines. MSHA initiated rulemaking regarding DPM in order to reduce the DPM exposure of underground

miners. Based on mining commodities, MSHA has divided the mining industry into two separate sections for regulation purposes: (a) coal mines and (b) M/NM mines.

2.4.1. Impact on Underground Coal Mines. In underground coal mines, MSHA imposes distinct requirements for diesel powered equipment usage. This is due to the possible presence of coal dust, explosive gas mixtures, and other related safety matters. MSHA also requires that any diesel equipment used in an underground coal mine must be approved by MSHA. Underground coal mine diesel equipment has been categorized by MSHA into two types: Type (I) permissible diesel equipment and Type (II) non-permissible equipment.

Type (I) permissible equipment is required in those underground mines that potentially have methane gas and/or coal dust explosive mixtures. Permissible equipment is mainly used in areas of the mine that are inside the last open crosscut (called inby areas). Permissible equipment consists mainly of HD production equipment that must be explosion proof and have stringent requirements for exhaust cooling systems and surface temperature controls. As of July 2002, according to MSHA, the requirement for each piece of permissible diesel equipment used in any underground coal mine is a maximum emission of 2.5 g/hr. of DPM (Safety, 2001b). Most permissible diesel equipment use exhaust filtration systems in order to meet the MSHA emission requirement of 2.5 g/hr.

Type (II) non-permissible diesel equipment can be used in the areas of the underground coal mines where use of permissible equipment is not essential. Non-permissible equipment does not require surface temperature and exhaust cooling controls. MSHA further categorizes non-permissible diesel equipment in two types (a) non-permissible light duty (LD) equipment and (b) non-permissible HD equipment (MSHA,

2014). As of January 2005, MSHA requires that each non-permissible HD diesel equipment used in an underground coal mine must emit less than 2.5 g/hr. of DPM, whereas each non-permissible LD diesel-powered equipment added in an underground coal mine after May 2001 must emit less than 5.0 g/hr. of DPM (MSHA, 2014). Other diesel engine vehicles which meet the United States Environmental Protection Agency (EPA) emission standards are considered in compliance with LD provisions, even if they exceed DPM emissions of 5.0 g/hr. LD diesel engines that meet the Unites Sates EPA standards and emit more than 5.0 g/hr. can be an important source of DPM in the underground coal mine air even though MSHA regulations allow their usage without emission control (A. Bugarski, Janisko, & Cauda, 2011).

2.4.2. Impact on M/NM Mines. After July 2001, MSHA requires that any diesel powered engine introduced in a M/NM in the US must be either certified to meet or exceed the particulate matter (PM) emission requirements specified by the EPA (Safety, 2001a). This requirement does not pertain to diesel engines used in ambulances or in firefighting equipment as these vehicles are used according to the mine's firefighting and evacuation plans.

2.5. US DPM REGULATIONS AND PERMISSIBLE EXPOSURE LIMIT

MSHA published two rules related to miners' exposure to DPM in underground coal (MSHA, 2014) and M/NM mines (Safety, 2001a). These regulations, implemented in the two mining sectors, differ significantly in term of implementation and DPM exposure determinations. The DPM regulatory approach implemented in M/NM mines is focused on monitoring DPM exposure in mine atmospheres. They encourage the use of Personal

Protective Equipment (PPE) and different administrative and engineering controls. The United States DPM Permissible Exposure Limit (PEL) for M/NM mines was implemented in May 2008. MSHA monitor DPM by employing a sampling methodology developed by NIOSH to measure Total Carbon (TC) concentration (Tomko, Stackpole, Findlay, & Pomroy, 2010). The PEL for TC on an average eight-hour shift basis is 160 $\mu g/m^3$. TC is defined as the sum of EC and OC when both EC and OC are analyzed by using the standard NIOSH 5040 method (M. E. Birch & R. A. Cary, 1996; Safety, 2001a). TC is used as a measure of DPM because reported studies have shown that DPM is generally (70% to 90%) made up of TC (Oanh et al., 2010; Shah et al., 2007; Warner et al., 2003). The relationship between EC and OC fractions in untreated exhaust from diesel engines depends on operating conditions, type of engine, fuel composition, and many other factors. The EC fraction in DPM increases with engine speed and operating load. A study conducted in underground metal mines where diesel-powered equipment is extensively used in the mining process reported that EC concentrations average about 75% of TC concentrations; whereas TC concentrations were found to make up, on average, 72% of total DPM concentrations (McDonald, Zielinska, Sagebiel, & McDaniel, 2002; Zielinska et al., 2002). Another study conducted in several underground M/NM mines showed strong linear correlation between EC and DPM and between EC and TC concentrations when Diesel Particulate Filter (DPF) systems were not used (JD Noll, Bugarski, Patts, Mischler, & McWilliams, 2007). A relatively recent study (James Noll, Gilles, Wu, & Rubinstein, 2015) determined the relationship between EC and TC from several DPM measurements that were conducted in the United States and the Australia. This particular study suggested that generally an EC value of 127 or 128 $\mu g/m^3$ represents a TC value of 160 $\mu g/m^3$.

Contrary to M/NM mines, DPM regulations implemented in underground coal mines are not compliance based; as the primary focus is to control DPM concentration by utilizing different available technologies that reduce DPM at the point of generation. Therefore, MSHA does not enforce DPM monitoring for compliance determinations in underground coal mines.

2.6. DPM EXPOSURE MEASUREMENTS

In underground metal mines, MSHA and operators routinely measure ambient concentrations and personal exposure to CO, CO_2, NO, NO_2, DPM, and other pollutants to verify compliance with exposure limits (Safety, 2001a; Tomko et al., 2010). Routine measurements of in-use emissions of CO and measurements of personal exposures to CO and NO_2 are a requirement when operating diesel engines in underground coal mines (Safety, 2008).

In order to assess the potential environmental and health impact of diesel emissions, ambient and indoor exposure measurement is primarily used. In occupational settings, three basic types of sampling techniques are used: (a) personal, (b) breathing zone, and (c) general air (Leidel, Busch, & Lynch, 1977). In the case of personal sampling, a measurement or sampling device is worn by the miner during his normal work shift. In breathing zone sampling, other individual samplers not worn by the miner measure concentrations from the breathing zone of the miner for whom exposure is to be obtained. These are typically hung from the roof and moved from place to place as the miner's work location changes. Area sampling or mine air sampling is a technique where concentrations are sampled or measured from fixed locations in the mine. In underground M/NM mines,

a miner's exposure is usually determined by the personal sampling technique (Safety, 2001a, 2008). This is due to the non-existence of an established relationship between area sampling and personal sampling concentrations (Chow et al., 2002; Leidel et al., 1977). The following section describes methods used to determine DPM concentrations in the United States M/NM mines as coal mines do not use ambient exposure monitoring for DPM compliance.

2.6.1. Shift-Average Based Monitoring. The concentration of DPM can be measured by several shift-average based measurement methods. This include the NIOSH 5040 (used by MSHA for compliance determination), respirable combustible dust, and size selective sampling method. Among shift-average based DPM measurement techniques, the NIOSH 5040 method is considered to be the best approach that can measure DPM. The NIOSH 5040 method is a direct approach, it can quantify OC and EC at low (5 µg) level, and it is less likely to suffer from interferences by mineral sources or other combustibles. The NIOSH 5040 method can therefore quantify DPM in situations where other shift-average methods may not be suitable (Birch, 2002; Ramachandran & Watts, 2003; Watts & Ramachandran, 2000). The NIOSH 5040 method has been adopted in this research. A detailed description of the NIOSH 5040 method is described in the following section.

The NIOSH 5040 method: The NIOSH 5040 methods is an established technique to measure DPM concentration in underground mines. This is the most accurate method that is used to determine the concentration of DPM in mines. The NIOSH 5040 technique is an analytical method that measures EC and OC components of a DPM sample collected on a quartz fiber filter (Birch, 2002). The NIOSH 5040 method differentiates carbon content into organic and elemental components, which makes it more versatile as compared

to the other carbon analytical methods. MSHA considers TC to be the most appropriate surrogate for DPM as TC contributes over 80% of the particulate matter present in diesel exhaust (M. Birch & R. Cary, 1996; Birch, 1998). Major interferences that are typically found in underground M/NM mines can affect TC analysis. These interferences are mechanically generated dust that may contain OC and/or EC, cigarette smoke, oil mist, ammonium nitrate/fuel vapors from explosive material, and welding fumes (B. K. Cantrell et al., 1993; McCartney & Cantrell, 1992; Safety, 2001a). However, because dust in M/NM mines generally does not have high carbon content, results of TC and EC measurements are not significantly influenced by carbon from mineral dust (J. D. Noll, Timko, McWilliams, Hall, & Haney, 2005). Size-selective samplers used during DPM sampling can effectively remove EC and OC contamination from mineral dust, but these are not effective in removing sub-micrometer aerosols from cigarette smoke or oil mist (Birch, 2002; Borak, Sirianni, Cohen, Chemerynski, & Wheeler, 2003). Avoiding cigarette smoke or oil mist is not always possible when taking personal samples and because these contaminants interfere only with the OC analysis, MSHA proposed using sub-micrometer EC as a surrogate for DPM (Birch & Noll, 2004). In a typical M/NM mine environment, no other sources of sub-micrometer EC are known. Thus, EC can be used as a surrogate for DPM (Birch & Noll, 2004).

The current DPM sampling protocol requires that both personal and area samples be collected simultaneously over the miner's full shift (Tomko et al., 2010). The personal sample is used to assess personal exposure to TC and EC. One area sample (or sometimes more than one) is used to assess the relationship between TC and EC. As a part of the alternative procedure to determine TC exposure levels, EC concentrations obtained by

personal exposure sampling are multiplied by the ratio of TC to EC obtained from area sample measurements (Safety, 2001a; Tomko et al., 2010). The TC/EC ratio is determined from one or more samples collected in the main exhaust course of the mine because OC interferences are expected to be negligible in those samples (Safety, 2001a; Tomko et al., 2010). This EC based approach to determining TC exposures is used to minimize the potential for overestimating a miner's exposures to TC due to various artifacts that primarily affect the measurement of the OC fraction of TC.

The NIOSH 5040 method requires four sampling components: a specialized wearable pump designed to deliver a constant volume flow with an accurate timing device, tygon tubing, a 10 mm nylon cyclone, and a DPM filter cassette. Field samples are collected by a sampling medium that consists of a 37 mm cassette preceded by a 10 mm nylon cyclone. Air is drawn at a flow rate of 1.7 liters per minute using a calibrated constant flow sampling pump through the nylon cyclone. The nylon cyclone has a cut-point of 4.0 µm and an impactor with a cut-point of 0.8 µm at a volume flow rate of 1.7 liters per min. These settings serve to physically eliminate most of the mechanically generated mineral dust from diesel aerosol. Before sampling, the cassette and cyclone assemblies are connected to the calibrated sampling pump by using plastic tubing. Personal DPM samples are collected by fitting these sampling trains on miners; whereas area sampling is conducted by installing the monitoring setup at desired locations in the mine. After the collection of a DPM sample, the cassettes are sealed and sent to a laboratory for analysis. Cassettes are opened and a 1.5 cm^2 rectangular shaped portion of the filter is removed using a metal punch. This procedure allows three individual sample analyses for each sample collected (Ramachandran & Watts, 2003). In the laboratory, a thermo-optical method is

utilized to analyze the sample. In the thermal-optical method, separation of OC and EC is accomplished through temperature and atmospheric control (Grenier, 1998; Turcotte, Edwardson, & Laflamme, 1998).

2.6.2. Real-time Monitoring. DPM regulations, endorsed in the United States by MSHA triggered development of instruments that can estimate DPM exposure in real-time. Generally these monitors use photo-acoustic methods or condensation counters to measure respirable combustible dust and then display an equivalent DPM concentration. Although the NIOSH 5040 is a standard method used for DPM compliance determination in the Unites States M/NM mines, this method is based on determining shift-average DPM concentrations. Thus, it inherently involves an issue of "lag time" since it requires a post-collection laboratory analysis for DPM determination. It may take two weeks to get laboratory results and miners could be potentially overexposed to DPM during that time. Like any other shift-average based measurement method, the NIOSH 5040 method is not suitable to detect rapid changes in DPM levels, which may occur over the course of monitoring. In order to determine any change in DPM levels caused by changing mining activities, more than one mine air sample may have to be collected using the NIOSH 5040 method. This may increase the amount of work and cost involved in DPM monitoring. These limitations of the NIOSH 5040 method can be addressed by the use of real-time DPM monitoring devices. Although use of real-time DPM monitors is relatively new in the mining industry, real-time DPM monitors can almost instantly quantify the generation rate of DPM as well as its relative magnitude, and highlight mine situations where DPM levels are relatively high for substantial time periods.

Most real-time monitors (both prototypes and commercial units) that have been developed for mine use face serious challenges to accurate determination of DPM concentrations. The difficulties are due to increased vulnerability to mine atmospheric conditions such as oil mist, mineral dust, presence of moisture, and other particles. Another big challenge is applicability of real-time monitors in different mining conditions and the lack of a standard/unified calibration method for these units. NIOSH has been closely involved in the development of various instruments that measure airborne DPM concentration (H. Wu & Gillies, 2008). The following paragraph describes the review of various real-time monitors (except the Airtec monitor that is described in a later section) that were used for DPM monitoring in mines or in the laboratory.

The relationship between a TSI Dusttrak real-time aerosol monitor and the NIOSH 5040 method was investigated by a team of researchers. They found that the average TSI Dusttrak mass concentration is linearly correlated with TC concentration from the NIOSH 5040 method (Stephenson et al., 2006). Arnold et al. (2008) used a photo acoustic monitor, the NIOSH 5040 method, and a Dusttrak nephelometer for measuring DPM in Nevada gold mines. They determined real-time EC by a photo acoustic monitor, EC and TC by the NIOSH 5040 method and TC by the Dusttrak nephelometer. The EC and TC values obtained by the NIOSH 5040 method were found to be 50% of the respective values obtained from the Dusttrak and the real-time photo acoustic monitor (Arnott, Arnold, Mousset-Jones, Kins, & Shaff, 2008). Gillies and Wu (2008) measured real-time DPM in three different mines in Australia by a modified personal dust monitor (D-PDM). The D-PDM was modified especially to measure real time DPM in mines. They correlated D-PDM mass concentration with TC and EC obtained by the NIOSH 5040 method and

proposed several mine specific correlation equations (A. Gillies & H. Wu, 2008). Griffith (2012) determined DPM by using a real-time monitor and NIOSH 5040 method and showed that real time DPM monitor's accuracy decreased with more usage and high level of OC (Griffith J. F., 2012). Although several real-time DPM monitoring devices have been tested by various researchers, the following section will specifically focuses on the evolution of the FLIR Airtec real-time DPM monitor. The FLIR Airtec monitor is a commercial real-time DPM monitor that was adopted for this research. The FLIR Airtec monitor was selected for this research because, as compared to other real-time DPM monitors, the Airtec is the only small, efficient and rugged real-time DPM monitor that has been tested extensively and found satisfactory.

2.6.2.1. FLIR Airtec real-time DPM monitor. The FLIR Airtec real-time DPM monitor is based on a technique developed at the NIOSH Pittsburgh research laboratory (Janisko & Noll, 2008; James Noll & Janisko, 2007). The Airtec measures the EC component of DPM and has been tested in both the laboratory and in different mining conditions where its performance was reported to be satisfactory (Janisko & Noll, 2008, 2010; James Noll & Janisko, 2007; James Noll & Janisko, 2013; James Noll, Janisko, & Mischler, 2013; JD Noll, Patts, & Grau, 2008; J Noll, Volkwein, Janisko, & Patts, 2013).

2.6.2.1.1. <u>Working principal of the Airtec</u>. The Airtec has four key components: an impactor, a filter, a pump, and an optical measuring circuit. Air is drawn at a set flow rate (1.7 or 0.85 liters per minute) through an impactor and through a filter within the instrument, collecting EC from the air sample. The light intensity transmitted through the filter is then measured by an optical sensing circuit. Increase in EC accumulation on the filter cassette causes the output voltage to decrease. Laser absorption is related with EC

concentration by comparing the drop in voltage due to EC accumulation with a calibration curve. Changes in voltage are recorded by a data logger and a microcontroller is used to calculate and display the real-time output on an LCD screen of the monitor. In addition to the realtime display, data is logged internally that can be downloaded to a personal computer with a USB port. The monitor provides a five minute rolling average of EC concentrations that is calculated by recording a data point every minute. The Airtec also provides TC and the eight hour Time-Weighted Average (TWA) EC concentrations.

The Airtec preferentially selects DPM particles by two mechanisms. First, many potential interfering agents are removed by a particle size selector and second, use of light absorbance limits detection primarily to highly absorbing materials such as black carbon rather than on less absorbing materials such as silicates or condensed water (Keith, 2011; Takiff & Aiken, 2010). Figure 2.2 shows the circuit diagrams of the FLIR Airtec real-time DPM monitor (Keith, 2011), whereas the FLIR Airtec monitor is shown in Figure 2.3 (Keith, 2011; Takiff & Aiken, 2010).

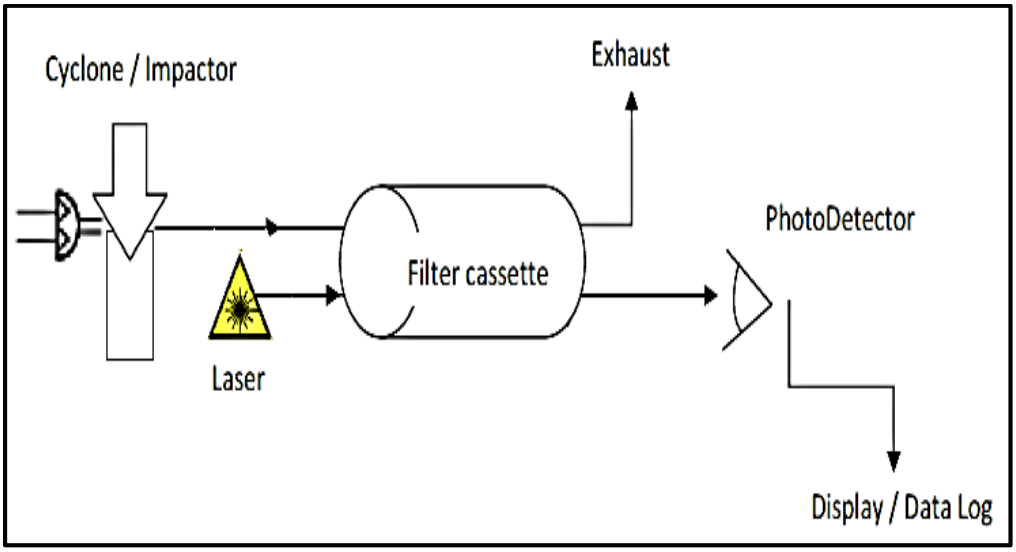

Figure 2.2 FLIR Airtec real-time DPM monitor circuit (Keith, 2011)

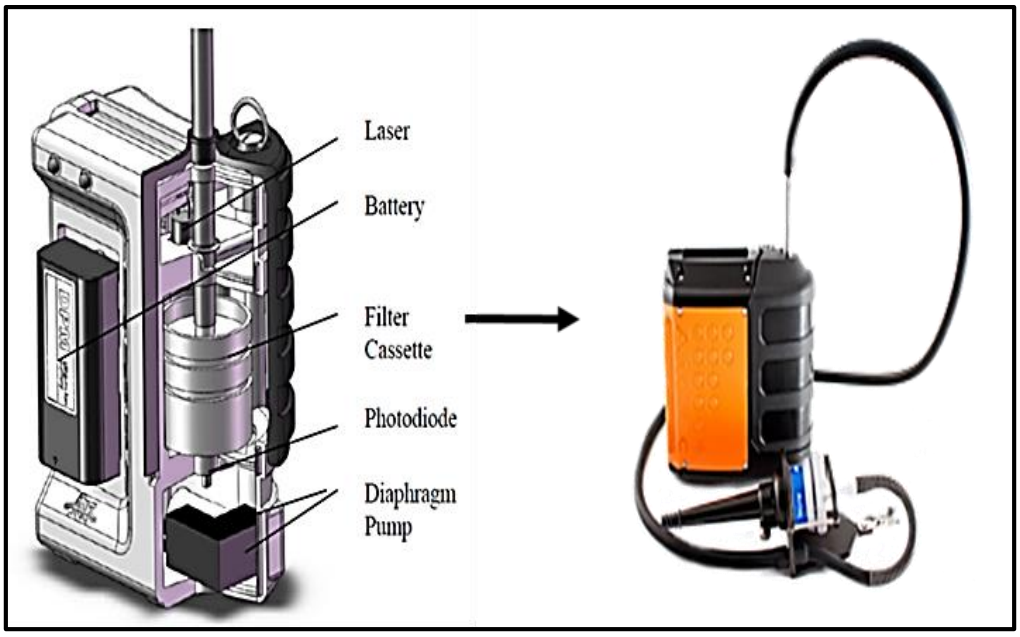

Figure 2.3 FLIR Airtec real-time monitor (Keith, 2011; Takiff & Aiken, 2010)

2.6.2.1.2. <u>Evolution of the Airtec and its use to measure DPM</u>. This section describes the evolution of the Airtec monitor and the results of various laboratory and field studies performed with the prototype and with the commercially available FLIR Airtec DPM monitor.

Noll and Janisko (2007), Janisko and Noll (2008), and Noll et al. (2008) determined EC concentrations by an "EC monitor" and the NIOSH 5040 method. The researchers concluded that the real-time EC monitor is not prone to any interference from sudden shock or from dropping. Mine area sampling results showed that the real-time EC monitor estimated slightly higher TWA EC than the NIOSH 5040 method. (Janisko & Noll, 2008; James Noll & Janisko, 2007; JD Noll et al., 2008).

The EC monitor used by Noll and Janisko (2007), Janisko and Noll (2008), and Noll et al. (2008) was subsequently licensed to ICX Technologies Incorporate. Takiff and

Aiken (2010) used the licensed version of a beta prototype of the real-time EC monitor to measure DPM and concluded that the EC monitor can efficiently determine EC concentrations in mines (Takiff & Aiken, 2010).

Janisko and Noll (2010) used a beta prototype ICX DPM monitor [similar to the monitor that was used by Takiff and Aiken (2010)] for mine DPM measurements in mines. The ICX DPM monitor was able to provide average EC over the previous five, ten, fifteen minutes, and for the eight-hour. It used a rolling average concentration for EC measurement. Janisko and Noll (2010) concluded that the ability to perform well-executed tests and to interpret the information that real-time monitors provide is an essential part of a sophisticated DPM measurements program (Janisko & Noll, 2010).

Noll, et al., (2013) conducted comprehensive laboratory analysis of the commercial version of the ICX real-time DPM monitor that was later branded as the Airtec. Airtec could be used for both area and personal sampling. Laboratory analysis of the commercial Airtec was conducted to check its performance under different testing conditions. In this study, a calibration curve (line of best fit) was developed for the Airtec monitor. The developed calibration is applicable only when EC mass collected onto the filter cassette does not exceed 276 µg. This is because at EC mass over 276 µg the optical density measurement becomes inaccurate due to optical saturation. The 276 µg of EC mass is equivalent to 338 $\mu g/m^3$ of TWA EC concentration when the flow rate of Airtec is set at 1.7 liters per minute, and 676 $\mu g/m^3$ with 0.85 liters per minute flow rate. Laboratory results on the Airtec monitor showed that mineral dust can interfere with the monitor only in the absence of a size selector; whereas no influence of oil mist or humidity was observed. The monitor has not detected the presence of cigarette smoke unless DPM was already present

on the filter; however, in enclosed cabs where the operator was smoking cigarettes, sampling results indicate that smoke has been shown to cause a bias to the measurement of the Airtec. In laboratory testing, the Airtec instrument meets the NIOSH accuracy criteria (James Noll et al., 2013).

Noll and Janisko (2013) determined the potential interferences of dust, humidity and oil mist on the FLIR Airtec monitor performance in limestone and granite mines. They concluded that if the effect of spatial variability is considered, the FLIR Airtec readings were equivalent to the NIOSH 5040 method values. The results of this study by Noll and Janisko (2013) showed that dust and high humidity did not affect the FLIR Airtec reading when an impactor was used. They concluded that besides the known potential interferences, the presence of some other submicron aerosols in the monitoring environment could potentially cause a bias in the FLIR Airtec results (James Noll & Janisko, 2013).

Gillies et al. (2014) discussed several ambient monitoring practices used in underground mines and concluded that real-time DPM ambient monitoring practices are gradually being accepted as an engineering tool to optimize the DPM control strategies (ADS Gillies et al., 2014)

Khan and Gillies used the commercially available version of the FLIR Airtec alongside the NIOSH 5040 method to determine the DPM concentrations in metal and nonmetal mines and identified high DPM sources. The front-end loaders and dump trucks were the main sources of DPM in metal mine, whereas in nonmetal mine load-haul dumps were major DPM contributors (M.U. Khan & Gillies, 2015a).

Khan and Gillies published early findings of a study in a mine using high-percent biodiesel and noticed that the TWA EC values resulted from the FLIR Airtec monitor were usually higher than the TWA EC obtained by the NIOSH 5040 method. A correlation equation between TWA EC measurements by both (FLIR Airtec and NIOSH 5040) methods was developed during initial research findings (M. U. Khan & Gillies, 2015b). Although the initial research reported the presence of a possible bias in TWA EC values of the FLIR Airtec, however the results of that study were based on limited evidence. No other studies have tested the ability of the Airtec to determine DPM from biodiesel exhaust. Given the utility of the Airtec monitor and the increased trend to use biodiesel fuel in the mining industry, a critical need exists to correlate the results from a real-time DPM monitor and the NIOSH 5040 method for high-percent biodiesel exhaust measurements. This study addresses this need and tests the Airtec, perform its field-calibration, and suggests a correction factor for biodiesel exhaust determination.

2.6.2.2. Advantages of real-time DPM monitoring. The use of real-time DPM monitoring is gaining popularity in the mining industry. Real-time DPM monitors offer several benefits over conventional shift-average based DPM measurement methods. Real-time monitoring methods are relatively new and so far no real-time DPM monitor has been accepted as a standard. However, current instrumentation developments allow improved real-time monitoring of ventilation parameters with particular emphasis on gases, respirable dust, and DPM (M.U. Khan & Gillies, 2015a). Real-time DPM monitors can provide significant information about the DPM situation in mines which cannot be

achieved by other TWA methods. Some other advantages of real-time DPM monitors are as follows:

- Real-time DPM monitors can almost instantly quantify the levels of DPM.
- Real-time DPM monitors can provide the information of trends of DPM concentrations throughout a working shift.
- Real-time monitoring of DPM is vital to understand frequent changes that occur in DPM concentrations in underground mines.
- Real-time monitoring can be used to design and implement better DPM control strategies.
- Real-time DPM monitor can be used to optimize the number of diesel-powered equipment used in any active stope.
- The cost of monitoring DPM can be reduced significantly by employing real-time DPM monitoring. This cost reduction allows a corresponding increase in DPM sampling at active mine openings, that ultimately leads to an improved mine environment.
- DPM monitors can pin point high DPM exposure zones in underground mines.
- Identification of high DPM zones allows efficient modification of mine ventilation, operator positioning and other work practices.

2.7. ROLE OF VENTILATION IN DPM DILUTION AND CONTROL

DPM is an unavoidable pollutant in mine air mixture, which makes controlling DPM an important aspect of mine ventilation plans. DPM concentration levels in underground mines can be controlled in part by providing adequate ventilation, using

biodiesel, altering the design and types of diesel engines, employing exhaust after-treatment devices, and using environmental cabs and PPE. Although use of each approach can help to control the concentration of DPM in mines, DPM dilution by ventilation is likely the most important and is essential. McPherson stated that in any underground facility where personnel are required to enter, the dilution of pollutants by providing sufficient airflows is a main objective of an underground ventilation program (Mc Pherson, 2012).

MSHA considers Particulate Index (PI) and specific nameplate Ventilation Rate (VR) to determine total airflow requirements for M/NM mines. PI is related to the DPM and nameplate VR is associated with other gases from the diesel engine exhaust. Overall airflow requirements for N/NM mines are less stringent as compared to underground coal and gassy mines. In M/NM mines, stope ventilation requirements are not dictated by any specific guidelines because it depends upon many factors, which include stope geometry, stope dimensions, in-place airflow distribution systems, level of diesel equipment activity in a stope, etc. Since no specific requirements exist for stope ventilation, miners who stay at mine work faces are directed to vacate the work areas if the concentrations of poisonous gasses from diesel engine exhaust reach a certain Threshold Limits Value (TLV). However, to date, no TLV is assigned for DPM concentrations because real-time DPM monitors have only recently become available and MSHA DPM regulations do not directly consider elevated short term DPM levels a serious health threat. MSHA does not require real-time DPM monitoring at M/NM mines' work areas. However, it is possible that elevated short term DPM levels can effect miners' health badly. Dilution of DPM by proper ventilation

is therefore important. A critical need exists to investigate stope ventilation parameters to determine means of effective DPM dilution and better quality air.

CFD modelling techniques have now became a recognized tool to understand complex airflows and behavior of various gases and dust particles in three dimensional space. CFD simulations can provide uniquely valuable information for initial research concepts and novel alternatives. Numerical simulations using CFD technique have been successfully adopted in various mine ventilation related research areas. Several studies have used CFD to simulate the behavior of DPM in mines and examined the effect of different ventilation practices on DPM concentration in different mining conditions. One study used a CFD model to simulate DPM distribution and temperature in sloped dead-end entries that were ventilated with a push tube and blower fan system. This research suggested an increase in air flow rates for decreasing DPM concentrations at work faces (Yi Zheng, Lan, Thiruvengadam, Tien, & Li, 2017). However, it did not evaluate quantitatively the effect of change in duct diameter, duct inlet velocity, and duct position with respect to the dead-end on the DPM levels. In fact we have been unable to identify any research which has exclusively examined the effect of ventilation related parameters on the dilution of DPM in a dead-end mine entry. This study will examine some ventilation related parameters that play an important role in the ventilation of dead-end mine entry. These ventilation parameters include the duct inlet velocity, duct diameter, optimum combination of duct diameter and velocity, total air quantity, and the location of duct inlet with respect to the dead-end.

2.8. RATIONALE FOR PHD RESEARCH

The intrinsic lag-time associated with the NIOSH 5040 method can be completely avoided by utilizing commercially available real-time DPM monitors. However, the focus of real-time DPM monitors has been on conventional diesel fuels. To the author's knowledge, no measurements have been performed in high-percent biodiesel exhaust. Considering the advantages of biodiesel in terms of DPM emission and its wide use in the mining industry, there is a great need to test the Airtec monitor for measuring DPM in mine situations with a high-percent biodiesel. This study reports around three hundred hours of real time data collected in active underground metal mines which use high-percent biodiesel almost exclusively.

The second fundamental limitation of the standard NIOSH 5040 method is its inability to detect elevated DPM levels for short, but significant durations and its inability to discriminate transient DPM levels that are encountered in any typical underground M/NM mine. This research will provide a significant data base regarding transient DPM levels at the work faces and in exhaust air drifts of underground metal mines. The data collected during this study regarding DPM transient levels provides a first look at DPM transients in underground metal mining operations. In addition, through careful logging of mine activity, the present study relates DPM transient levels with diesel equipment activity in mines. No research work has been reported to date, to the author's knowledge, that has comprehensively studied real-time DPM concentrations in active underground metal mines and its association with specific diesel equipment activities.

Study of DPM transient levels is critical because it will provide evidence of the actual time-varying DPM concentrations at work faces and in exhaust air drifts. It is quite

possible that the personal TWA DPM exposure of a miner may remain below PEL even though he is exposed to very high levels of DPM concentration for short durations. High level of DPM may harm miners' health even when their PEL remain within allowable limit. Although the health effects of miners' short term exposure to very high DPM levels are not established, researchers in the health sector can utilize the present results to examine realistic short term DPM exposures. This would allow for determination of whether short term exposure limit would be appropriate for DPM.

3. FIELD ASSOCIATION OF THE FLIR AIRTEC AND THE NIOSH 5040 METHOD IN HIGH-PERCENT BIODIESEL EXHAUST

3.1. OVERVIEW

MSHA employs the NIOSH 5040 method for DPM compliance purposes in the United States underground metal and nonmetal mines. The NIOSH 5040 DPM sampling method is a recognized procedure used to measure DPM concentration. This technique can quantify DPM concentrations even at very low levels. Although the NIOSH 5040 method is an accurate way to measure DPM exposure, the method requires that the exposure sample be submitted to a laboratory for analysis. The process of obtaining results from the laboratory means that there is a significant time lag before an accurate exposure determination can be made. During this time, miners can potentially be overexposed to high airborne levels of DPM (Takiff & Aiken, 2010). In addition, the NIOSH 5040 method provides only a TWA value of DPM concentration. Significant information about the changing mine environment due to changes in work activity cannot be obtained by utilizing the NIOSH 5040 method. This obvious limitation can be adequately addressed by using real-time DPM monitoring devices. Real-time monitoring of DPM is vital to gain an accurate picture of rapid changes in DPM levels in the mine atmosphere. The outcomes of various real-time DPM monitoring studies have revealed that the mining industry now has access to an enhanced tool to better understand the mine atmosphere in the context of DPM (Janisko & Noll, 2008; James Noll et al., 2013; H. W. Wu, Gillies, Volkwein, & Noll, 2009).

Given the utility of real-time DPM monitoring and the increased trend to use biodiesel fuel in the mining industry, a critical need exists to correlate the results from a

real-time DPM monitor and the NIOSH 5040 method for high-percent biodiesel exhaust measurements. Although the Airtec real-time monitor has been tested and calibrated for regular diesel fuel (Janisko & Noll, 2008, 2010; James Noll & Janisko, 2007; James Noll & Janisko, 2013; James Noll et al., 2013; JD Noll et al., 2008), no significant research has been done to confirm its applicability in biodiesel exhaust measurements. A possible bias between the Airtec and the NIOSH 5040 has been observed and reported in the preliminary findings of recent research (M. U. Khan & Gillies, 2015b). The section expands upon the preliminary results to provide a comprehensive evaluation of the Airtec performance in high-percent biodiesel exhaust concentrations. DPM measurements have been performed in active mines using the Airtec real-time monitor along with the standard NIOSH 5040 method. The DPM samples were collected from five different underground metal mines over approximately one year. The TWA EC results from both methods were compared, and results identify a trend of slight overestimation by the Airtec for EC concentrations ranging from 0 to 200-$\mu g/m^3$. A bias correction for high-percent biodiesel exhaust is developed.

3.2. RESEARCH METHODOLOGY

Research methodology of both DPM monitoring methods adopted in this research is described in the following sub sections.

3.2.1. TWA Monitoring Method. The NIOSH 5040 method has been employed to measure standard shift-average DPM concentrations. This is an established analytical method which is used to measure the EC and OC components of a DPM sample collected on a quartz fiber filter (Birch, 2002). This method differentiates carbon content into organic

and elemental components, which makes it more versatile as compared to the other carbon analytical methods. In the NIOSH 5040 method, a personal DPM sample is collected by fitting sampling trains on a miner whereas area sampling is conducted by installing the monitoring setup at a specific location in the mine. After the collection of either type of DPM sample, the cassettes are sealed and sent to a laboratory for analysis (detail of the NIOSH 5040 method is given in Section 02).

3.2.2. Real-time Monitoring Method. The FLIR Airtec real-time DPM monitor has been used to measure real-time DPM concentrations in the present study. This monitor was originally developed and tested by a group of researchers working with NIOSH (Janisko & Noll, 2008, 2010; James Noll & Janisko, 2007; James Noll & Janisko, 2013; James Noll et al., 2013; JD Noll et al., 2008). The Airtec measures the EC component of DPM and has been tested in the laboratory and in numerous mining conditions. The performance of the Airtec was reported to be satisfactory (Janisko & Noll, 2008, 2010; James Noll & Janisko, 2007; James Noll & Janisko, 2013; James Noll et al., 2013; JD Noll et al., 2008; J Noll et al., 2013). The Airtec has four key components, an impactor, a filter, a pump, and an optical measuring circuit. Air is drawn at a set flow rate through an impactor and then through an internal filter that collects EC from the air sample (details of the Airtec evolution and its working principal are described in Section 02).

3.2.3. DPM Monitoring Process. DPM samples were collected from five underground metal mines in the United States. The mines were highly mechanized and use heavy duty underground diesel equipment for all mining operations. These mines use high-percent biodiesel as a main fuel for diesel equipment. The mines' diesel fleet include haul trucks, drill machines, front-end loaders, load haul and dumps, back hoes and other heavy-

and light- duty diesel equipment that is typically used in any large metal mining operation. The mines generally work seven days a week with two 10-hour shifts per day. The production of these mines varies from 5200 to 4000 tons of ore per day. The width of mine individual openings generally varies from 9 to 10 meters. These openings are considered large, and the air velocities at some mine locations are very low (less than 0.5 m/s). The mine opening heights are highly variable; at some places, mine entries are about 4 meters in height, whereas at other locations, these openings can be as much as 24 meters high. The depth of the studied mines varies from 275 to 350 meters from the surface. Safety precautions were taken by the research team members throughout the data collection phase as they worked in mines. After identifying a number of high DPM concentration areas in these mines, the mine management implemented a procedure requiring all personnel to wear respirators in these locations. Respirators were worn by all miners and research team members throughout their stay at mine locations with higher DPM concentrations. During face work, miners were almost exclusively confined in their environmental cabs.

DPM area samples were collected at numerous locations in the selected mines for a period of nearly one year. Figure 3.1, Figure 3.2, and Figure 3.3 present the mine entries in mines X, Y, and Z, respectively. Figure 3.4 shows the roof drilling operation in a mine Z. Sampling was conducted near the working faces, in exhaust air drifts and in fresh air drifts during a variety of mining activities. The DPM area sampling was performed by installing the Airtec real-time DPM monitor and NIOSH 5040 DPM sampling pump side-by-side at several locations in the mines. A similar approach has been adopted by other researchers while evaluating the performance of real-time DPM monitors in the field (Janisko & Noll, 2008, 2010; James Noll & Janisko, 2007; James Noll & Janisko, 2013;

JD Noll et al., 2008; H. W. Wu et al., 2009). Results from real-time and shift-average based measurements are compared by installing both types of monitors at the same location for each sampling duration. DPM monitors installed for measurements in mine Y and mine Z are shown in Figure 3.5 and Figure 3.6, respectively. The pumps were calibrated at 1.7 liters per minute as prescribed by the NIOSH 5040 sampling method protocol. Figure 3.7 shows the sampling pump calibrations setup for the NIOSH 5040 method. The SKC DPM sampling cassettes were used to collect samples for the NIOSH 5040 method. The SKC impactor is a sampling device that is used by MSHA for DPM compliance evaluations. The NIOSH 5040 DPM sampling was performed by using two types of pumps; GILAir and AIRCHEK. The EC values from the real-time monitors were obtained by connecting the Airtec to a laptop and downloading the data directly from the monitor with help of a manufacturer provided software. The NIOSH 5040 samples were sent to a laboratory for standard 5040 analysis. The EC values obtained from both methods were then converted into equivalent eight-hour shift-average EC concentrations for the sake of consistency. All samples were collected under close observation by the research team members. During sampling, the monitoring equipment was regularly checked, and measurements which encountered any kind of error (for example, flow rate error, clogging of the Airtec filter cassette, or flow rate error of the NIOSH 5040 monitors) were discarded.

3.3. RESULTS AND DISCUSSION

Results and discussion are discussed in following sub sections.

3.3.1. TWA EC Comparison. A scatter-plot of all TWA EC results collected from the five metal mines is shown in Figure 3.8. The results obtained by the two methods show

noticeable differences in measured EC values. The range of EC concentration obtained during this study varies from 8 to 725 µg/m^3. The results of TWA EC concentration from both methods were plotted by keeping EC from the Airtec as an independent variable (x-axis) and EC from NIOSH 5040 as a response variable (y-axis). Figure 3.8 shows a line of 45° slope (1:1 slope) for reference. If both methods were in perfect agreement, the data points in Figure 3.8 would fall directly on the 45° line. Any measurement point above the 45° slope line represents underestimation by the Airtec, whereas any data point below the 45° slope line reflects overestimation by the Airtec. The data in Figure 3.8 can be further subdivided into two separate EC ranges by considering the distinct behavior of the Airtec. The first range contains samples that have EC less than 200 µg/m^3, which is hereafter termed as the "lower EC concentrations." The second range has all samples corresponding to EC concentrations above 200 µg/m^3, which is hereafter termed as "higher EC concentrations." EC values obtained by the NIOSH 5040 method were found to be below 200 µg/m^3 for 55% of samples, whereas 45% of samples had EC over 200 µg/m^3. The scatter-plot shows that for lower EC concentrations, the Airtec slightly over estimated EC values in over 90% of the measurements. The difference in EC values between both adopted methods is not unexpected since the Airtec estimates EC using a calibration equation, whereas the NIOSH 5040 method uses a gravimetric approach to assess EC concentration. Although this difference in measured EC concentrations can occur due to the effect of spatial variability as described by Noll et al (2013), the presence of a clear trend for lower EC concentrations suggests that difference is not entirely due to the effect of spatial variability, as the inlets of both samplers were within close proximity to each other. In fact, if spatial variability is the only factor that could cause the difference in EC

measurements, then one would not expect any specific trend of overestimation or under-estimation by the Airtec real-time monitor. The behavior of the Airtec monitor at lower EC concentration levels indicates that some unknown effect in addition to that of spatial variability is influencing its results. The assumption that the EC differences are entirely due to the effect of spatial variability does not seem to be justified, as the EC scatter-plot in Figure 3.8 lies mostly on one side of the 45° slope line when concentrations of EC are below 200 µg/m^3.

The observed trend for lower EC concentrations is even more pronounced when percentage bias is viewed for the Airtec monitor as in Figure 3.9. Overall, 70.5% of the Airtec results were found within ± 20% of NIOSH 5040 results, whereas 29.5% samples showed difference of more than 20%. The Figure 3.9 shows the plot of percentage bias of the Airtec versus NIOSH 5040 measurements.

Figure 3.1 A mine entry in the mine X

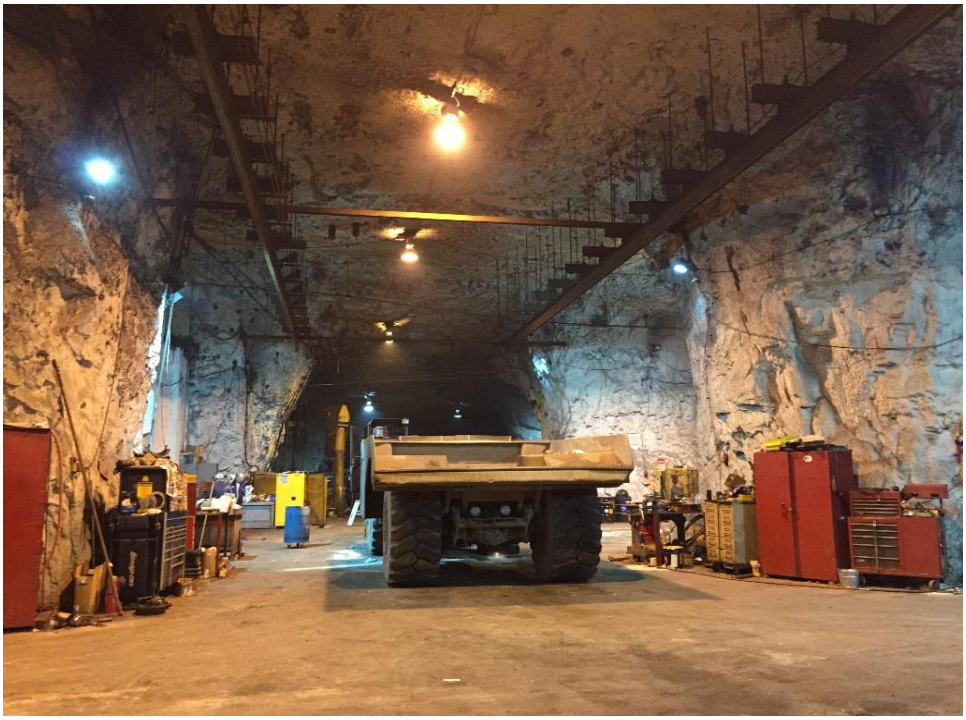

Figure 3.2 A mine entry in the mine Y

Figure 3.3 A mine entry in the mine Z

Figure 3.4 Roof drilling operation in the mine Z

Figure 3.5 DPM monitors installed in the mine Y

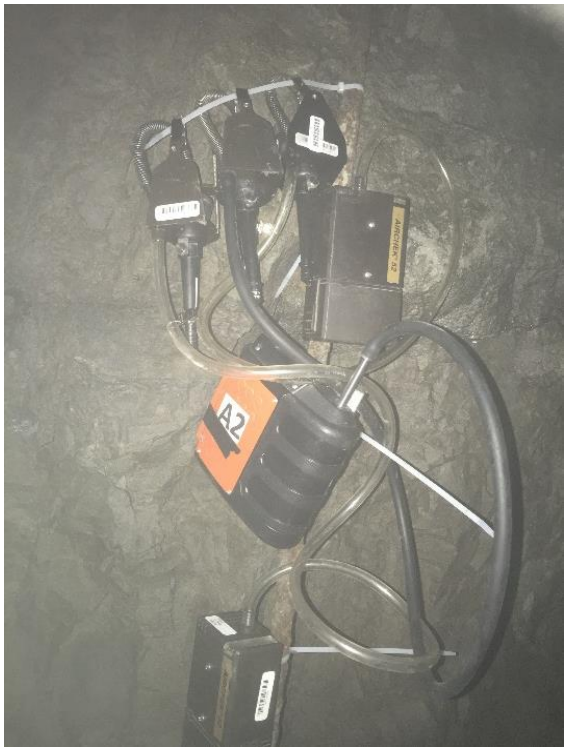

Figure 3.6 DPM monitors installed in the mine Z

Figure 3.7 The NIOSH 5040 DPM sampling pump calibrations setup

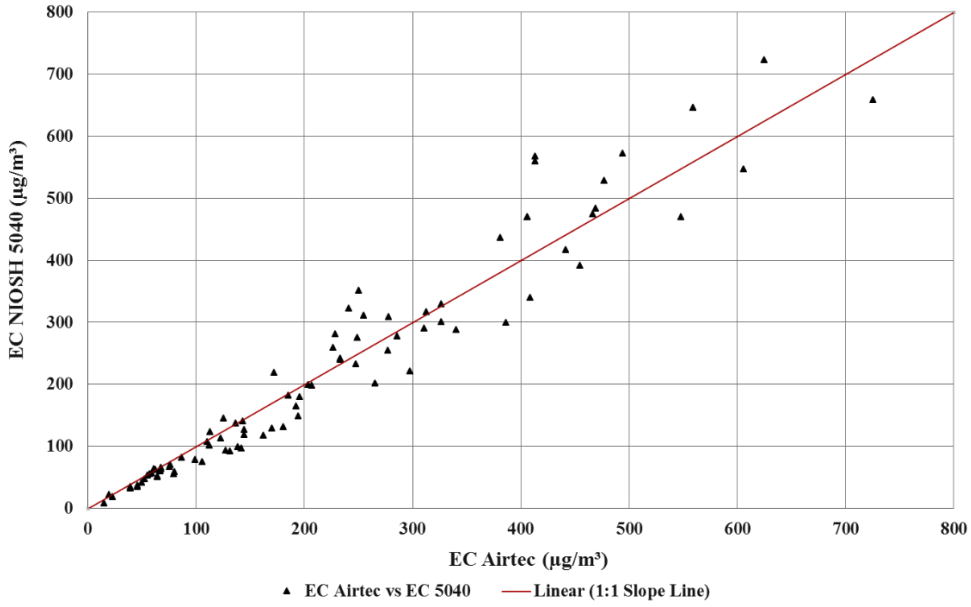

Figure 3.8 EC concentrations scatter plot between the Airtec and the NIOSH 5040

The data in Figure 3.9 reinforce the indication that a distinct behavior of the Airtec exists for lower EC concentrations. Percentage bias for lower EC concentrations showed that 63% of results were within ± 20%, whereas for higher EC concentrations a total of 80% samples lie within ± 20% of the NIOSH 5040 EC value. Average percent bias is calculated by dividing samples in various ranges of EC concentrations and averaging their bias. An average bias of zero value does not represent an exact estimation by the Airtec; rather, it represents that the Airtec overestimated and under-estimated (relative to the NIOSH 5040 method) the EC concentrations by equal amounts for different measurements. Average percent bias of the Airtec measurements for various EC ranges have been shown in Figure 3.10. Average percent bias was clearly highest (15.72 percent) for EC range between 0 to 200 µg/m^3, whereas in higher EC concentrations the bias was reduced and became negative for EC concentrations between 300 to 500 µg/m^3. The indication of a

strongly positive average percent bias at the lower EC concentration further strengthens the observation of EC overestimation.

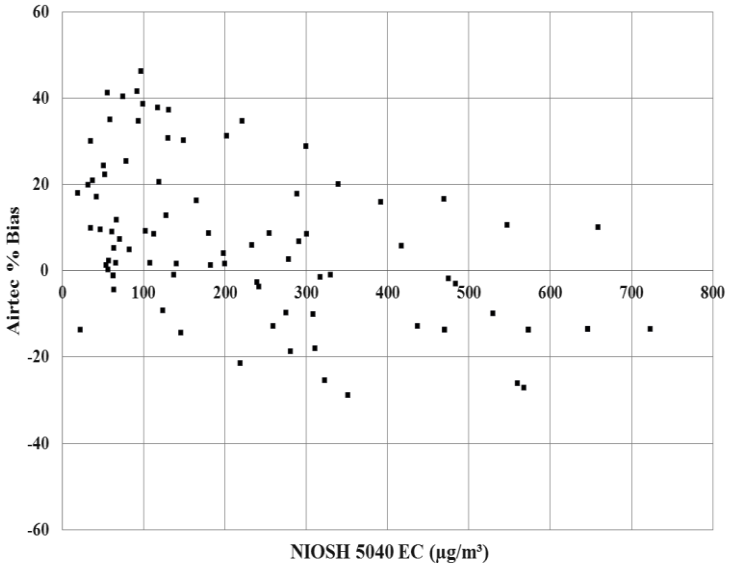

Figure 3.9 NIOSH 5040 versus Airtec percent bias

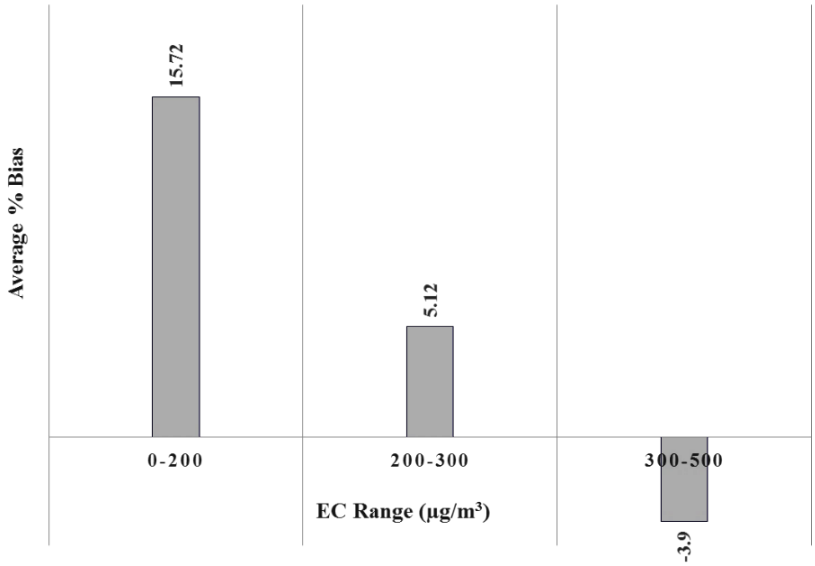

Figure 3.10 Airtec average percent bias

3.3.2. Real-time EC Profiles. In order to investigate possible causes of the bias in the Airtec measurements, data points showing the greatest bias have been examined in detail. The possibility was that the source of the bias could be specific diesel equipment, mining activity, or a particular location in the mine. Data points showing a high percent of bias were compared in both the lower and higher EC concentrations ranges. For each range, both positive and negative percent bias are plotted. Positive percent bias measurements are compared with each other, while negative percent bias measurements are compared with other negative percent bias values.

Figure 3.11 shows a comparison of three measurements for lower EC concentrations when the percent bias was positive. These measurements have relatively high positive bias and were conducted on different working days. For subsequent discussion the measurement locations were named station A, B and C. All three measurements in Figure 3.11 represent similar bias by the Airtec even though the measurement stations were situated at entirely different locations in the mine. Station A was located in the exhaust drift of the mine, which represents the final exhaust of the mine air (exhaust from several work faces and other activities). Station B was situated in the exhaust air drift, but does not represent the total exhaust of mine air. The distance from station A and station B was approximately 3 kilometer (km). Station C was near the work face at a distance of approximately 6 km from station A and 3 km from station B. All measurements presented in Figure 3.11 were performed on different days and represent an entirely different set of mining activities. Even though all three real-time plots show a markedly different pattern of EC loading on the Airtec filter cassette, each led to a high bias. Further consideration of mining activities performed during various time periods,

mine locations, and measurement days led to the conclusion that the high positive percent bias in the Airtec readings is not influenced either by a certain location in the mine or by some specific diesel equipment activity.

Figure 3.12 shows the real-time variation of three selected measurements for lower EC concentrations that have negative percent bias. The measurement locations were named as station D, E, and F. Station D is located in the fresh air drift, whereas stations E and F are situated at the mine in such a way that they capture DPM from several working faces and from the recirculated air by auxiliary mine fans. No major diesel activity was being performed near any of these measurement stations. All these measurements were performed on different days of the year and represent different diesel activities in the mine. Figure 3.12 shows a typical real-time graph obtained from the Airtec. It can be seen from Figure 3.12 that regardless of positive or negative biases, real-time EC progression similar to Figure 3.11 is obtained. Considering the maintained log of mining activities during these measurements, no specific activity or mine location could be identified as a cause for the bias in the Airtec measurements.

A plot of real-time EC concentrations by the Airtec monitor for higher EC concentrations is shown in Figure 3.13. This plot contains a comparison of measurements which showed a high-percent positive bias. The three real-time plots in Figure 3.13 pertain to different mine locations and represent different mining activities. The measurements were conducted on different days. Station G was located near the work face and was approximately 6 km away from the fresh air shaft. On the measurement day at station G, several activities were being performed at the work face including drilling, explosive loading, mucking, and rock bolting. The results of these activities are evident by

increasingly high EC concentration as time passed (Figure 3.13). Station B is situated in the exhaust air drift around 3 km away from the active work face. Station C was also located in the mine exhaust airway, in a typical mine setting. Station C represents the DPM exiting from station G plus DPM from hauling trucks. The only commonality among all the real-time data shown in Figure 3.13 was the positive bias. Although the plots represent entirely different sets of mining activities the bias does not seem to have been triggered by a specific activity.

Figure 3.14 shows a comparison of real-time EC plots when the Airtec showed negative bias for higher EC concentrations. Station G captures the exhaust exiting the work face when different pieces of diesel equipment were operating at the work face including a front-end loader, a face drill, and a rock bolter. Station C was located around 300 m away from station G. In addition to the DPM exiting from the station G, station C also captured the DPM from several haul trucks in the process of mucking. Both station C and G are the exact same stations at the same mine, which in Figure 3.13 showed a positive bias. Station H was situated in another mine and primarily represents the exhaust from a face drill machine. The Figure 3.14 represents a typical real-time EC graph obtained by the Airtec. No specific distinction that may highlight any cause of specific bias in the Airtec measurement can be identified.

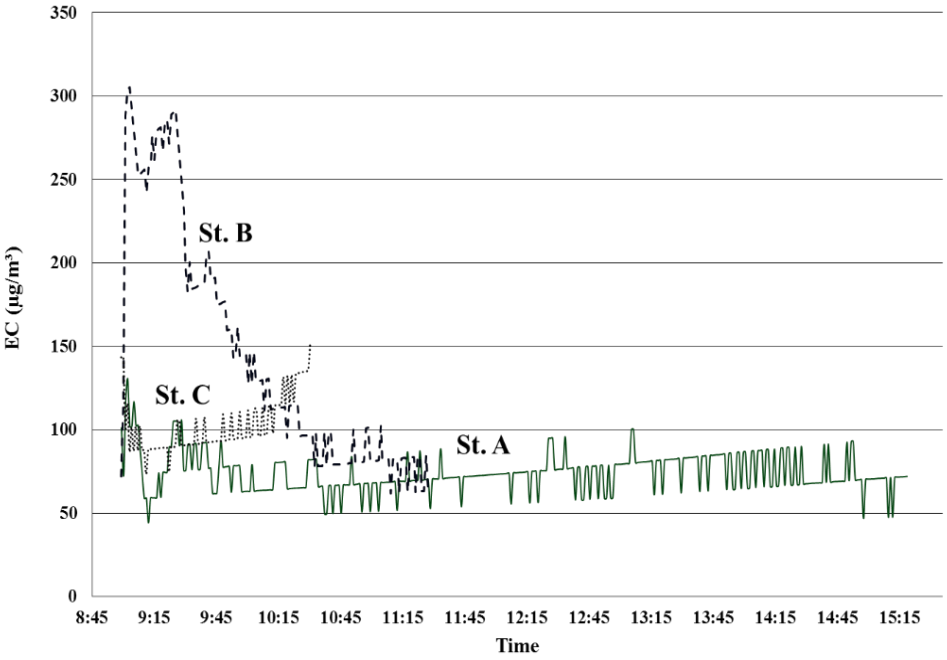

Figure 3.11 Real-time EC plots for positive bias at lower TWA EC

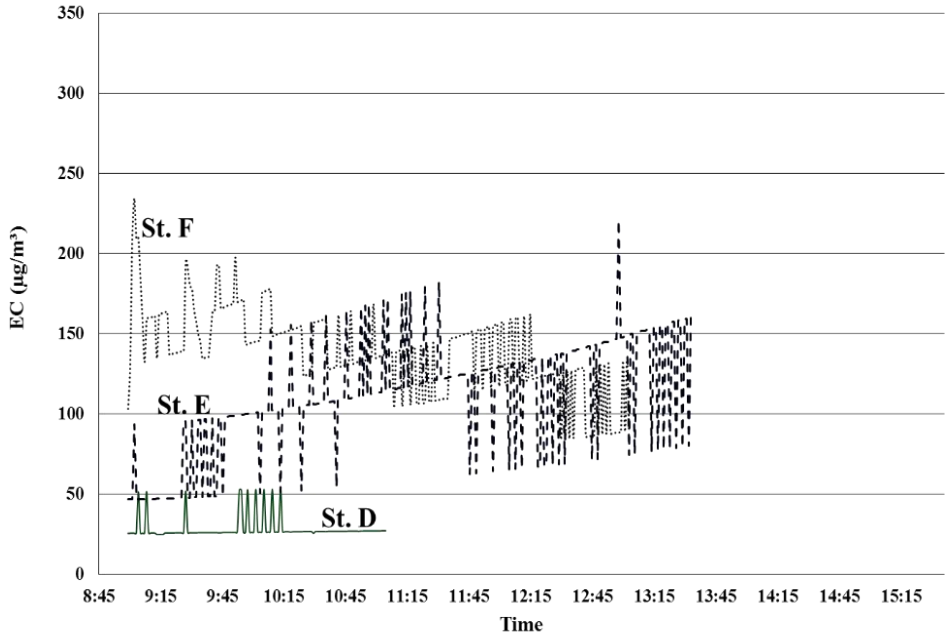

Figure 3.12 Real-time EC plots for negative bias at lower TWA EC

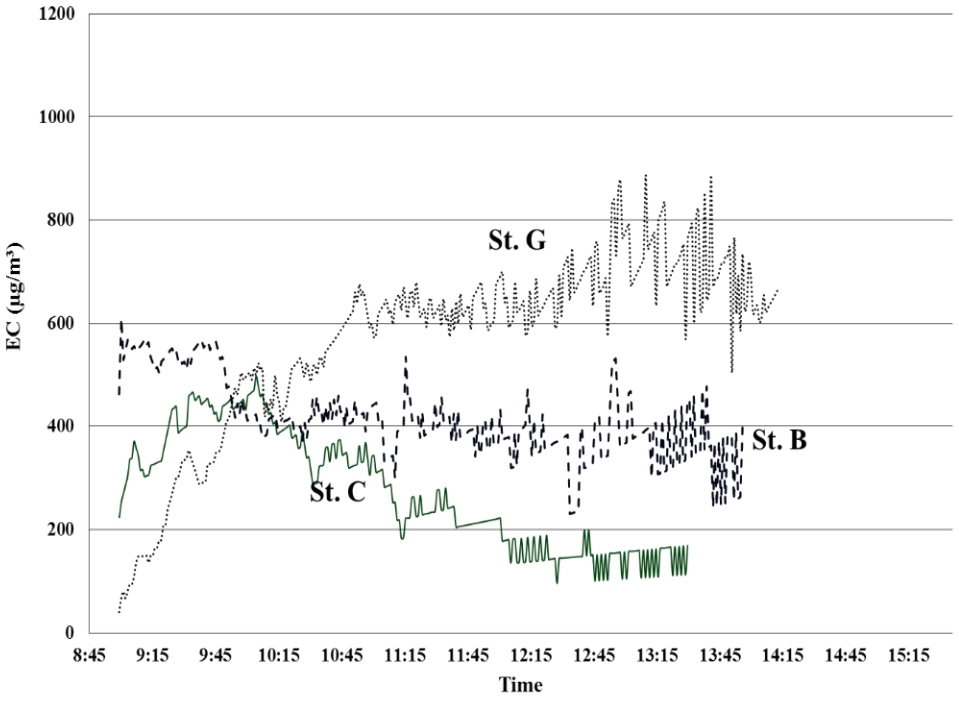

Figure 3.13 Real-time EC plots for positive bias at higher TWA EC

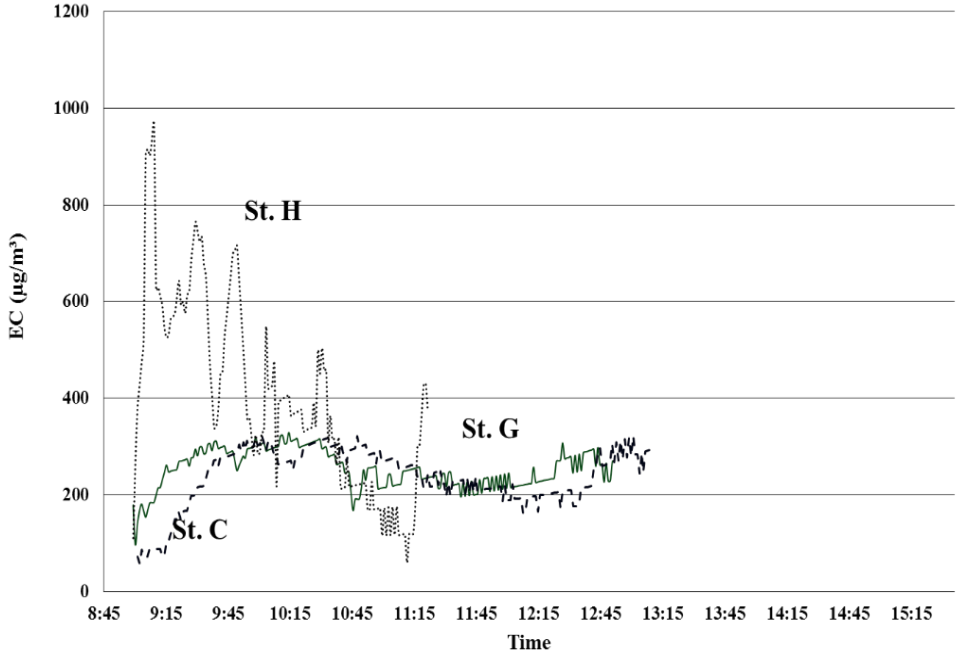

Figure 3.14 Real-time EC plots for negative bias at higher TWA EC

3.3.3. Bias Correction for Low EC Concentrations. The presence of a distinct overestimation trend in Figure 3.8 suggests that for better EC estimation by the Airtec, a correction factor is required at concentrations below 200 µg/m^3 for high-percent biodiesel exhaust measurements. Figure 3.8 shows that data points lie equally on both sides of the 45° slope line when the EC concentration is higher than 200 µg/m^3, thereby indicating no specific trend in bias. The absence of any specific trend in determining EC by the Airtec in higher EC concentrations (above 200- µg/m^3) suggests that no further correction is needed for higher EC concentration range. The ability of the Airtec to measure DPM at higher EC concentrations is deemed satisfactory and therefore no correction is suggested for EC concentrations above 200-µg/m^3.

The overestimation trend of the Airtec has been further investigated by considering the EC concentrations ranging from 0 to 200 µg/m^3. The EC range from 0 to 200 µg/m^3 is very important as the PEL for DPM lies within this range. As per MSHA rule, any DPM value above 160 µg/m^3 of TC (equivalent to approximately 130 µg/m^3 of EC) in metal and nonmetal mines is considered an over-exposure. Accurate estimation of EC in the range from 0 µg/m^3 to 130 µg/m^3 is of central importance, as this may dictate the applicability of the Airtec monitor for DPM compliance determinations. Since any EC value above 130 µg/m^3 is usually considered as over-exposure, accuracy of the Airtec in determining EC values above 130 µg/m^3 is less critical in the context of DPM compliance determinations.

Figure 3.15 presents a scatter-plot of EC concentrations by the Airtec and the NIOSH 5040 method for EC values up to 200 µg/m^3. In Figure 3.15, the x-axis represents EC by the Airtec monitor, whereas the y-axis presents EC by the NIOSH 5040 method. From the complete data set of 90 comparison points, a total of 49 samples were found to

lie in the concentration range from 0 to 200 µg/m^3. These samples were randomly divided into two subsequent data sets identified as "training set" and "validation set." The training set included 85% of the sample data. The validation set had the remaining 15% of the data points. The training set was used to develop the correlation by using the least square regression technique, and a strong correlation with high value of correlation coefficient (R^2 = 0.92) was obtained. The correlation equation Eq. (1) is the line of best fit with the intercept forced to be zero. An independent validation of the prediction equation was achieved by using the data points (validation set) that were held back during the formation of the correlation equation.

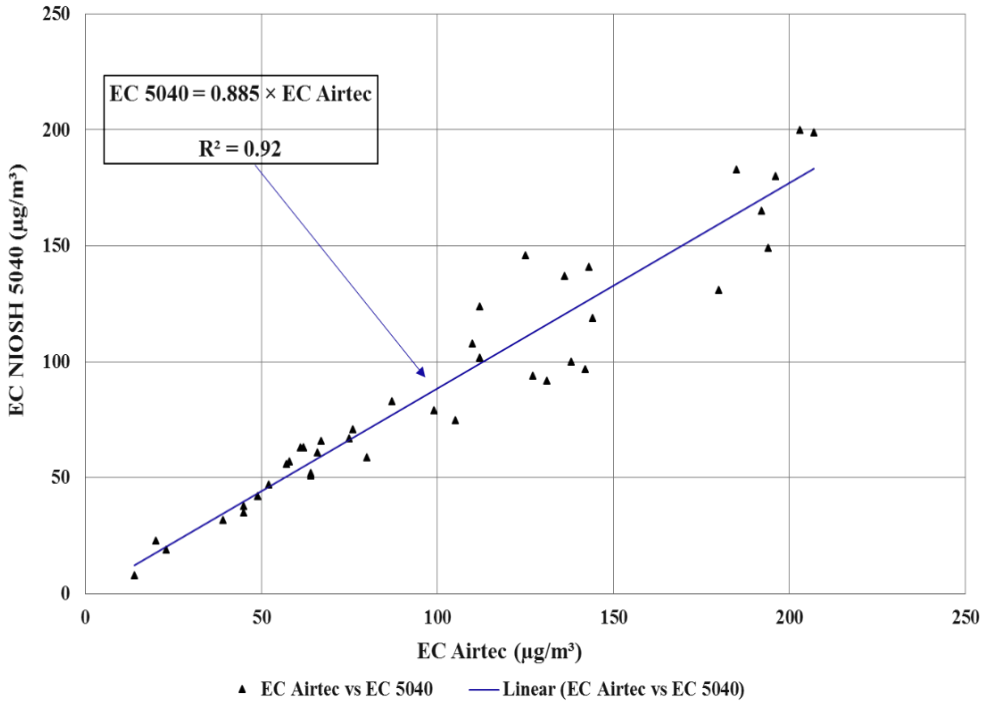

Figure 3.15 EC concentrations Airtec versus the NIOSH 5040 method

$$EC\ (5040) = 0.885 \times EC\ (Airtec) \qquad \text{Eq. 1}$$

3.3.4. Model Validation. To authenticate the accuracy of the developed correlation, EC values of the validation set were predicted by using the relation of Eq. (1). Figure 3.16 shows the plot of predicted versus actual EC concentrations for the data points of the validation set. A 45° slope line is also plotted in Figure 3.16 for reference. The predicted and measured values lie on both sides of the 45° slope line, which denies the presence of any one-sided trend by Eq. (1) and confirms that the proposed relation is applicable in EC concentrations ranging from 0 to 200 µg/m^3, when used under similar mining conditions.

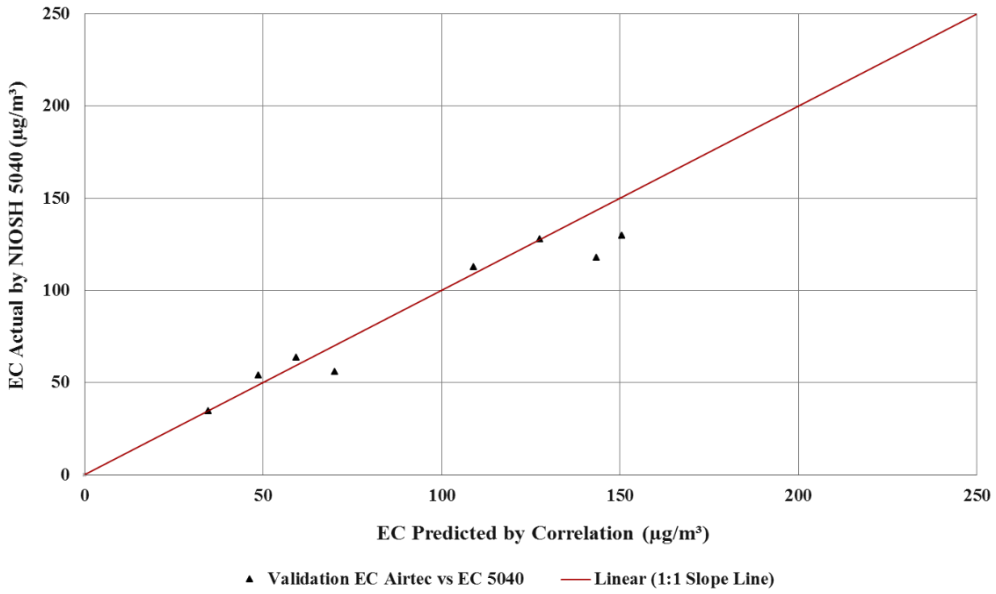

Figure 3.16 EC concentrations predicted versus actual

3.4. SUMMARY

Real-time DPM monitoring devices are gaining in popularity because of their ability to quickly understand the details of rapidly changing mining environments. Extensive DPM sampling has been conducted in several underground metal mines in the

Unites States that use over 70% biodiesel in the diesel fuel mixture. The Airtec real-time DPM monitor was tested against the standard NIOSH 5040 DPM sampling method under a variety of mining conditions. Comparison showed that the Airtec usually overestimated the EC concentrations when EC is less than 200 $\mu g/m^3$. A correlation is proposed, and a strong correlation with high value of correlation coefficient ($R^2 = 0.92$) is observed. The proposed equation can be used for accurate estimation of EC concentration by the Airtec monitor when used under similar mining conditions. The correlation equation was validated by an independent set of samples, and its prediction capability was found to be satisfactory. Results showed that no correction is required for the Airtec when EC concentration exceeds 200 $\mu g/m^3$. This study showed that with the given correction, the Airtec has a potential to be used as an alternative to the NIOSH 5040 method for assessing EC in similar underground mines. DPM monitoring with the Airtec is quick, easy, and provides more information than the time-weighted average results of the NIOSH 5040 method.

Although not specifically investigated in the current study, a possible reason for bias in the Airtec measurements might be due to the presence of some non-absorbing aerosols in high-percent biodiesel fuel mixture, as filter-based light extinction techniques are reported to be affected by the presence of absorbing particles, non-absorbing particles, and humidity (Arnott et al., 2003; Bond, Anderson, & Campbell, 1999; Coen et al., 2010; Lack et al., 2008; LaRosa, Buckley, & Wallace, 2002). The Airtec works on the principal of “light extinction” which includes the effect of light absorption and scattering (James Noll & Janisko, 2013). Bond et al (1999) reported that light extinction is affected by the presence of non-absorbing particles that can cause either an enhanced light absorption or

light scattering (Bond et al., 1999). Noll and Janisko (2013) noted that in the presence of DPM particles, light absorption will be dominant to light extinction, whereas if scattering aerosols are also collected with DPM, light scattering will have more influence (James Noll & Janisko, 2013). High-percent biodiesel fuel mixture could have some non-absorbing sub-micron aerosols, which would affect the light extinction of the monitor at lower EC concentrations (less than 200 µg/m^3). Various researchers have reported that when only EC particles are present on the filter cassette, light absorption will be the dominant phenomenon, whereas light scattering will dominate when some other scattering aerosols are also collected with EC (Bond et al., 1999; James Noll & Janisko, 2013). The presence of non-absorbing particles may have a pronounced effect at lower EC concentrations due to multiple light scattering, with the effect increasingly damped as EC accumulation on the filter cassette and laser absorption takes over the charge from laser scattering. Considering the results of this particular study, it seems that the influence of non-absorbing particles reduces with significant EC accumulation on the filter cassette, and the Airtec monitor predicts EC concentrations without bias for higher (> 200 µg/m^3) EC.

4. WORK FACE AND EXHAUST AIR DRIFT MEASUREMENTS

4.1. OVERVIEW

Underground miners are exposed to different levels of DPM concentrations throughout their work shift. A miners' DPM exposure may depend upon many factors: the types of diesel engines used in a mine, the miners' work location with respect to the diesel equipment usage, the nature of the job performed by miner, ventilation arrangements for each work stope, overall efficiency of the mine ventilation operation, the miners' adoption of good work practices, and their use of environmental cabs and personal protective equipment while staying at or near work zones. Generally, any underground mine that relies primarily on diesel equipment to conduct mining operations results in the highest DPM concentration being observed at or near the active work faces (active mining zones). This is because multiple diesel-powered machines are often being used at each active mining zone. Thus, underground miners who work at and or near the work faces have a higher probability of being exposed to severe levels of DPM concentrations as compared to those miners who are less involved in work-face activities. The harmfulness and severity of DPM exposure to miners has been a critical issue. Recent categorization of DPM into group 1 (type of agents) by the IARC suggests that, miners' exposure to high DPM concentrations even for short duration can have some deleterious effects on their health (Cancer, 2012). Thus, the realization of the presence of high-level DPM concentrations at active mining zones and understanding their variations with respect to the diesel equipment activities is vital. Since face workers have the highest potential to be exposed to high DPM concentrations, real-time monitoring of DPM at work faces demands careful attention.

Real-time monitoring of DPM concentrations at active mining zones is important because high DPM concentrations for short (less than an hour) and even significantly longer (less than three hours) durations cannot be identified by the standard TWA NIOSH 5040 DPM monitoring method.

This section identifies and describes a number of DPM measurement scenarios that are found in many underground mines by illustrating a series of real-time and shift-average based DPM determination in several underground metal mines in the Unites States. Extensive DPM area samples were collected at various mines locations including work faces and exhaust air drifts which were situated near (400 m to 700 m) work faces. High DPM area sampling concentrations were observed at work faces and in exhaust air drifts. This section also highlights the importance of real-time DPM area measurement by demonstrating that active mining zones do in fact have very high DPM concentrations. Finally, this section illustrates the DPM progression with time at the work faces and in exhaust air drifts, showing that in any underground mine, high DPM concentrations can occur over both relatively for long and short time periods.

4.2. DETAILS OF STUDIED MINES AND MONITORING PROCESS

DPM samples were collected from underground metal mines in the United States. The studied mines were highly mechanized and used dozens of diesel-powered pieces of equipment to perform all major mining operations. These mines use high-percent biodiesel as the main fuel for their diesel equipment. The diesel fleet of all mines includes haul trucks, drill machines, frond-end loaders, load-haul-dumps, back hoes and other heavy and light duty diesel equipment that is typically used in any large metal mining operation. All

mines generally work seven days a week with two ten-hour shifts per day. The production of these mines vary from 4000 to 5200 tons of ore per day. The width of the mine openings generally varies from 6 to 10 meters; these openings are considered large and the air velocities at some mines locations are very low (less than 0.5 m/s). The heights of mines openings are highly variable. At some places, mine entries are about 7 meters in height whereas at other locations these openings can be as much as 35 meters high. The depth of the mines studied varies from 275 to 350 meters from the surface. All mines have intake and exhaust ventilation shafts and employ several auxiliary fans for ventilation purposes. Most of the work faces have push and pull ventilation arrangement and use blower fans that are installed with ventilation ducts to push the fresh air at work face, whereas exhaust fans are used both with and without ventilation ducts to pull out the polluted air from the work face. Safety precautions were taken by the research team members throughout the data collection phase as they worked in the mines. After identifying a number of high DPM concentration areas in these mines, the mine management implemented a procedure requiring all personnel to wear respirators in these locations. Respirators were worn by all miners and research team members throughout their time in higher DPM concentration areas.

4.3. RESEARCH METHODOLOGY

The FLIR Airtec real-time DPM monitor (described in the previous sections) has been used for real-time DPM measurements, whereas the shift-average DPM concentrations were measured by employing the TWA NIOSH5040 method (discussed in previous Sections).

DPM area samples were collected at several work faces and at exhaust air drifts in the selected mines for a period of nearly one year during a variety of mining activities. The DPM area sampling was performed by installing the Airtec real-time DPM monitor and the NIOSH 5040 DPM sampling pump side-by-side at measurement locations. Standard and recommended sampling protocols have been followed for both adopted monitoring methods. Real-time monitoring provided the variations in DPM levels, whereas the NIOSH 5040 method delivered the TWA DPM concentrations for each measurement. All samples were collected under close observation by research team members. The monitors were regularly checked during sampling and those measurements that encountered any sort of error (for example, flow rate error, clogging of the Airtec filter cassette, or flow rate error of the NIOSH 5040 monitors) were discarded. Detailed logs of diesel equipment activities in the monitoring areas were maintained, and the effect of different mining activities on the levels of DPM is discussed in the following sections.

4.4. RESULTS ANALYSIS

Results from DPM area measurements at work faces and in exhaust air drifts were divided into separate categories. In order to better understand the relationship between the usage of diesel equipment and DPM concentrations resulting from their use, DPM measurements at the mine faces and in the exhaust air drifts were subdivided into three distinct EC concentrations ranges: (a) low (0 to150 $\mu g/m^3$), (b) intermediate (150 to 300-$\mu g/m^3$), and (c) high (above 300 $\mu g/m^3$). This subdivision is based on the mean EC concentration as determined by the Airtec monitor. The mean EC for each measurement is determined by calculating the simple average of EC concentrations obtained by the Airtec

monitor over each collection period. Each subdivided section combines different measurement results that represent similar levels of DPM concentrations under various mining circumstances.

4.5. DPM MONITORING AT THE WORK FACES

The EC concentration data gathered at various work faces during the course of this study has been analyzed. The real-time EC concentration graphs obtained by the Airtec DPM monitor were plotted. Figure 4.1 shows the representative plots of EC concentrations observed at the mines' work faces. It can be seen from Figure 4.1 that, the DPM levels at the work faces can become very high. In some cases, instantaneous EC concentration at the work faces was as high as 900 $\mu g/m^3$ (Figure 4.1). Work face measurements results revealed that the concentrations of DPM were quite high during most of the monitoring period. The miners' direct exposure to such high concentrations can be dangerous to their health. The details of diesel equipment activities during DPM monitoring at the work faces are described in the following sections (4.5.1 to 4.5.3). To facilitate discussion, distinct DPM measurements at the work faces are identified as F1, F2, F3, F4, F5, F6, F7, F8, and F9. Each DPM measurement from F1 to F9 is an individual work face measurement performed at an active work face in one of several mines.

4.5.1. Cases Representing Mean EC below 150 $\mu g/m^3$. Figure 4.2 shows three representative plots of real-time EC concentrations for cases that have mean EC values (measured by the Airtec) below 150 $\mu g/m^3$.

Measurement F1: The monitoring occurred over a period of about three hours and forty minutes. During the measurement duration, a jumbo drill of 212 kW was involved in

drilling. Drilling operation continued for around three hours during the monitoring period. The maximum instantaneous EC concentration was noted to be about 130 µg/m^3 (Figure 4.2, plot F1), whereas the TWA concentration determined by the Airtec monitor was 87 µg/m^3. The TWA TC and EC values determined by the NIOSH 5040 method were 155 µg/m^3 and 83 µg/m^3, respectively.

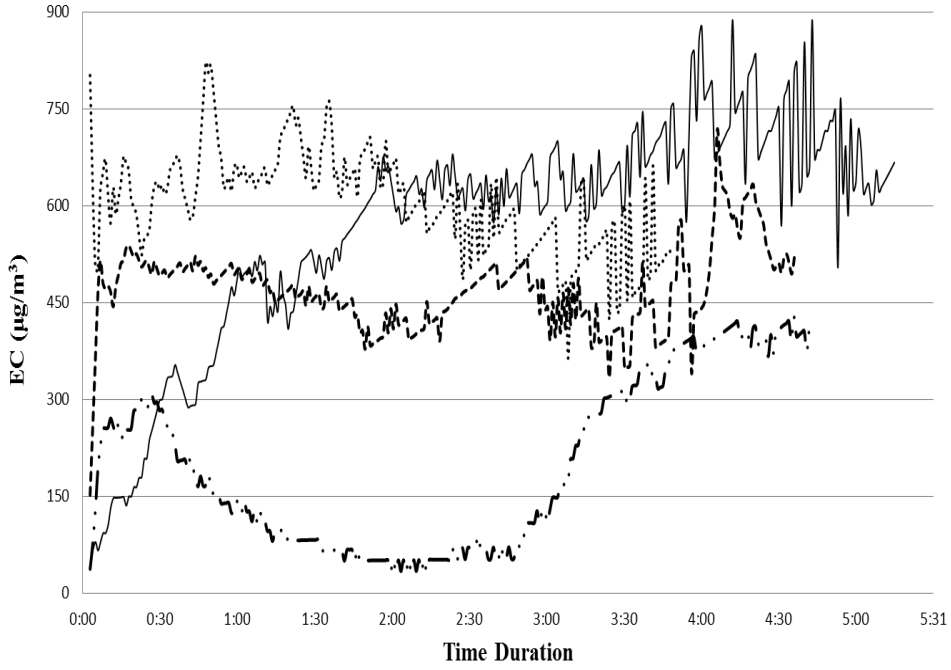

Figure 4.1 Real-time plots of EC concentrations at work faces

Measurement F2: The plot F2 in Figure 4.2 represents DPM concentrations generated by a jumbo drill that was used for face drilling. The jumbo drill utilizes a Caterpillar (CAT) diesel engine having 186 kW of power. Monitoring lasted for about an hour as the monitors were stopped when drilling operation was finished. The duration of measurement F2 was

relatively shorter than many other measurements since this measurement was performed in order to determine the level of DPM concentrations produced by a single jumbo drill in a particular work stope. During this particular measurement, the maximum instantaneous EC concentration observed by the Airtec was about 140 µg/m^3. The TWA TC and EC measured by the NIOSH 5040 method were 259-µg/m^3 and 95 µg/m^3, respectively, whereas the TWA EC concentration determined by the Airtec monitor was 127 µg/m^3.

Measurement F3: The monitoring period for plot F3 in Figure 4.2 was the shortest measurement duration performed during this study. A jumbo drill with 212 kW engine power was operating during measurement in the mine area under observation. Monitoring stopped when the drilling operation finished. During the monitoring period, instantaneous EC concentrations by the Airtec were observed to be above 150 µg/m^3 several times. The TWA TC and EC concentrations measured by the NIOSH 5040 method were 235 µg/m^3 and 137 µg/m^3, respectively, whereas the TWA EC measured by the Airtec monitor was 136 µg/m^3.

4.5.2. Cases Representing Mean EC from 150 µg/m^3 to 300 µg/m^3. Figure 4.3 shows three real-time EC concentrations plots for cases that have shown the mean EC concentrations between 150 µg/m^3 to 300 µg/m^3.

Measurement F4: DPM monitoring duration for measurement F4 lasted for about five hours. A 212 kW jumbo drill, a CAT Front-End Loader (FEL) having 280 kW, and two Volvo dump trucks (each above 355 kW) were involved in various mining activities during measurement. After about 30 minutes of monitoring, a fire drill exercise was performed at the mine site, which resulted in the shutdown of all mining activities and running equipment throughout the mine. It can be seen (Figure 4.3) from the real-time plot of

measurement F4 that the EC concentration started decreasing when fire drill exercise began (time duration at around 30 minutes). The fire drill exercise continued for over two hours. During a fire drill, all miners had to report to the underground mine workshop situated near the main mine shaft. The travelling distance from the work face under observation to underground workshop was around 7 km. After approximately two hours and forty minutes, the work at face resumed with a drill machine, a dump truck and one FEL. The work resumption quickly resulted an increase in DPM concentrations in the work area. This increase in DPM can be seen in Figure 4.3 plot F4. EC concentrations started increasing rapidly and reached above 300 $\mu g/m^3$ within an hour of work resumption. The NIOSH 5040 method TWA TC and EC concentrations for F4 were 197 $\mu g/m^3$ and 149 $\mu g/m^3$, respectively, whereas the Airtec measured the TWA EC concentration as 194-$\mu g/m^3$.

Measurement F5: This particular DPM concentration measurement (Figure 4.3, F5) at the face area lasted for about four hours. During the first two monitoring hours, only two work activities (face drilling and mucking) were being performed. A CAT FEL with 293 kW, three haul trucks (each above 298 kW) and one 186 kW jumbo drill were involved in mining operations. The measurement location at which DPM monitors were installed was not capable of capturing full DPM exhaust emitted by the FEL and haul trucks as the FEL was in constant movement (entering and exiting the measurement zone) during work. Drilling operation stopped after about two hours of monitoring. During the last measurement hour, a 186 kW roof bolter entered into the monitoring area and joined face work with the FEL and haul trucks. For measurement F5, the TWA values by the NIOSH 5040 method resulted in concentrations of TC and EC of 530 $\mu g/m^3$ and 351 $\mu g/m^3$, respectively. The TWA EC concentration measured by the Airtec was 250 $\mu g/m^3$.

Measurement F6: The monitoring period for measurement F6 lasted for about three and a half hours. Mucking activity was ongoing at the face area while DPM monitors were installed. A CAT FEL with 293 kW and three dump trucks each with power of above 298-kW were involved in the mucking operation. Consistent high levels of DPM were observed as the TWA TC and EC determined by the NIOSH 5040 method was 376 µg/m^3 and 330-µg/m^3, respectively, whereas the Airtec monitor resulted in the TWA EC concentration of 326 µg/m^3.

4.5.3. Cases Representing Mean EC above 300 µg/m^3. Figure 4.4 shows three representative real-time EC graphs from the face measurements that have mean EC Airtec values above 300 µg/m^3. Although all cases in Figure 4.4 represent overall high EC, distinct EC trends of increasing, decreasing, consistent, and random concentrations are observed for short and long periods of time.

Measurement F7: Monitoring F7 lasted for approximately six hours and thirty minutes. Mucking and face drilling were the primary mining operations being performed during the first two hours of the measurement period. Afterwards, a roof bolting accompanied the mucking and drilling operation. For mucking operation a CAT FEL of 280 kW and three Volvo dump trucks each with power of 355 kW were used. A jumbo drill of 212 kW was used for the face drilling operation. A roof bolter with 186 kW started its operation after a couple of monitoring hours. During monitoring, consistently high (over 350 µg/m^3) EC concentrations were seen (Figure 4.4, plot F7). The TWA EC value measured by the Airtec was 454 µg/m^3, whereas the NIOSH 5040 method resulted in TWA TC and EC concentrations of 564 µg/m^3 and 392 µg/m^3, respectively.

Measurement F8: The DPM measurement duration for F8 time series was approximately five and a half hours. Four activities were performed at the work face during monitoring. These activities included loading of explosive (charging) in the drill holes, mine roof rock bolting, mucking and face drilling. The explosive charger had a power of 93 kW, and the power of the roof bolter was 186 kW. For the mucking operation a CAT FEL was being used, which has a power of 280 kW along with two Volvo haul trucks each, 355 kW. The power of the jumbo drill was 212 kW. During first monitoring hour, only mucking was performed, whereas in the second monitoring hour, a jumbo drill started face drilling, which was followed by a roof bolter in the third monitoring. During the third to forth hour, mucking operation stopped and the charging was performed only in last thirty minutes of the monitoring period. Very high DPM concentrations were observed as a result of simultaneous multiple mining activities. The profile F8 indicates that the existing ventilation arrangements were not adequate for the amount of diesel equipment being used in the stope. This is evident by an increasing trend of real-time EC concentrations throughout the monitoring duration. The TWA EC value by the Airtec was 606 $\mu g/m^3$, whereas the TWA TC and EC measured by the NIOSH 5040 method were 872 $\mu g/m^3$ and 548 $\mu g/m^3$, respectively.

Measurement F9: The duration of monitoring for measurement F9 was around four hours. DPM concentrations at the face during F9 measurement were among the highest face concentrations observed during this study. Scaling, face drilling and mucking were performed in the area under observation during measurement. The drilling operation did not contribute to the DPM concentrations because the drill machine was electric and no DPM generation would be anticipated by its operation. Scaling continued during the first

half hour with a scaler of 129 kW, whereas a CAT FEL of 280 kW and four haul trucks each with power of above 298 kW were involved in the mucking operation. The mucking operation continued throughout the monitoring period. This particular work face location was situated near the mine's final exhaust shaft, which meant that the air entering the work stope for face ventilation was already contaminated by DPM exhausts from several other work faces. The average TWA NIOSH 5040 TC concentrations of air entering the work stope was around 100 µg/m^3. This average value (100 µg/m^3) was calculated by averaging several NIOSH 5040 TWA TC values measured for the air that ventilates the work stope of F9. The TWA TC and EC concentrations measured for F9 by the NIOSH 5040 method were 902 µg/m^3 and 723 µg/m^3, respectively, while the TWA EC by the Airtec monitor was found to be 625 µg/m^3.

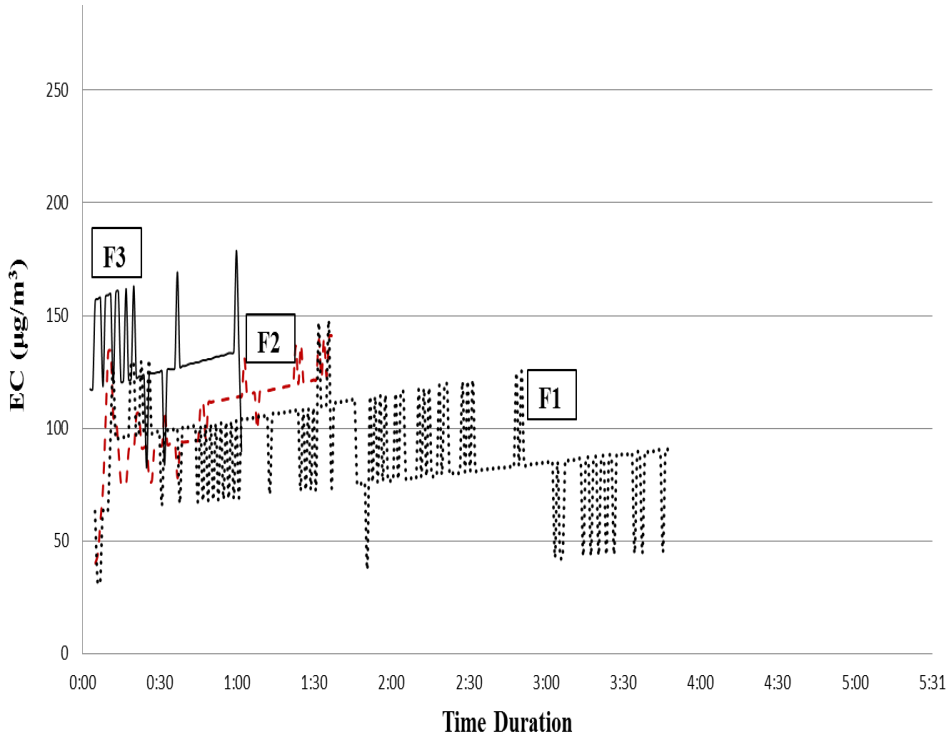

Figure 4.2 Real-time plots of EC at work faces when mean EC is below 150 µg/m^3

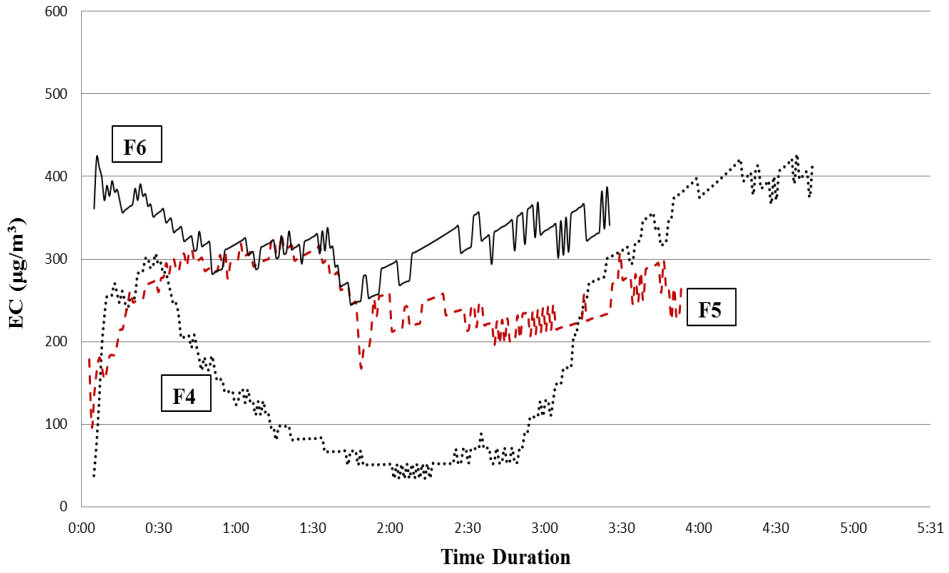

Figure 4.3 Real-time plots of EC at work faces when mean EC is from 150 to 300 µg/m^3

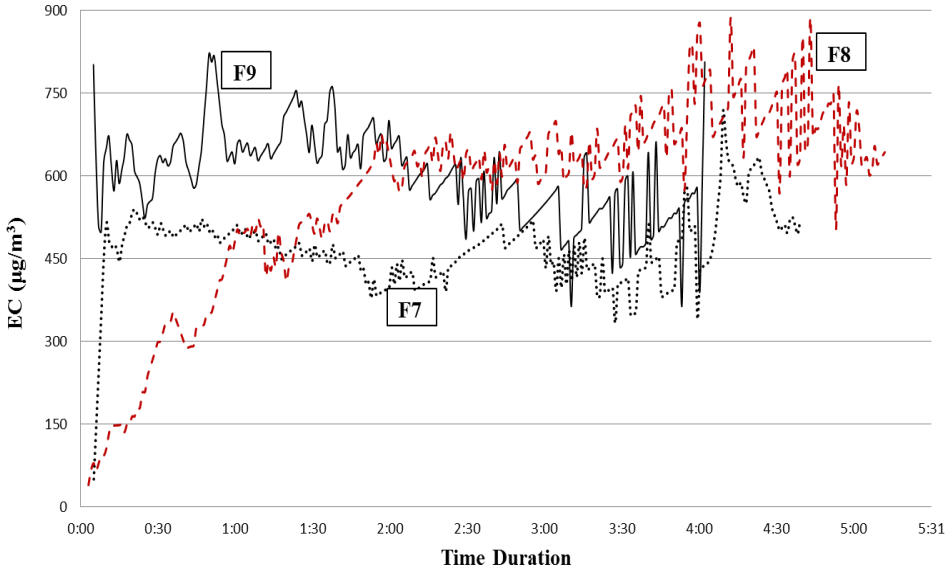

Figure 4.4 Real-time plots of EC at work faces when mean EC is above 300 µg/m^3

4.6. DPM MONITORING IN THE EXHAUST AIR DRIFTS

Real-time DPM measurements were also conducted in several different exhaust air drifts of the studied mines. All exhaust measurements locations in mines are situated in the near proximity (400 m to 700 m) of the work faces. DPM concentrations are captured in the near exhaust drifts in order to examine their levels as opposed to the work-face concentrations. In general, lower concentrations of DPM were observed in the exhaust air drifts as compared to the work-face concentrations. The locations where monitors were installed vary from 400 to 700 meters from the work face. Monitoring was conducted for different time durations and activities. Figure 4.5 shows a representative plot of real-time EC concentrations for exhaust air drift measurements. It can be seen from Figure 4.5 that in some cases, the instantaneous EC concentrations by the Airtec monitor were above 750 $\mu g/m^3$. As for the face measurements, in order to better understand the effect of different levels of diesel equipment activities on the DPM concentrations in the exhaust air drifts, the measurements are subdivided into three sections based on their mean EC values as determined by the Airtec monitor. The exhaust air drift measurements showed DPM concentrations generally less than the face measurement levels. A total of nine exhaust air drift measurements arbitrarily named as E1, E2, E3, E4, E5, E6, E7, E8 and E9 are presented in the following sections (4.6.1 to 4.6.3).

4.6.1. Cases representing mean EC below 150 $\mu g/m^3$. Measurements E1, E2 and E3 represent cases that have mean EC concentrations (by the Airtec monitor) below 150 $\mu g/m^3$. Figure 4.6 shows the real-time EC progression of these measurements with time.

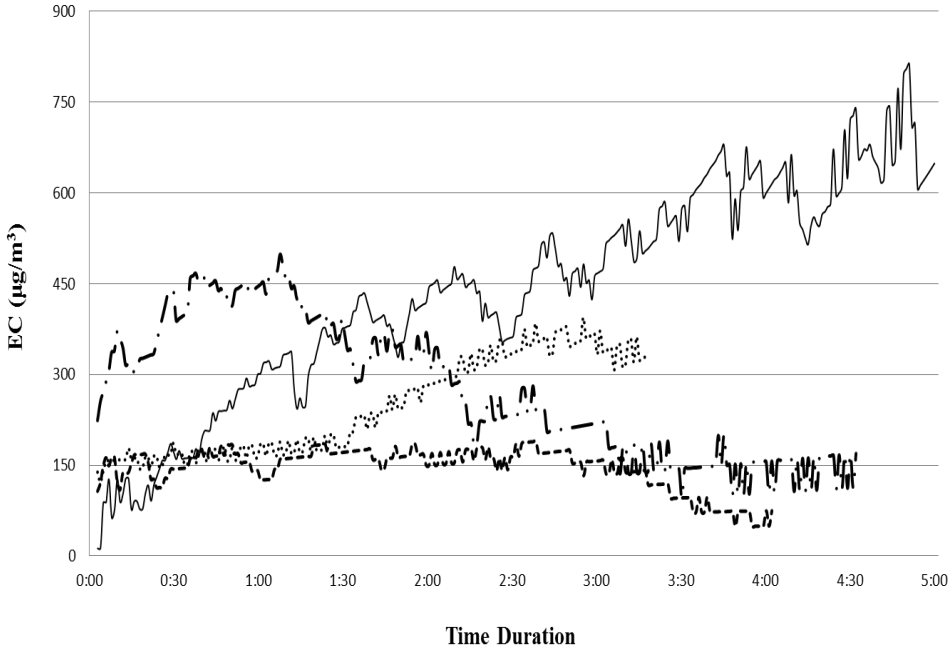

Figure 4.5 Real-time plots of EC concentrations in exhaust air drifts

Measurement E1: DPM measurement E1 lasted for three hours and forty minutes. During the monitoring period, a jumbo drill of 212 kW was operating at the work face. Drilling operation lasted for about three hours. The TWA TC and EC determined by the NIODH 5040 method were 125 µg/m^3 and 71 µg/m^3, respectively, whereas the TWA EC value determined by the Airtec monitor was 76 µg/m^3.

Measurement E2: Monitoring duration for measurement E2 lasted for about two hours and thirty minutes. Only one CAT FEL of 280 kW was working inside the monitoring zone. Apart from the FEL, no other significant diesel equipment activity was observed. The FEL was being used for removing and clearing the rock debris from the work face area in order to prepare the face for the drilling operation. The TWA TC and EC concentrations determined by the NIOSH 5040 method were 222 µg/m^3 and 141 µg/m^3, respectively. The Airtec monitor measured TWA EC as 143 µg/m^3.

Measurement E3: For measurement E3, no extensive work was observed at the work face or near exhaust air drift. Monitoring duration lasted for over four hours. A roof bolter of 73 kW was working during the first two and a half monitoring hours, whereas a fork lifter of 104 kW was at work between the first and the second hour of monitoring. Diesel equipment operation continued for about two and a half hours and then stopped. It can be observed in Figure 4.6 plot E3 that the real-time EC concentrations started decreasing when mining activity finished and reached as low as around 50 µg/m^3. For measurement E3, the TWA TC by the NIOSH 5040 method was 142 µg/m^3, whereas the TWA EC concentrations were 100 µg/m^3 and 138 µg/m^3 by the NIOSH 5040 and the Airtec monitors, respectively.

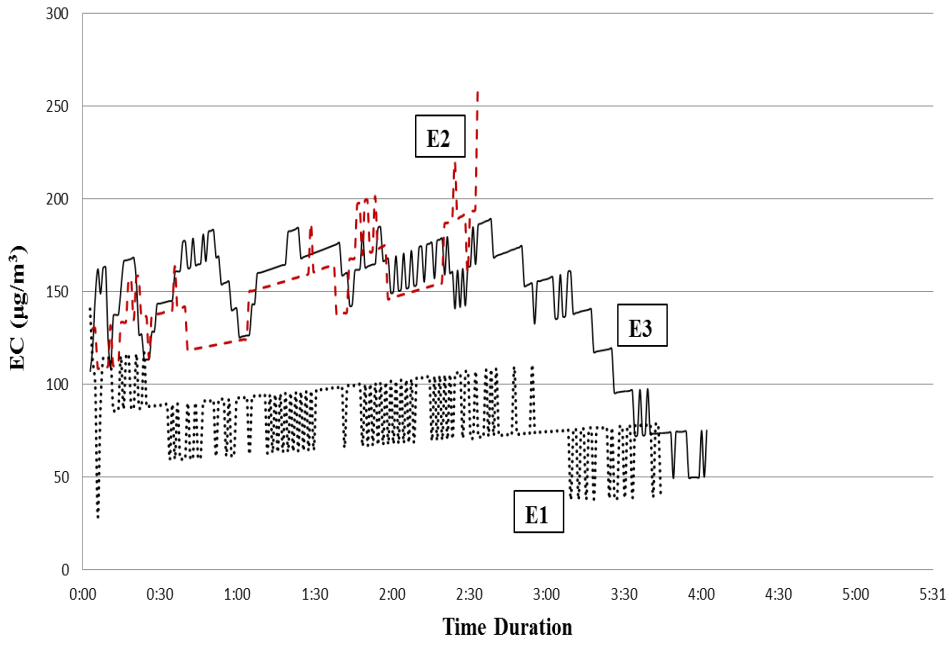

Figure 4.6 Real-time plots of EC in exhaust air drifts when mean EC is below 150 µg/m^3

4.6.2. Cases representing mean EC from 150 µg/m^3 to 300 µg/m^3. Figure 4.7 shows the exhaust air drift measurements cases (E4, E5 and E6) that have the mean EC concentrations (by the Airtec monitor) above 150 µg/m^3 but below 300 µg/m^3.

Measurement E4: The monitoring E4 (Figure 4.7) in the exhaust air drift was conducted for more than three hours. A CAT roof bolter was working at the face during the monitoring period. The power of roof bolter was 160 kW. No other significant diesel equipment activity was being performed in the area under observation except some occasional trips by mini man haul jeeps of around 19 kW. It seems that the DPM concentrations observed in this particular case E4 were higher than the usual expectation for the level of diesel equipment activities performed at the time of measurement. It is possible though that the high DPM concentration might be the result of some previously conducted activity in the mine or even a bad engine condition for a specific piece of diesel equipment used at the time of monitoring. However, the exact reason of significant higher DPM concentrations in measurement E4 is unknown. The TWA TC and EC measured by the NIOSH 5040 method were 278 µg/m^3 and 199 µg/m^3, respectively, whereas the Airtec monitor measured the EC concentration as 207 µg/m^3.

Measurement E5: Plot E5 in Figure 4.7 represents the exhaust air drift concentrations of the work face measurement represented by F5 in the previous section (4.5.2). Measurement continued for more than four hours. During the first two monitoring hours both face drilling and mucking were being performed. A CAT FEL with 293 kW, a 186 kW jumbo drill, and three haul trucks each above 298 kW were involved in different mining operations. Drilling operation stopped after about two monitoring hours. During the last measurement hour, a roof bolter of 186 kW power entered into the monitoring area and joined face activities

with FEL and haul trucks. The TWA measurement by the NIOSH 5040 method resulted in concentrations of TC and EC as 471 µg/m^3 and 323 µg/m^3, respectively. The TWA EC concentration measured by the Airtec was found to be 241-µg/m^3. For the same diesel equipment activities, the work face TC and EC concentrations by the NIOSH 5040 method were 530 µg/m^3 and 351 µg/m^3, respectively. The difference in TC and EC values between F5 and E5 represents the difference in DPM levels of work face and exhaust air drift for similar diesel activities. This also showed that the work faces usually have the highest overall DPM, and the concentrations of DPM are being diluted while moving out from the work face to the exhaust air drift.

Measurement E6: This particular measurement (E6) was performed in the exhaust air drift over a period when mucking occurred at the face area. Monitoring lasted for about four and a half hours. In the first two hours, a CAT FEL 280 kW and three haul trucks each with a power of 355 kW were involved in the mucking operation. Mucking stopped after about two hours, while FEL remained in operation even during the next hour and then departed from the monitoring area. Real-time EC concentrations up to 500 µg/m^3 were seen during monitoring. The E6 profile shown in Figure 4.7 indicates that high concentrations were seen when multiple pieces of diesel equipment were in operation. However, once the FEL left the monitoring area, the EC concentration started decreasing. The NIOSH 5040 TWA TC and EC concentrations for E6 were 313 µg/m^3 and 202 µg/m^3, respectively, whereas the TWA EC by the Airtec monitor was 265 µg/m^3.

4.6.3. Cases representing mean EC above 300 µg/m^3. Figure 4.8 shows the exhaust drift measurements cases E7, E8, and E9 which have mean EC concentrations (by the Airtec monitor) above 300 µg/m^3.

Measurement E7: Monitoring duration for E7 lasted for approximately five and a half hours. Mining activities including mucking, face drilling, explosive charging, and roof bolting were performed during measurement. This particular measurement (E7) was conducted in the exhaust air drift at the same day and time when measurement F8 was performed at the work face. In fact, plot E7 in Figure 4.8 represents the concentrations of DPM in the exhaust air drift for the face measurement F8 described in the previous section (4.5.3). A CAT FEL 280 kW, and two Volvo haul trucks each with a power of 355 kW were involved in the mucking activity. Face drilling started in the second monitoring hour by a 212 kW jumbo drill and continued until the end of the measurement. A roof bolter of 186-kW power started operation in the third monitoring hour, whereas the explosive charger, which has a power of 93 kW, worked during the last thirty minutes of monitoring period. The mucking operation was suspended from the third to forth hours, and resumed afterwards. It was observed that multiple diesel equipment operations at the work face resulted in very high DPM concentrations in the exhaust air drift. The increasing trend of real-time EC concentrations in plot F7 of Figure 4.8 showed that the ventilation arrangements were not adequate for the diesel equipment used in the work stope. For measurement E7, the TWA EC concentration by the Airtec was 441 $\mu g/m^3$, whereas the TWA TC and EC values determined by the NIOSH 5040 method were 607 $\mu g/m^3$ and 417 $\mu g/m^3$, respectively. It was noted the TWA TC and EC concentrations by the NIOSH 5040 method for measurement E7 are less than the respective values of measurement F8. This behavior is similar to what we have observed in the case of measurements F5 and E5. This showed that work faces contain the highest concentrations of DPM.

Measurement E8: A number of activities continued at the face area while the measurements were being performed at a location in the exhaust air drift. The measurement location in the exhaust air drift was approximately 400 meters away from the face area. Monitoring lasted for about four and a half hours while face activities including mucking, face drilling, and roof drilling continued. A CAT FEL 280 kW, and three haul trucks each with power of above 298 kW were involved in mucking, whereas a 186- kW jumbo drill was used for face drilling. Another jumbo drill 146 kW was used for roof drilling. Similar to plot E7, since multiple activities continued at the work face during the monitoring period, increasing trends of real-time EC concentrations were observed in plot E8, as shown in Figure 4.7. The TWA TC and EC values by the NIOSH 5040 method were 808 µg/m^3 and 539 µg/m^3, respectively, whereas the Airtec monitor measured TWA EC as 396 µg/m^3.

Measurement E9: The total measurement duration for E9 was around three and one half hours. Monitoring was conducted in the exhaust air drift while drilling and mucking continued at the work face. A jumbo drill of 186 kW was used for drilling, whereas a CAT FEL 280 kW, and three haul trucks (each above 298 kW) were involved in the mucking operation. After an hour and a half, drilling stopped, whereas mucking lasted through the duration of monitoring. Real-time EC concentrations of as much as 600 µg/m^3 were observed by the Airtec monitor. After the drilling operation was finished, a decrease in real-time EC concentrations was observed (Figure 4.8, plot E9). The respective TWA concentrations of TC and EC by the NIOSH 5040 method were found to be 700 µg/m^3 and 530 µg/m^3, whereas the Airtec monitor measured TWA EC as 477 µg/m^3.

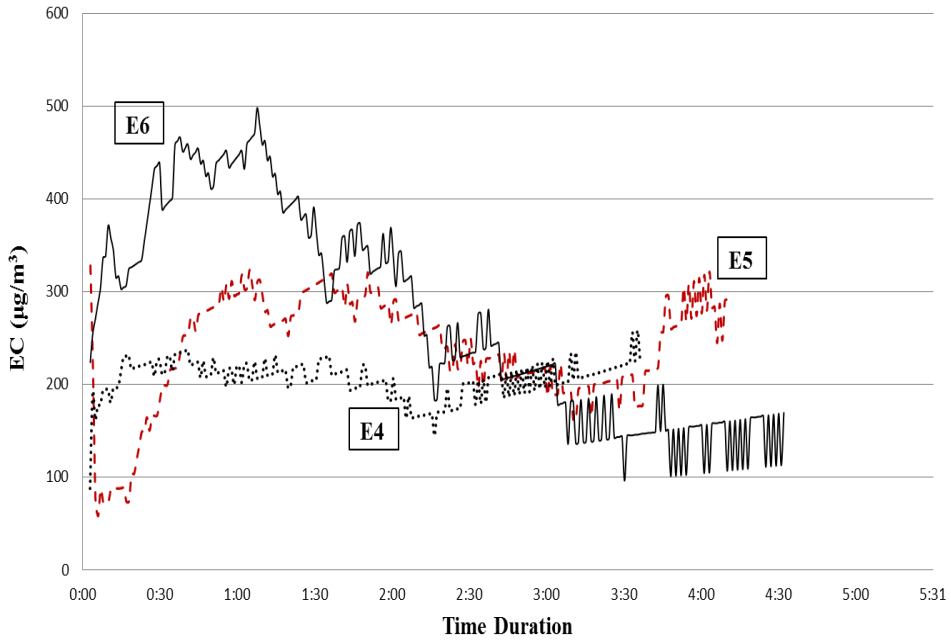

Figure 4.7 Real-time plots of EC in exhaust air drifts when mean EC is from 150 to 300-µg/m^3

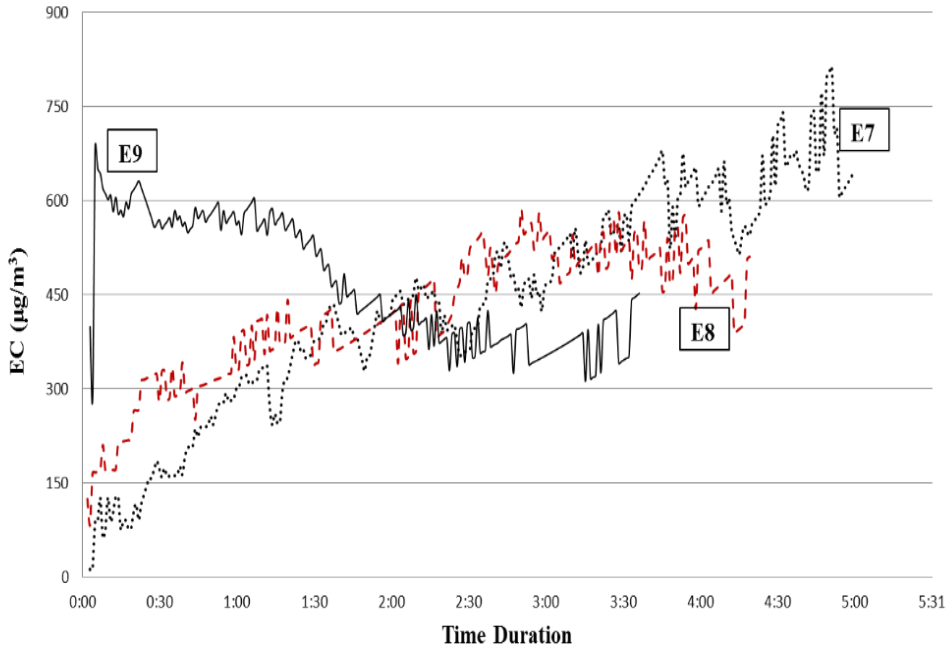

Figure 4.8 Real-time plots of EC in exhaust air drifts when mean EC is above 300 µg/m^3

4.7. SUMMARY

This section presents a series of real-time DPM area monitoring at the work faces and in the exhaust air drifts situated near the work faces. Several measurements were performed at active mines sites in the United States, which employ both heavy- and light-duty diesel-powered equipment and use diesel equipment as a primary source to conduct all major mining operations. All of the studied mines use high-percent biodiesel as a primary fuel type for all diesel equipment.

Based on mean EC concentrations measured by the Airtec monitor, the DPM measurement results from work faces and from the exhaust air drifts were subdivided in to three levels: low, intermediate, and high. This subdivision was performed in order to compare distinct DPM measurements with similar DPM levels and present numerous mining situations that can happen at various locations in any underground mine. This subdivision also helps to highlight various mining scenarios and investigate the relationship between the use of diesel equipment, its resulting DPM emissions, and their effect on DPM levels in a typical mine work stope. The DPM time variations do not follow any rigid patterns. In underground mine stopes, all kinds of DPM profiles have been observed, including decreasing, increasing, essentially constant, and random. In an active mine site, hundreds of variables participate to determine the precise levels of DPM concentration. Although there is no fixed behavior of DPM concentrations in mine stopes, certain generalities about the levels of DPM concentrations with respect to the mine locations and the use of diesel equipment can be identified. DPM levels observed at the mine work faces indicate that high DPM concentrations can occur near the work faces for most of the work shift. Face measurements F1, F2, and F3 showed low levels of DPM

concentrations only because they do not represent an active work face. In measurements F1, F2, and F3, low DPM values resulted because only one piece of diesel equipment was used and the measurements were conducted for short durations. Similar to face measurements, high DPM levels are observed in the near-face exhaust drifts. However, the overall levels of DPM concentrations were found to be generally lower in exhaust air drifts than at work faces. As might be expected, the levels of DPM concentrations were lower in exhaust drifts as compared to the work face, even on the same days. Not surprisingly, multiple pieces of diesel equipment resulted in higher levels of DPM levels both at the work faces and in exhaust air drifts. Consistently increasing trends of DPM levels resulted when the ventilation arrangements were not adequate. Lastly, real-time monitoring is significant because it can help us to analyze, understand, and interpret the mine air environment and allow us to improve the mine air quality.

5. DPM EXPOSURE FREQUECIES IN UNDERGROUND MINES

5.1. OVERVIEW

After observing several cases/scenarios of real-time DPM monitoring and considering the presence of high DPM concentrations at work faces and in exhaust air drifts (Section 4), the next logical step was to evaluate the Frequency Distributions (FD) of DPM concentrations at the mines' work faces and in exhaust air drifts. Identification of DPM concentration frequency distributions at working zones in underground mines is significant, since this can allow estimation of the likelihood of DPM levels faced by miners at certain mine locations. This section presents DPM frequency distribution models that can be used to estimate the miners' probable DPM exposures during their stay at and or near working zones in underground mines.

The importance and need to determine short-term exposure limit (STEL) for DPM while determining DPM PEL for compliance purposes is described in this section. Considering the severe hazardous health effects linked to the miners' exposure to diesel exhaust and the availability of real-time monitoring devices, the potential value of STEL is proposed in this section. Although no real-time DPM monitor has been identified as a standard, several studies have reported satisfactory measurement results utilizing commercially available real-time DPM monitors. Any real-time DPM monitor that satisfactory determine DPM concentrations can be used for DPM STEL measurements until a real-time standard method is approved. This section also discusses the importance of measuring instantaneous DPM and the significance of DPM area sampling technique.

5.2. MINE AREA DPM EXPOSURE FREQUENCY DISTRIBUTIONS

The real-time DPM monitoring data attained during this study by the Airtec monitors was analyzed with respect to the measurements' locations (work faces and exhaust air drifts). Thousands of mine-area DPM exposure samples were recorded for numerous work faces and exhaust air drift measurements. Mine-area DPM exposure frequencies were analyzed by using the Wolfram Mathematica 10.4 software package. Exposure frequency values represent the total number of recordings for which DPM concentrations have reached that specific concentration ($\mu g/m^3$ of EC) value. Thus, exposure frequencies are the frequencies of EC measurements for a certain EC concentration value in $\mu g/m^3$. The term exposure frequency should not be mixed with the miners' exposure to DPM or PEL, since exposure frequency represents the DPM exposures of certain mines areas under consideration. The following sections presents DPM exposure frequency distributions for mines' work faces (Section 5.2.1) and for exhaust air drift measurements (Section 5.2.2).

5.2.1. DPM Frequency Distribution for Work Face Measurements. DPM measurements at the work faces were analyzed for each individual measurement day by employing Wolfram Mathematica 10.4. The exposure frequency distribution plots were generated for all work face measurements. Figure 5.1, 5.2, 5.3, and 5.4 show few representative frequency distribution plots of DPM measurements conducted at various work faces along with fitted distribution patterns. Each plot represents an individual measurement location. All generated plots were analyzed to determine the best fit statistical distribution by using Wolfram Mathematica 10.4. The frequency distributions of DPM concentrations at the work faces did not generally follow a normal distribution. In fact, no

statistical distribution was able to completely represent all face measurements cases. However, over half of the face measurements cases appreciably followed the lognormal distribution. A Weibull distribution pattern also provided a reasonable representation of some work face measurements. The lognormal and Weibull distributions had the most difficulty in capturing cases that had overall low EC concentrations with narrow EC range. Statistical parameters including mean, median, standard deviation, skewness, and kurtosis were individually determined for all measurements. Table 5.1 provides the values of statistical parameters for work face measurements. Table 5.1 shows that the mean EC concentrations varies from 90 $\mu g/m^3$ to 764 $\mu g/m^3$, whereas the observed values of median were as low as 88 $\mu g/m^3$ and as high as 684 $\mu g/m^3$. The value of standard deviation changes from 18 $\mu g/m^3$ to 206 $\mu g/m^3$, whereas both positive and negative skewness was observed (Table 5.1). The variations in the values of mean, median, and standard deviation showed that all work face measurements covered a broad range of different activities under various mining situations. These mining conditions are typically encountered in most of the underground mines; thus, the findings of this research could be applicable to similar mining conditions.

5.2.2. DPM Frequency Distribution for Exhaust Air Drift Measurements. Similar to work faces measurements, DPM results obtained from all exhaust air drift measurements were analyzed for individual measurement. The DPM area exposure frequency distribution plots were generated for all exhaust drift measurements. Figure 5.5, 5.6, 5.7, and 5.8 show representative frequency distribution plots along with fitted distribution patterns for exhaust air drift measurements. Each plot represents an individual measurement. Wolfram Mathematica 10.4 was used to determine the best fitted statistical

distribution patterns for individual plots. Similar to work face measurements, the frequency distributions of DPM concentrations in the exhaust air drifts were not normally distributed. Like face measurement results, no single statistical distribution was capable of unanimously representing all exhaust drift measurements. Most exhaust measurements were convincingly represented by lognormal and Weibull distribution patterns. Measurements cases which had overall low EC concentrations with narrow range, were not efficiently presented by any of the statistical distribution. Statistical parameters such as mean, median, standard deviation, skewness, and kurtosis were individually determined for all exhaust air drift measurements. Table 5.2 provides the values of statistical parameters for all exhaust air drift measurements. The mean EC concentrations varies from 80 µg/m^3 to 469 µg/m^3, whereas the values of median ranges from 70 µg/m^3 to 460 µg/m^3. Both mean and median values for exhaust air drift measurements were lower than the respective values of work face measurements. The standard deviation values changes from 16 µg/m^3 to 290 µg/m^3, whereas both positive and negative skewness was observed (Table 5.2). The variation in the values of mean, median, and standard deviation was due to different work arrangements, showing that the measurements cover a wide range of mining activities. Similar mining conditions are typically encountered in most of the underground mines, and thus the findings could be applicable to other identical mines.

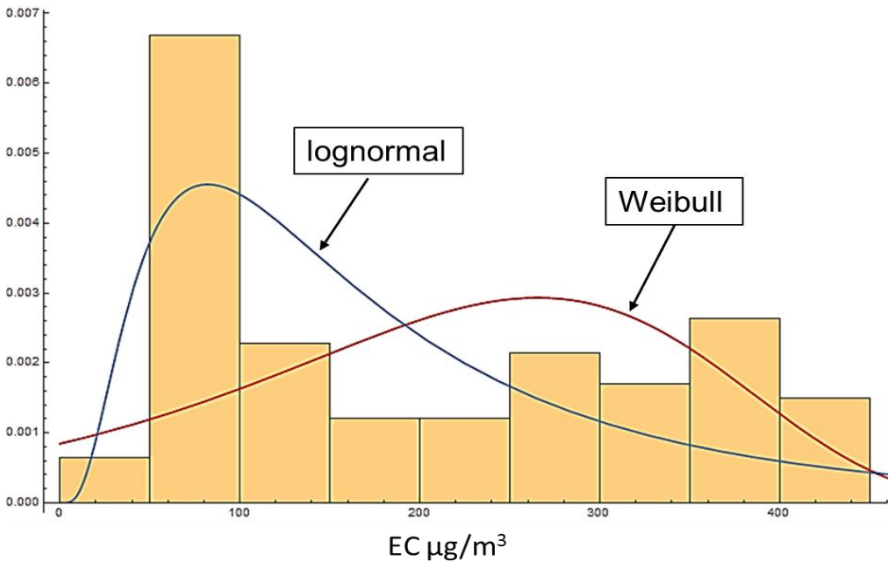

Figure 5.1 Frequency distribution plot of work face measurement A with lognormal and Weibull distribution fit

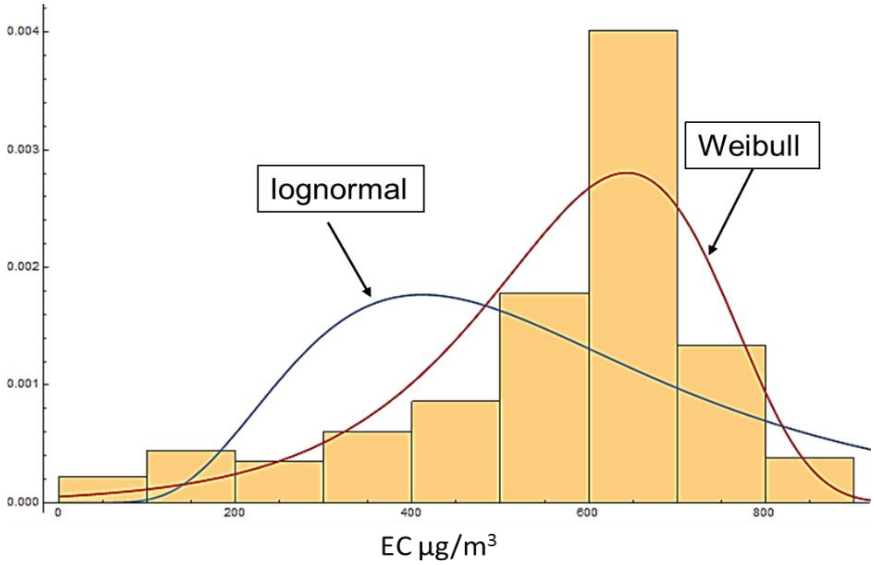

Figure 5.2 Frequency distribution plot of work face measurement B with lognormal and Weibull distribution fit

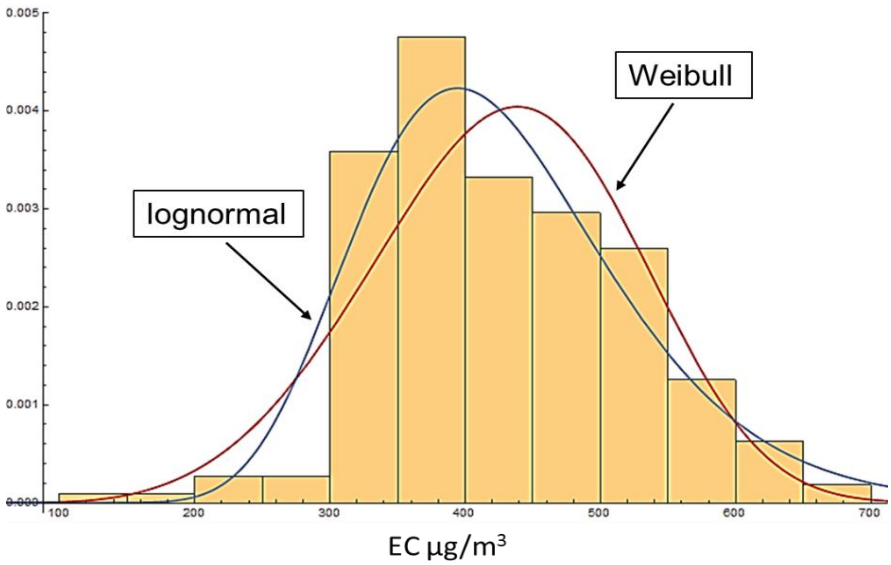

Figure 5.3 Frequency distribution plot of work face measurement C with lognormal and Weibull distribution fit

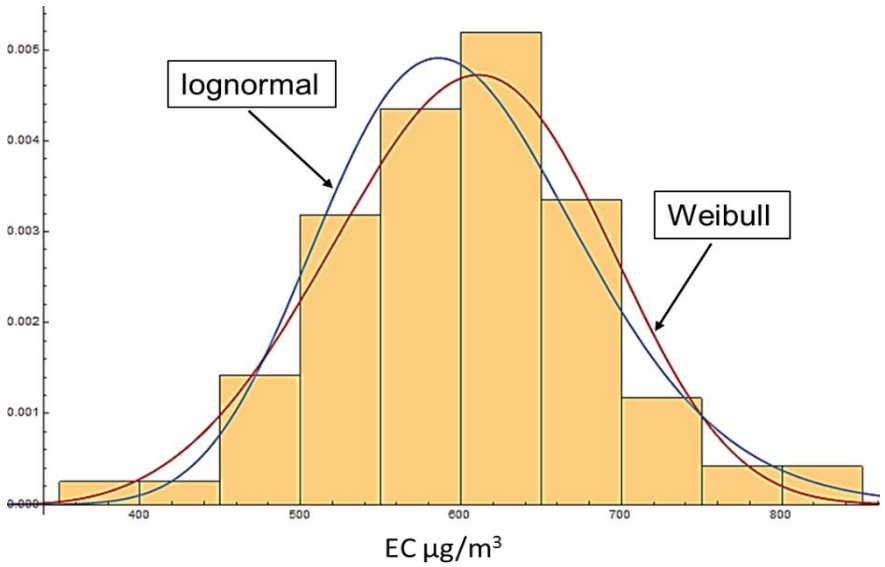

Figure 5.4 Frequency distribution plot of work face measurement D with lognormal and Weibull distribution fit

Table 5.1 Statistical parameters for all work face measurements

	Mean	**Median**	**Standard Deviation**	**Skewness**	**Kurtosis**
	$\mu g/m^3$	$\mu g/m^3$	$\mu g/m^3$		
1	479.921	495.604	65.2467	-0.692482	3.32859
2	468.521	471.936	67.9293	-0.794264	9.90799
3	299.597	303.78	65.0187	-0.18022	2.16332
4	199.515	166.958	131.81	0.325599	1.57233
5	175.249	168.538	69.154	0.637673	2.30179
6	567.386	619.413	175.761	-1.11635	3.80971
7	106.163	112.075	19.4852	-0.80232	4.19285
8	241.5	231.941	82.9738	0.15935	1.56948
9	253.749	251.735	40.6091	-0.423516	3.00682
10	426.951	412.214	92.5945	0.16565	3.09332
11	131.768	128.674	18.3487	0.127665	4.18685
12	334.396	297.44	155.975	1.4471	6.14143
13	332.113	335.639	33.7258	-4.63292	35.3818
14	178.354	163.254	73.9584	2.43802	8.44901
15	90.2297	88.346	20.4027	-0.33895	3.57331
16	173.965	173.581	22.123	-0.0371538	3.5051
17	602.677	609.147	80.5948	-0.0310487	3.3565
18	764.425	684.332	206.586	0.232791	1.85804
19	324.766	324.144	33.618	-0.0589265	3.13981

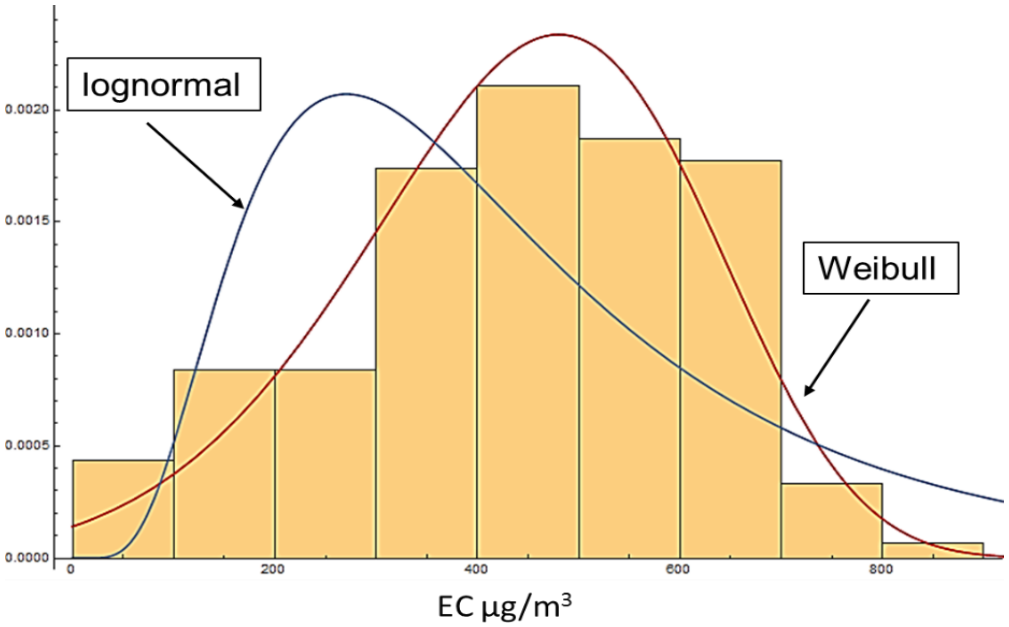

Figure 5.5 Frequency distribution plot of exhaust air drift measurement E with lognormal and Weibull distribution fit

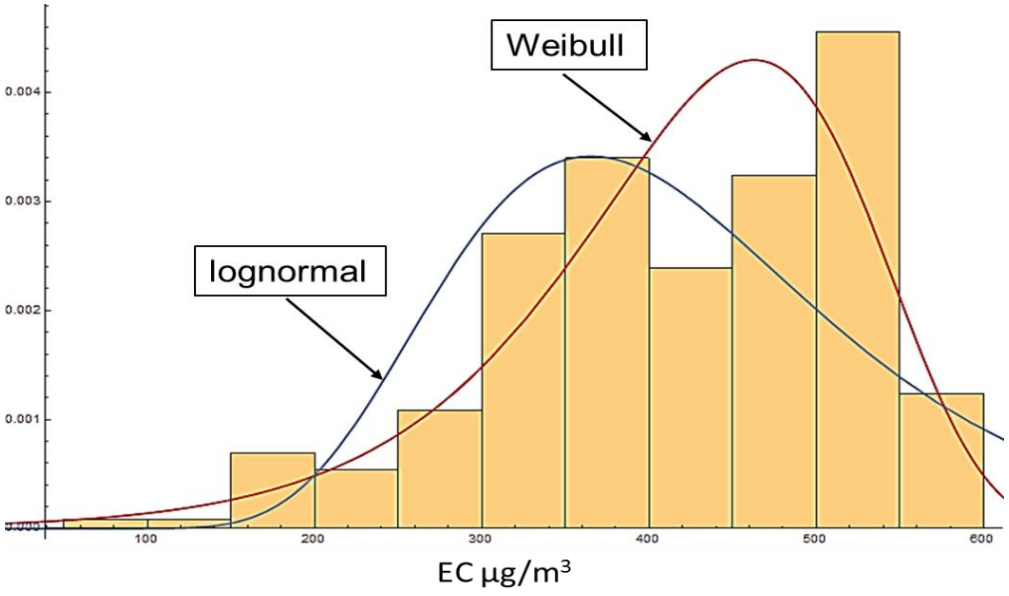

Figure 5.6 Frequency distribution plot of exhaust air drift measurement F with lognormal and Weibull distribution fit

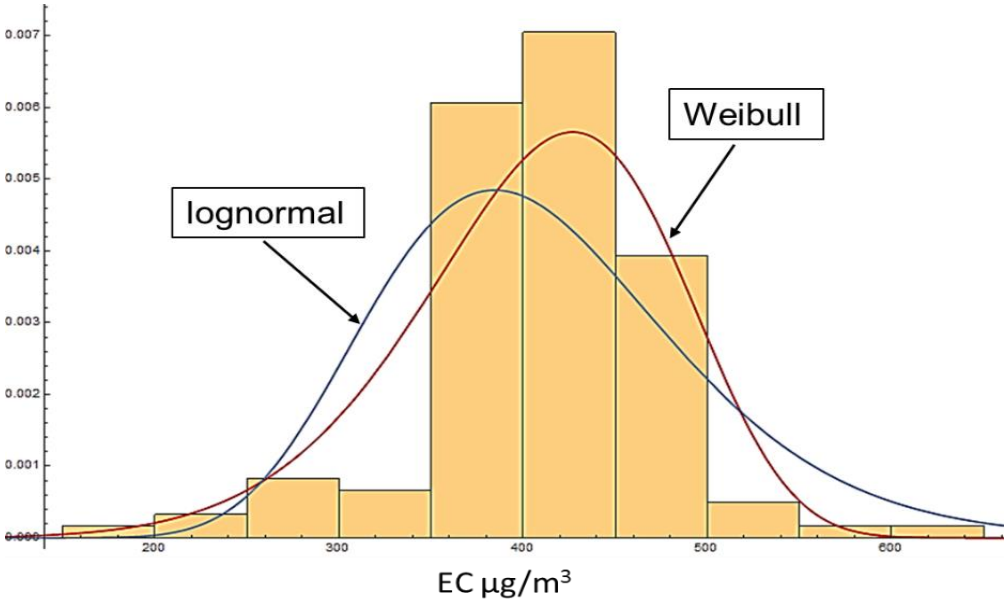

Figure 5.7 Frequency distribution plot of exhaust air drift measurement G with lognormal and Weibull distribution fit

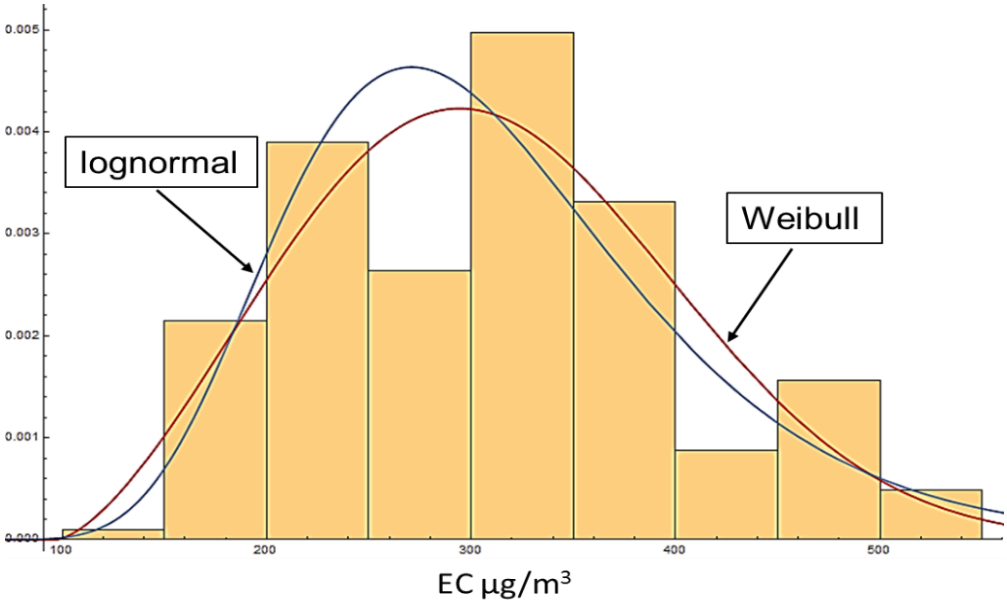

Figure 5.8 Frequency distribution plot of exhaust air drift measurement H with lognormal and Weibull distribution fit

Table 5.2 Statistical parameters for all exhaust air drift measurements

	Mean	**Median**	**Standard Deviation**	**Skewness**	**Kurtosis**
	$\mu g/m^3$	$\mu g/m^3$	$\mu g/m^3$		
1	392.567	277.196	290.504	1.67769	5.40337
2	438.328	450.667	175.706	-0.351971	2.41657
3	102.773	95.2385	16.8439	1.03366	3.26566
4	246.718	233.426	80.371	0.233831	1.44179
5	238.738	253.725	60.5666	-0.975537	3.64108
6	417.168	418.439	104.995	-0.621488	2.88367
7	409.078	413.607	68.5894	-0.904783	7.17824
8	280.586	282.615	26.5749	-0.80117	4.37396
9	464.336	460.971	57.5236	-0.0091439	2.38136
10	469.836	441.783	96.9933	0.149947	1.57512
11	273.155	253.227	112.659	0.221805	1.72411
12	144.749	157.269	34.7749	-1.18795	3.496
13	193.376	184.327	50.9777	0.594459	3.80161
14	80.3418	70.507	51.1768	1.68101	7.09698
15	310.491	314.651	91.0766	0.33929	2.54187
16	152.128	150.849	32.5506	2.90344	19.5767
17	82.7272	78.356	18.9486	-0.306183	3.10051
18	205.569	209.484	20.484	-1.26803	7.39852

5.3. MINERS' EXPOSURE ASSESSMENTS BY USING DPM FD MODELS

After analyzing the individual measurements for work faces and exhaust air drift measurements, DPM concentrations results for similar types of measurement locations were combined. DPM concentration results from all face measurements were combined, whereas all results from exhaust air drift measurements were pooled together. The pooling of results was conducted to reflect overall DPM concentrations at the work faces and in exhaust air drifts throughout the study period. Since both types of measurement locations (work faces and exhaust air drifts) represent numerous mining scenarios, the DPM concentration distributions achieved after pooling individual measurements can be considered as representative of DPM concentrations generally found at these locations in underground mines. The following section (5.3.1) describes the results and the distribution patterns of combined work faces measurements, whereas the Section 5.3.2 covers the distribution patterns of combined exhaust air drift measurements. Although both types of measurement locations (work faces and exhaust air drifts) have distinct mean and standard deviation values, both are positively skewed and seem to closely follow the lognormal and Weibull distributions (discussed in Section 5.3.1 and 5.3.2). Since the measurement places in exhaust air drifts were found near (400 m to 700 m) the work faces, both types of measurement locations can be represented either by lognormal or Weibull distribution. Thus, all measurements (from work faces and exhaust drifts) were finally combined to achieve a larger set of readings for detailed analyses. The results obtained after combining all data are discussed in Section 5.3.3.

5.3.1. Models Assessing DPM at the Work Faces. The distribution patterns of DPM concentrations obtained by measurements at work faces are shown in Figure 5.9 and

Figure 5.10. It is evident from Figure 5.9 and Figure 5.10 that the DPM face concentration results are not normally distributed; rather, they follow either a lognormal or a Weibull distribution pattern. Considering the shapes of fitted curves for both types of distributions (Figure 5.9 and Figure 5.10), Weibull distribution seems a better fit for DPM concentrations at work faces, although it yields slight conservative concentration values of mean and median. Statistical parameters for both lognormal and Weibull distributions for data from work face measurements were computed using Wolfram Mathematica 10.4. Table 5.3 shows the distribution parameters, and Table 5.4 shows the percentiles obtained by lognormal and Weibull distributions for work face measurements.

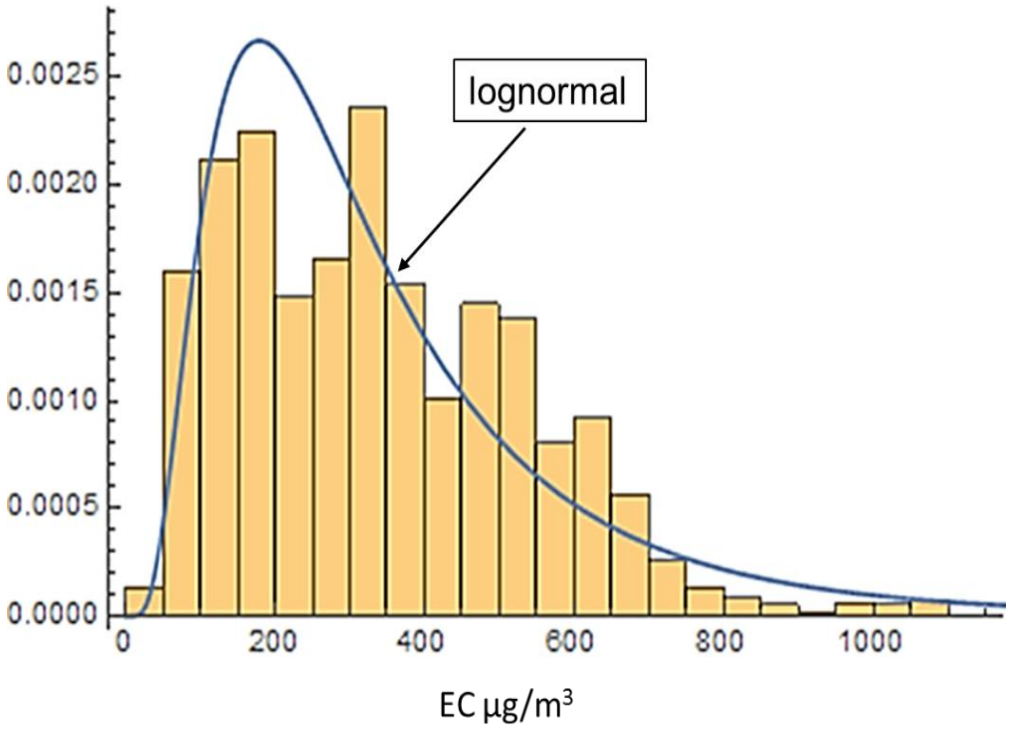

Figure 5.9 Frequency distribution of DPM concentrations during all work face measurements with lognormal distribution fit

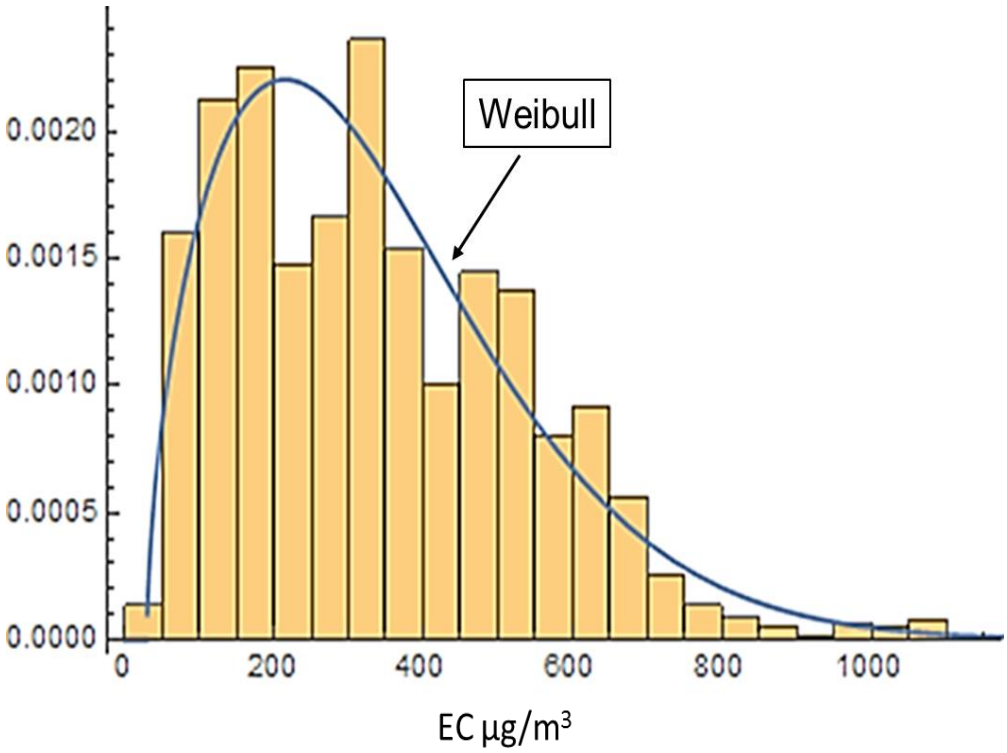

Figure 5.10 Frequency distribution of DPM concentrations during all work face measurements with Weibull distribution fit

5.3.2. Models Assessing DPM in Exhaust Air Drifts. The distribution patterns of DPM concentrations obtained by measurements in exhaust air drifts are shown in Figure 5.11 and Figure 5.12. Similar to all work face measurement results, DPM concentrations in all exhaust air drifts are not normally distributed; rather, they seem to follow either a lognormal or a Weibull distribution pattern. Statistical parameters for both lognormal and Weibull distributions for work face data were computed by Wolfram Mathematica 10.4. Table 5.3 shows the statistical parameters of both fitted distributions. Contrary to the work face measurements where Weibull distribution was a better fit, lognormal distributions seems a better fit for exhaust air drift measurements. Table 5.4 shows the percentiles obtained by lognormal and Weibull distributions for combined exhaust drift measurements.

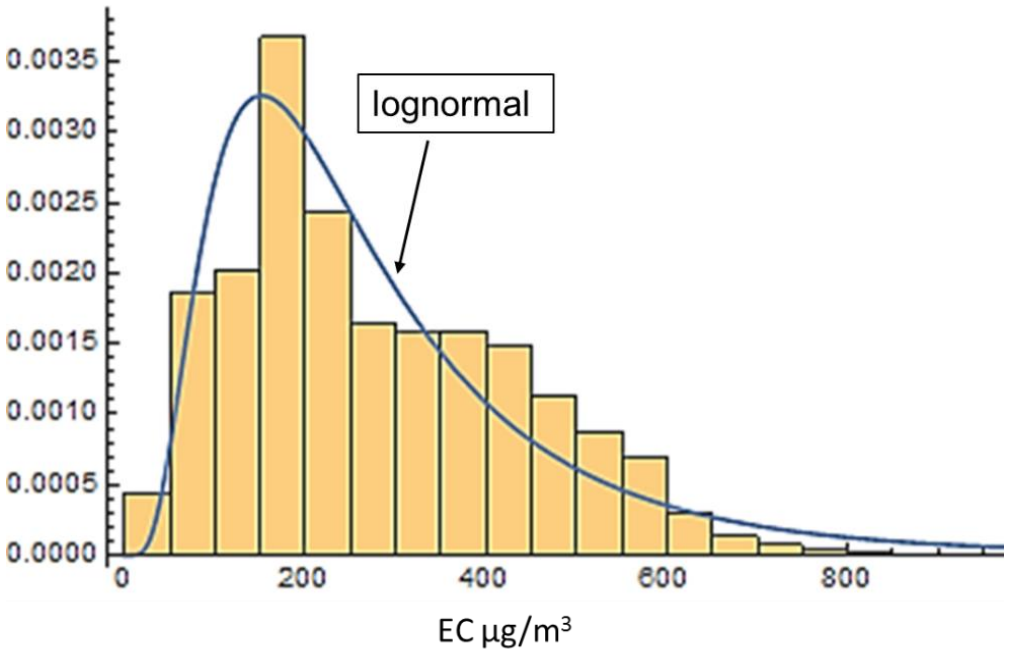

Figure 5.11 Frequency distribution of DPM concentrations during all exhaust drift measurements with lognormal distribution fit

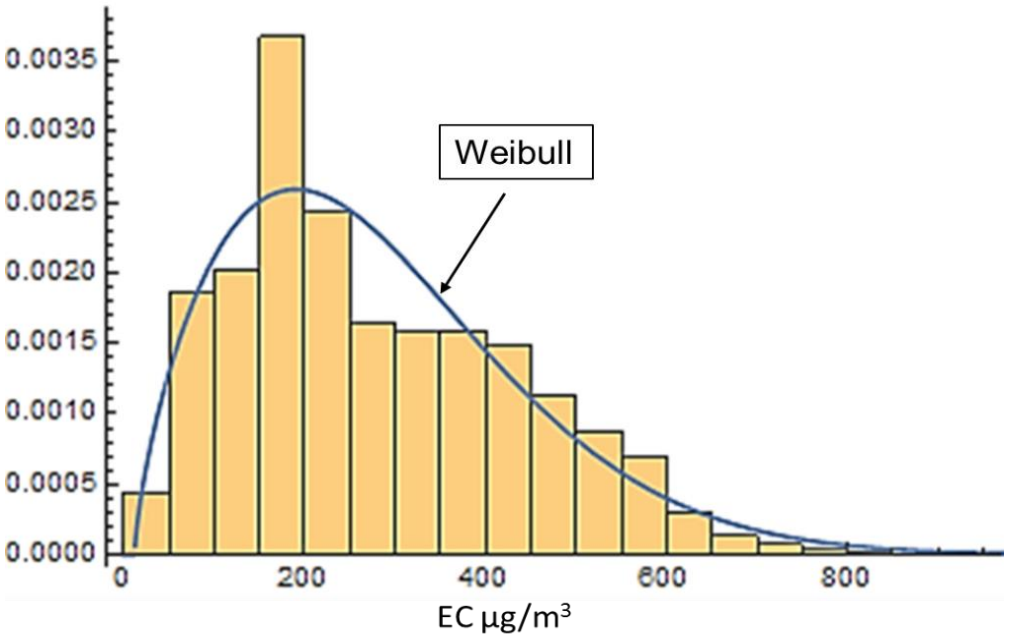

Figure 5.12 Frequency distribution of DPM concentrations during all exhaust drift measurements with Weibull distribution fit

5.3.3. Models Assessing DPM at Work Faces and Exhaust Air Drifts. Finally, all measurement data from work faces and exhaust drifts was combined and frequency distribution plots were created. Figures 5.13 and Figure 5.14 show the lognormal and Weibull distributions fitted to the combined data set. The combined data was best represented by a lognormal distribution since Weibull distribution missed the peak of distribution, as shown in Figure 5.14. The mean, median, and other statistical parameters of both types of distributions and their combination are described in Table 5.3. Table 5.4 provides percentiles for both lognormal and Weibull distributions along with their combined results.

Table 5.3 Statistical parameters of collective work faces, and exhaust air drift measurements along with their combined results

	Work Faces		**Exhaust Air Drifts**		**All Data**	
	Lognormal	**Weibull**	**Lognormal**	**Weibull**	**Lognormal**	**Weibull**
Normal Mean (μ)	5.6328	-	5.44693	-	5.4318	-
Normal SD (σ)	0.668486	-	0.652158	-	0.66716	-
Shape (α)	-	1.59103	-	1.69624	-	1.68357
Scale (β)	-	344.868	-	301.121	-	335.163
Location (μ)	-	29.9138	-	12.0843	-	12.3404
Mean	349.40	339.27	287.03	280.79	319.17	311.59
Median	279.44	303.82	232.045	254.69	255.48	281.93
SD	262.36	198.98	208.973	163.02	238.98	182.76
Skewness	2.674	0.9712	2.570	0.8684	2.666	0.8801

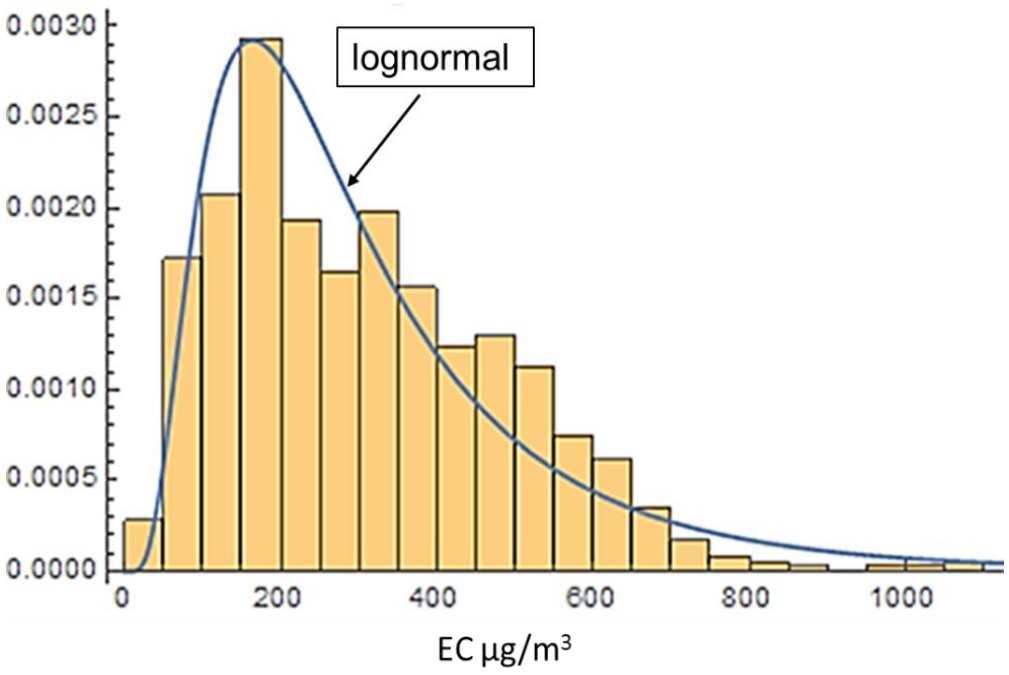

Figure 5.13 Frequency distribution of DPM concentrations for combined (work faces and exhaust air drifts) measurements with lognormal distribution fit

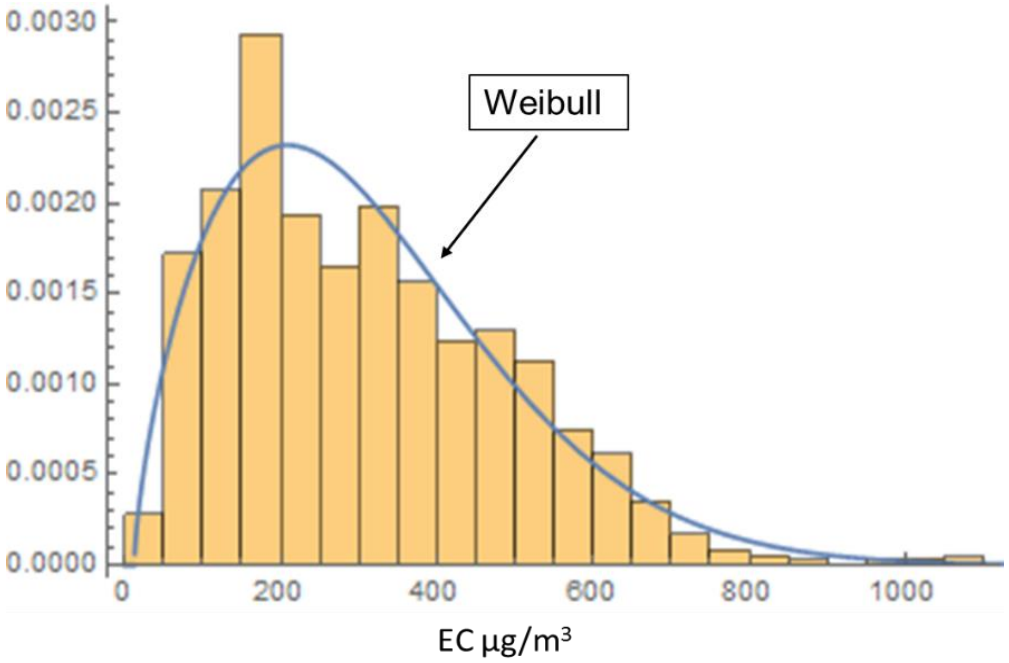

Figure 5.14 Frequency distribution of DPM concentrations for combined (work faces and exhaust air drifts) measurements with Weibull distribution fit

Table 5.4 Percentiles of collective work faces, and exhaust air drift measurements along with their combined results

	Work Faces		Exhaust Air Drifts		All Data	
Percentile	**Lognormal**	**Weibull**	**Lognormal**	**Weibull**	**Lognormal**	**Weibull**
1st	59.00	49.05	50.89	32.08	54.11	34.14
5th	93.05	83.23	79.37	64.35	85.26	69.76
10th	118.64	113.74	100.60	91.98	108.65	100.39
25th	178.02	187.51	149.46	156.54	162.90	172.24
50th	279.44	303.82	232.04	254.69	255.48	281.93
75th	438.64	453.37	360.25	377.14	400.68	419.26
90th	658.19	612.42	535.23	504.44	600.75	562.29
95th	839.12	717.21	678.33	587.07	765.52	655.45

5.4. NOTION TO MEASURE AND IMPLEMENT STEL DURING DPM PEL

The concept of measuring STEL is not new to the mining industry, as ACGIH, NIOSH, and MSHA have prescribed permissible exposure limits in terms of STEL and TWA for miners' exposure to underground mine gases including CO_2, CO, and many other mine contaminants. The American Conference of Governmental Industrial Hygienists (ACGIH) defines STEL as "A 15-minutes TWA exposure which should not be exceeded at any time during the workday, even if the 8-hour TWA is within the TLV-TWA. Exposures above the TLV-TWA up to the STEL should not be longer than 15 minutes and should not occur more than four times per day. There should be at least 60 minutes gap

between successive exposures in this range" (ACGIH, 1998). The main purpose of STEL is to prevent acute exposure and reduce associated health risks. STEL itself does not represent an independent exposure, instead, it enhances the compliance of the TWA limit by ensuring limited exposure to acute concentrations of such pollutants whose health effects are of a chronic nature.

The lack of instruments and procedures capable of measuring real-time DPM exposure, and uncertainty in the relationship between human exposure to diesel exhaust and chronic health effects has prevented the implementation of STEL determination during DPM PEL assessment. Recent technological developments in the area of real-time DPM monitoring provide tools and techniques that allow better estimation of DPM levels than ever before. The outcomes of various DPM monitoring studies have revealed that the mining industry now has access to enhanced tools that can help to better understand the mine atmosphere in the context of DPM (A. Gillies & H. Wu, 2008; James Noll & Janisko, 2013; James Noll et al., 2013; J Noll et al., 2013). The usage of real-time monitors is critical in determining STEL for DPM as the standard method that MSHA employs to determine the DPM PEL requires approximately two weeks to obtain results from the laboratory. The standard method of DPM PEL determination cannot provide any real-time or instant assessment of DPM exposure. In order to implement the idea of STEL during DPM PEL measurement, monitors are required that can almost instantly quantify DPM concentrations. Although no instant or real-time DPM monitoring method has of yet been recognized as a standard, real-time monitors are now available that can accurately estimate the concentrations of DPM under different mining conditions (Gaillard, McCullough, & Sarver, 2016; Gillies, 2011; A. Gillies & H. Wu, 2008; Janisko & Noll, 2008; M.U. Khan

& Gillies, 2015a; M. U. Khan & Gillies, 2015b; James Noll et al., 2013; JD Noll et al., 2008; H. Wu & Gillies, 2008). A recent study used a modified real-time DPM monitor for spot checking and reported satisfactory results (Gaillard et al., 2016). Several real-time DPM monitors have been developed and tested in the past decade and research is continuing to improve, check and confirm their DPM measurability under different mining conditions.

The availability of improved real-time DPM monitors, well recognized hazardous health effects of DPM exposure, and the categorization of DPM in group 1 agents by the IARC are some of those factors that have a potential to introduce the concept of measuring STEL for DPM during PEL determination. The recent realization of the associated severe health effect of DPM exposure by IACR suggests that miners' exposure to elevated levels of DPM even for a brief time period can be hazardous. Thus, only considering PEL determinations to ensure miners' safety does not seem adequate in the long term. The use of an instant DPM monitor along with DPM STEL determination should be encouraged to ensure safe working.

5.5. SIGNIFICANCE OF MINE AREA DPM SAMPLING

DPM monitoring in mines is relatively new as compared to dust or gas monitoring. MSHA does not employ mine area or real-time DPM sampling for compliance determination as these sampling results do not necessarily represent or reflect the miner's personal exposure to DPM. Numerous studies have reported high concentrations of DPM when area sampling was performed (Gaillard et al., 2016; Gillies, 2011; Janisko & Noll, 2008; M.U. Khan & Gillies, 2015a; M. U. Khan & Gillies, 2015b; JD Noll et al., 2008) at

various locations in different mines. It seems justifiable to assume that high DPM concentrations obtained by sampling at or near work faces do not necessarily reflect miners' personal exposure to those DPM levels because miners do not usually spend a complete eight hours of their work shift at high DPM concentration zones. In addition, those miners who work at high DPM concentrations areas are somewhat protected from elevated concentrations by utilizing environmental cabs and respirators. Although high DPM concentrations from area sampling have less influence in estimating miners' PEL, these concentrations can effect miners' overall exposure to DPM. Mine air quality is less likely to be improved unless mine management has a better understanding of the quality of air at different locations in the mine. DPM compliance determination neither provides enough information about the mine air quality at work faces, nor helps to understand the effect of any specific diesel equipment on the DPM contamination levels of mine air. DPM area sampling is important and critical in order to improve mine air quality and ensure safe working conditions, since PEL determination does not consider miners' exposure to high DPM levels as a threat until TWA exposure remains below 160 $\mu g/m^3$ of TC. Although DPM area sampling results do not represent the personal exposure of any miner working in an underground mine, the result contains significant information about the degree of cleanliness of the mine air and provide better understanding of the overall conditions of the mine air. Thus, along with personal sampling, DPM area sampling especially at active work zones should be encouraged.

5.6. SUMMARY

This section describes frequency distribution patterns of DPM concentrations encountered in underground mines' work faces and in exhaust air drifts. Distinct DPM measurements from work faces and exhaust air drifts were analyzed. It was found that the DPM concentrations at mine work faces and in exhaust air drifts were not normally distributed. Random frequency distribution patterns were observed for all measurements; however, lognormal and Weibull distribution were able to represent many work faces and exhaust air drift measurements. Results obtained from the work faces were combined. The data attained from all exhaust air drift measurements was also pooled together. Results of all work face and exhaust air drift measurements followed a lognormal and Weibull distribution. The work face concentration results are best represented by Weibull distribution, whereas exhaust air drift measurements closely followed a lognormal distribution. Finally, all measurements (both from the work faces and exhaust air drifts) were pooled and analyzed. DPM concentrations distribution obtained after combining all data from both types of measurement locations also followed lognormal and Weibull distribution. Lognormal distribution seems a better fit for fully combined data since Weibull distribution missed the peak of the data-set. Statistical parameters and percentiles were computed for each distribution. Based on work face concentration results, the most likely EC concentration that can happen at the work face was 339.27 $\mu g/m^3$ (Weibull distribution mean of all work face measurements). The most probable EC concentration for exhaust air drift measurements was 287.03 $\mu g/m^3$ (lognormal distribution mean of all exhaust air drift measurements). The percentile of all distributions showed that the chances of having area EC concentrations above 150 $\mu g/m^3$ at the work faces and in exhaust air

drifts are over 75%. This means a miner who visits work faces or exhaust air drifts (situated near to the active work face) has a 75% chance of exposure in areas where EC concentration is above 150 $\mu g/m^3$.

The distribution patterns identified in this section can be used to approximate the likelihood of DPM level to which a miner who works at active mining zones without environmental cab and a respirator is exposed. The notion to measure and implement STEL for DPM is highlighted. Mine air area sampling is important to ensure better air quality in mines. Area DPM sampling should be conducted more often alongside miners' personal exposure measurements to better understand the mine air environment.

6. WORK FACE AND SIMULTANEOUS DPM MEASUREMENTS

6.1. OVERVIEW

After identifying commonly encountered DPM concentrations at different mine locations (Section 4) and determining their frequency distribution patterns (Section 5), individual and simultaneous EC concentration plots of real-time DPM monitoring are examined in this section. Work face location is considered for individual measurements plots because work faces are the primary focus of diesel equipment activities and work face measurements are a natural point of comparison for measurements at other mine locations. The simultaneous measurement results are plotted for the work faces and exhaust air drifts, and for various inlet and exhaust air drift locations. Simultaneous measurements help to reveal the relationship between diesel equipment activities and their resultant DPM emissions at several mine locations at a certain time. These measurements are vital to explain variations in DPM levels at different mine locations. Simultaneous plots are also helpful in understanding dilution patterns of DPM concentrations at locations far from work faces. In this section, individual and simultaneous DPM measurements are divided into the three sub sections. First sub-section discusses few individual work face measurements, second sub-section provides work face and exhaust air drift simultaneous measurement results, whereas the third sub-section presents simultaneous measurements results from inlet and exhaust air drift measurements.

6.2. RESEARCH METHODOLOGY

The FLIR Airtec real-time DPM monitor (described in Section 2) has been used for real-time DPM measurements. DPM area samples were collected at several work faces, exhaust air drifts, and inlet air drifts in the selected mines during a variety of mining activities. Simultaneous measurements were conducted by installing the Airtec monitors simultaneously at different measurement locations. All samples were collected under close observation by research team members. The monitors were regularly checked during sampling and those measurements that encountered any sort of error (for example, flow rate error, clogging of the Airtec filter cassette) were discarded. Detailed logs of diesel equipment activities in the monitoring areas were maintained.

6.3. INDIVIDUAL WORK FACE MEASUREMENTS

This research comprises a series of work face measurements, some of these measurements plots are discussed in previous sections. This section exclusively focuses on several specific individual work face measurements that exemplify the effect of using multiple diesel-powered equipment on work face DPM levels. These measurements are included as work face DPM concentrations can be considered as a benchmark for other mine locations, since maximum DPM levels are mostly observed at or near work faces. In order to facilitate the discussion, face measurements discussed in this section are arbitrarily named as Z1, Z2 and Z3.

6.3.1. Measurement Z1. Figure 6.1 shows work face EC concentration plot for measurement Z1. Monitoring duration lasted for about five hours. A 212 kW jumbo drill, a 280 kW CAT FEL, two 355 kW haul trucks participated in work face activities. A fire

drill exercise was executed at the mine during monitoring. According to the existing mine procedure, during the fire drill all kind of work must be suspended and all miners must report to an underground mine workshop. The work at the face was stopped when fire drill exercise begun. The time when fire drill started is shown in Figure 6.1. It is evident from Figure 6.1 that EC concentrations decreased from around 300 µg/m^3 to about 50 µg/m^3 during the fire drill exercise since there was no activity during this time. Face work resumed after about three hours of monitoring and the EC concentrations began to increase right after the work was resumed. Figure 6.1 shows that within two hours of work redemption the Airtec monitor recorded an increase to EC concentration above 400 µg/m^3.

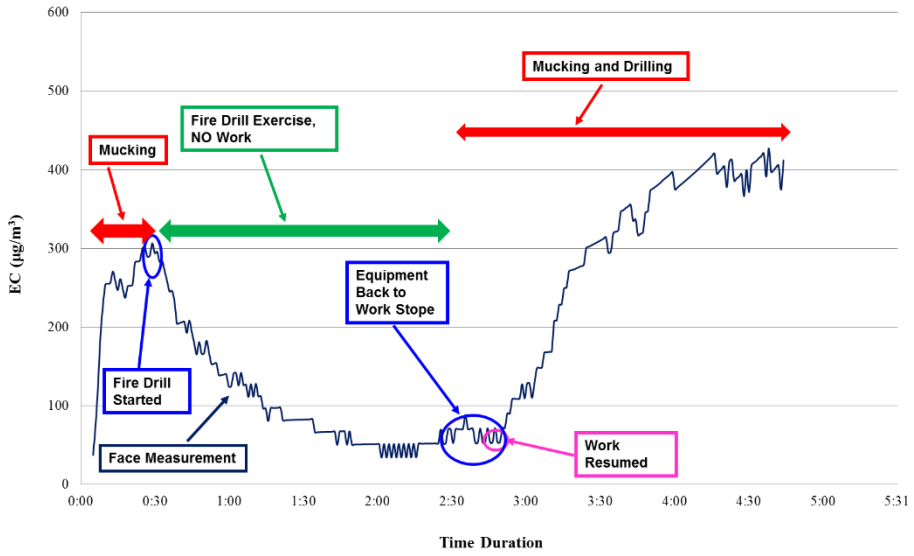

Figure 6.1 EC plot for work face measurement Z1

6.3.2. Measurement Z2. Figure 6.2 shows the EC concentration plot for work face measurement Z2. The duration of monitoring lasted for more than 5 hours. A 186 kW drill, a 129 kW scaler, and 280 kW CAT FEL participated in work face activities. Details of

activities at the beginning and completion of the monitoring time are shown in Figure 6.2. Drilling operation suspended at about the fortieth monitoring minute. A decrease in EC concentration right after the suspension of drilling operation can be seen in Figure 6.2. During the next two monitoring hours, only one scaler was in operation. At the beginning of the third monitoring hour, drilling resumed and joined the face activity with a scaler. Sudden increase in EC concentrations was shown by the Airtec monitor after drilling resumption. Later on at about 03 hour and 50 minutes a FEL joined face activities and a further increase in EC concentrations was measured by the Airtec monitor as shown in Figure 6.2.

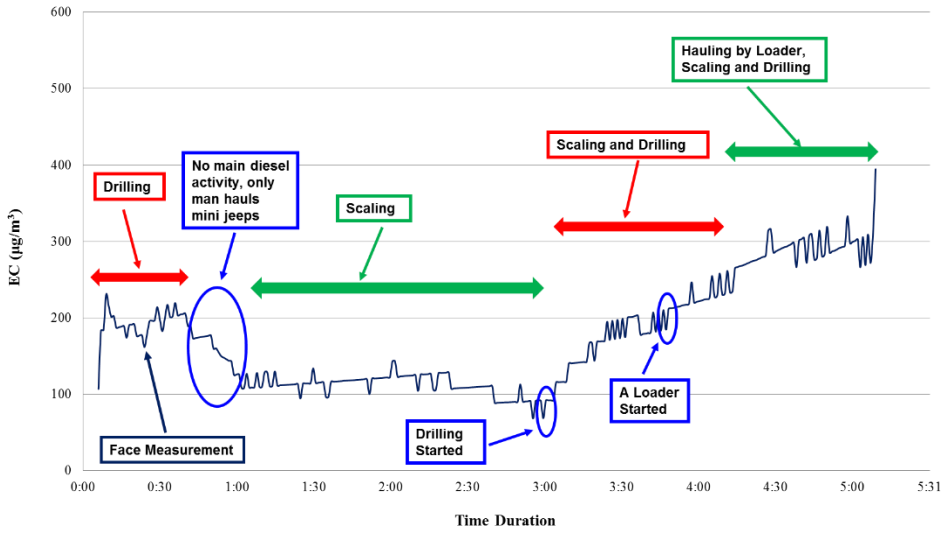

Figure 6.2 EC plot for work face measurement Z2

6.3.3. Measurement Z3. Figure 6.3 shows work face measurement Z3. This particular face measurement is one of the high EC concentration measurements by the Airtec monitor. The EC concentrations remained above 500 µg/m^3 almost throughout

monitoring duration. Measurement lasted for about four hours. Overall three activities were being performed at the work face, these include mucking, face drilling, and scaling. However the drilling operation did not contribute substantially to the DPM concentration as the drill machine was electrically driven. A 280 kW CAT FEL, four 298 kW haul trucks and a 129 kW scaler contributed towards the accumulation of DPM concentration. Detail of activities is shown in Figure 6.3. This shows that the Airtec monitor can be used to measure very high DPM concentrations for significantly long durations.

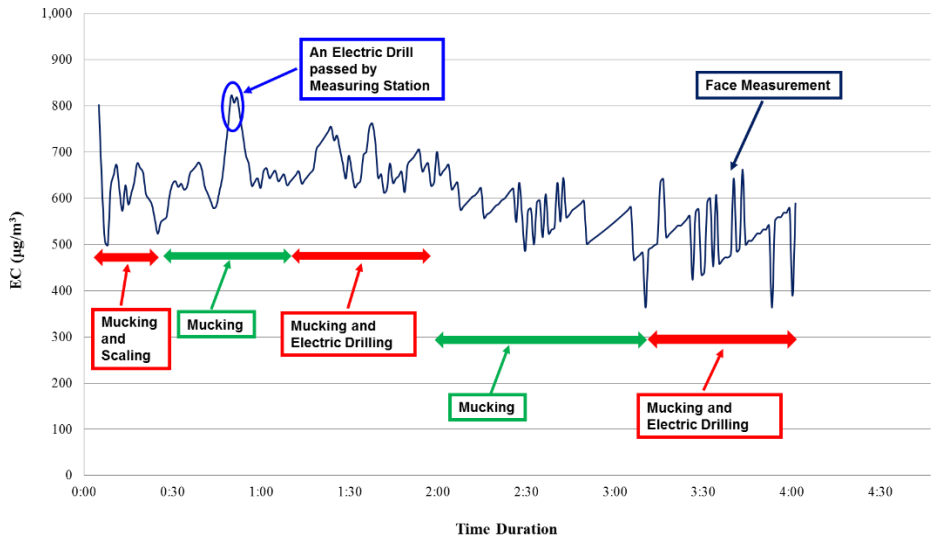

Figure 6.3 EC plot for work face measurement Z3

6.4. WORK FACE AND EXHAUST AIR DRIFT MEASURMENTS

Figure 6.4 shows a generic schematic of work face and exhaust air drift measurement locations. Arrows in Figure 6.4 represent the direction of the airflow whereas triangles represent measurement locations. Figure 6.4 also shows a combination of ventilation fan and duct system, whereas work face and exhaust air drift measurement

locations are captioned. In order to facilitate the discussion, work face and exhaust air drift measurements are arbitrarily named as B1, B2, B3, B4, B5, and B6.

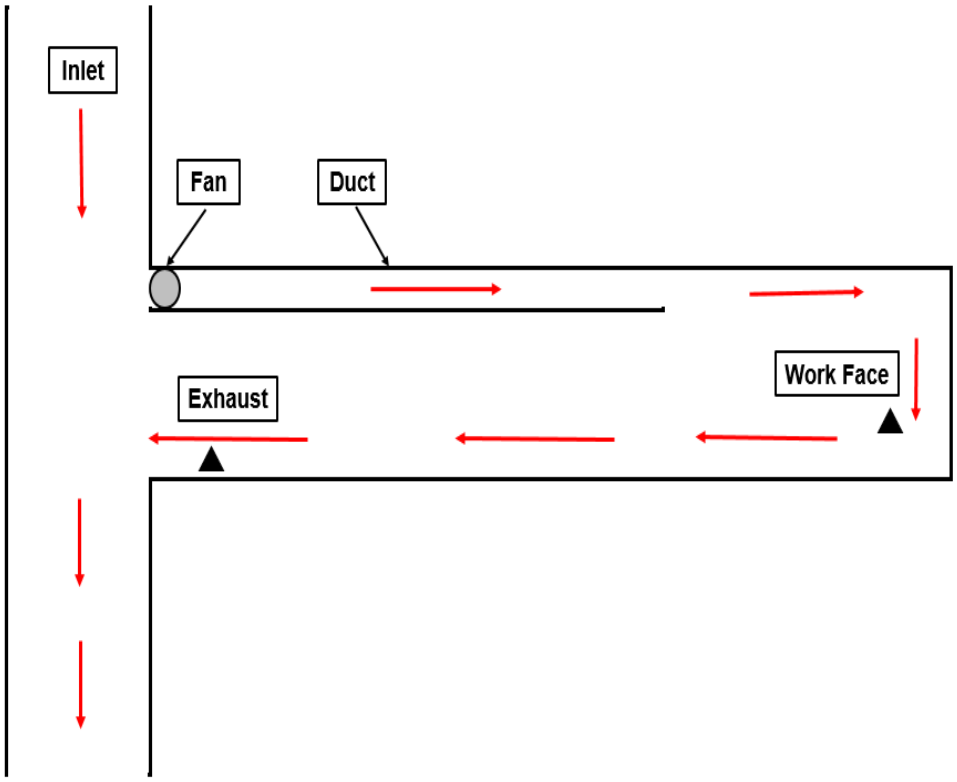

Figure 6.4 Schematic of work face and exhaust air drift measurements

6.4.1. Measurements B1. Figure 6.5 shows plots of measurements B1 that were conducted at the work face and exhaust air drift. Monitoring duration lasted for around five and a half hours. Several mining activities were being performed at the time of monitoring and overall high DPM concentrations were observed at both measurement locations. A 280 kW FEL, two 355 kW dump trucks, a 212 kW jumbo drill, a 186 kW roof bolter and one 93 kW roof bolter participated in work face activities during monitoring process. The duration of each activity is shown in Figure 6.5. During monitoring, consistent movement

of diesel vehicles was observed in between both measurement locations. Multiple face activities resulted in continuously increasing levels of DPM at both measurement stations. A consistently increasing DPM trend shows that the ventilation arrangements were not adequate.

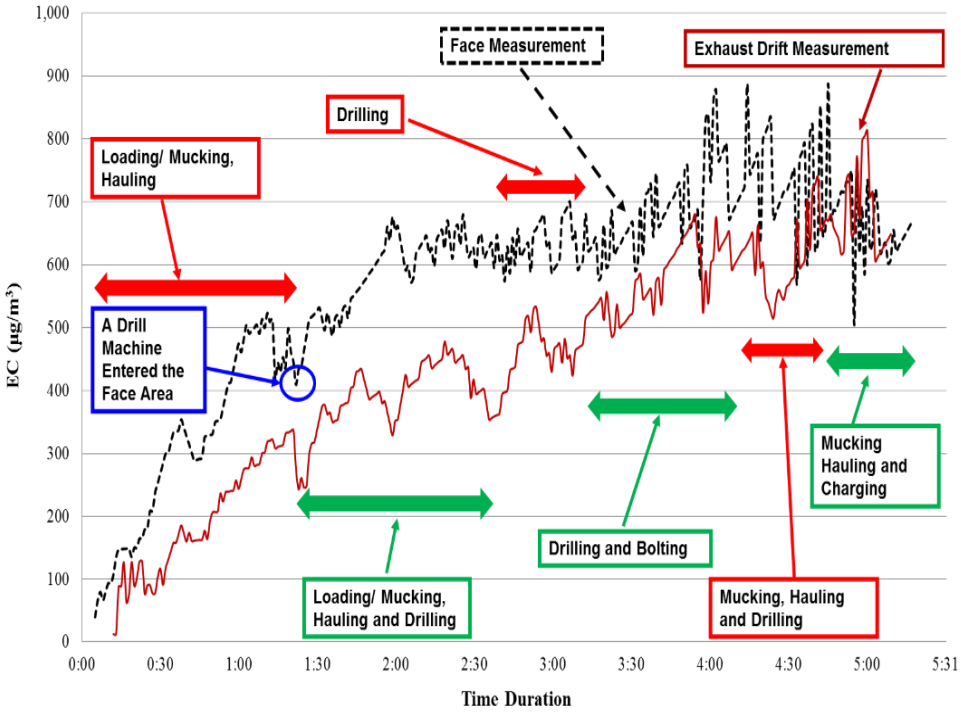

Figure 6.5 Work face and exhaust air drift EC during measurements B1

6.4.2. Measurements B2. Figure 6.6 shows the EC concentration profiles of work face and exhaust air drift for measurements B2. The monitoring durations was around five hours. Multiple diesel equipment activities were being performed at the work face. Face drilling was performed by a 212 kW jumbo drill during first ninety minutes of monitoring. Drilling activity was followed by a measurement break and both monitors were restarted

after about 5 minutes. A 129 kW scaler joined drilling operation for the next one and half hour. A 280 kW loader and three 298 kW haul trucks joined the face work during last ninety minutes. Detail of activities is illustrated in Figure 6.6. Both exhaust air drift and work face measurements showed almost similar levels of DPM throughout monitoring period.

6.4.3. Measurements B3. Figure 6.7 illustrates EC concentration plots of work face and exhaust air drifts for measurements B3. The monitoring period lasted for about four and a half hours. A 293 kW CAT FEL, three 298 kW haul trucks, one 212 kW jumbo drill and one 129 kW roof bolter participated in mining activities. Overall similar levels of DPM concentrations were observed at both measurement stations. After about one hour of monitoring, a sudden depression in the work face EC concentration is observed, however the exact reason of this particular depression is not known. Detail of activities is shown in Figure 6.7.

6.4.4. Measurements B4. Figure 6.8 shows the work face and exhaust air drift EC profiles of measurement B4. A number of activities including mucking, face drilling and roof drilling were being performed during the measurements. Monitoring duration was about four and a half hours. A 280 kW CAT FEL, three 298 kW haul trucks, a 186 kW drill jumbo and a 146 kW roof drill participated in work face activities. Detail of activities starting and finishing time is given in Figure 6.8. Overall high DPM concentrations were seen at both measurement stations throughout the monitoring period.

6.4.5. Measurements B5. Figure 6.9 shows EC plots of wok face and exhaust air drift for measurements B5. Measurements were performed for around three and half hours. Mucking and scaling were both underway during the monitoring period. A 280 kW CAT

FEL, three 293 kW haul trucks and a 129 kW scaler contributed at work face activities. Details of activity starting and stopping times are identified in Figure 6.9. Due to some issues, the ventilation fan went off during the first one and a half monitoring hour, thus no active ventilation system was in place for the work face area. However mining activities at the work face remained active during this period. An accumulation of DPM concentration occurred at the work face due to the lack of ventilation. After the ventilation fan was turned on, a sudden depression in the work face concentrations was observed. This rapid decrease in EC concentrations is likely due to the sudden push of fresh air that had not completely mixed with previous stagnant air at face. An intensive increase in the work face concentrations was observed just after the depression. This peak in EC concentrations could be the result of complete mixing of the fresh air with previously accumulated DPM that was swept by the ventilation afterwards.

6.4.6. Measurements B6. Figure 6.10 shows EC concentrations of work face and exhaust air drift for measurements B6. Monitoring duration was a little less than four hours. A 160 kW roof bolter worked at the face during monitoring period. Other than a roof bolter, no significant diesel activity was observed at the monitoring area, however some occasional trips were made by 19 kW man haul mini jeeps. One surprising observation is that EC concentrations for the exhaust drift measurement location were higher than the face measurement for some time intervals. This is because the monitor installed in the exhaust air drift location was capturing DPM from such work areas whose DPM was not captured by the monitor that was installed at work face measurement location. DPM concentrations observed in this case seems relatively high, this can be because the air entering the work face was already polluted by diesel equipment from other working areas.

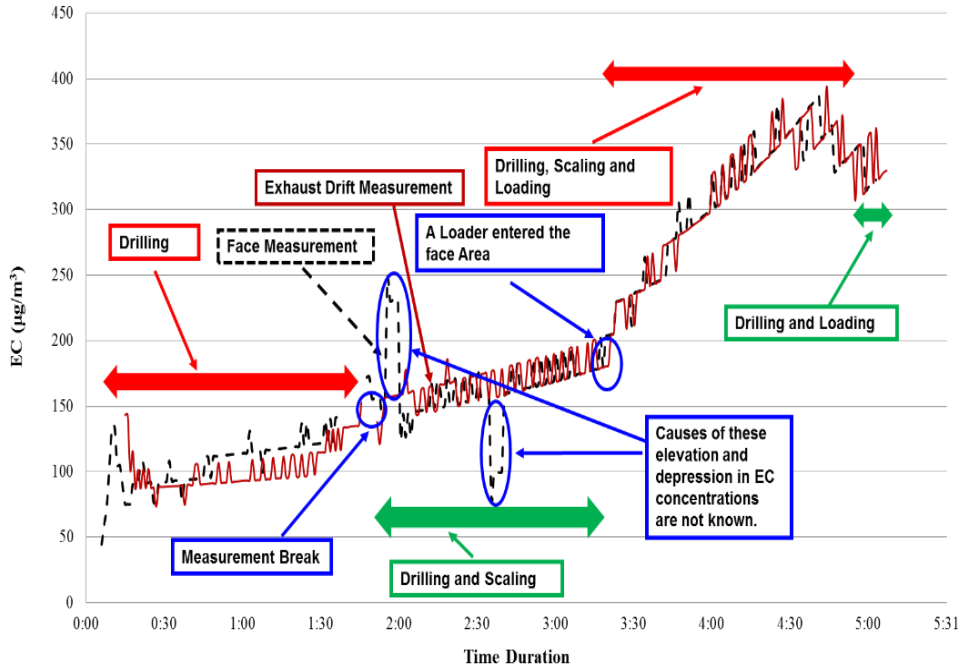

Figure 6.6 Work face and exhaust air drift EC during measurements B2

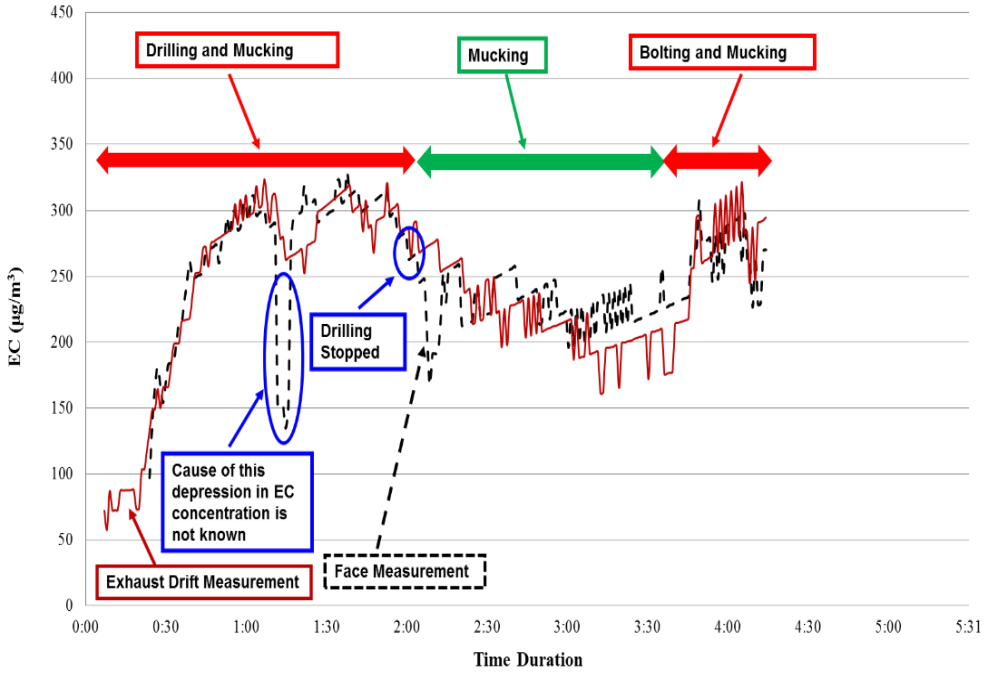

Figure 6.7 Work face and exhaust air drift EC during measurements B3

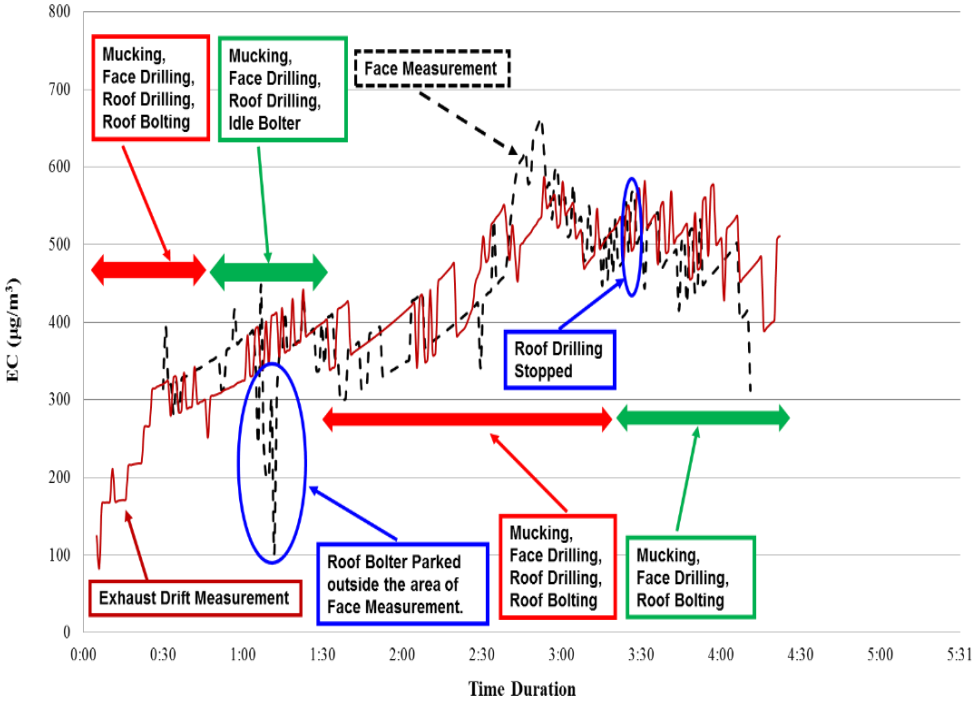

Figure 6.8 Work face and exhaust air drift EC during measurements B4

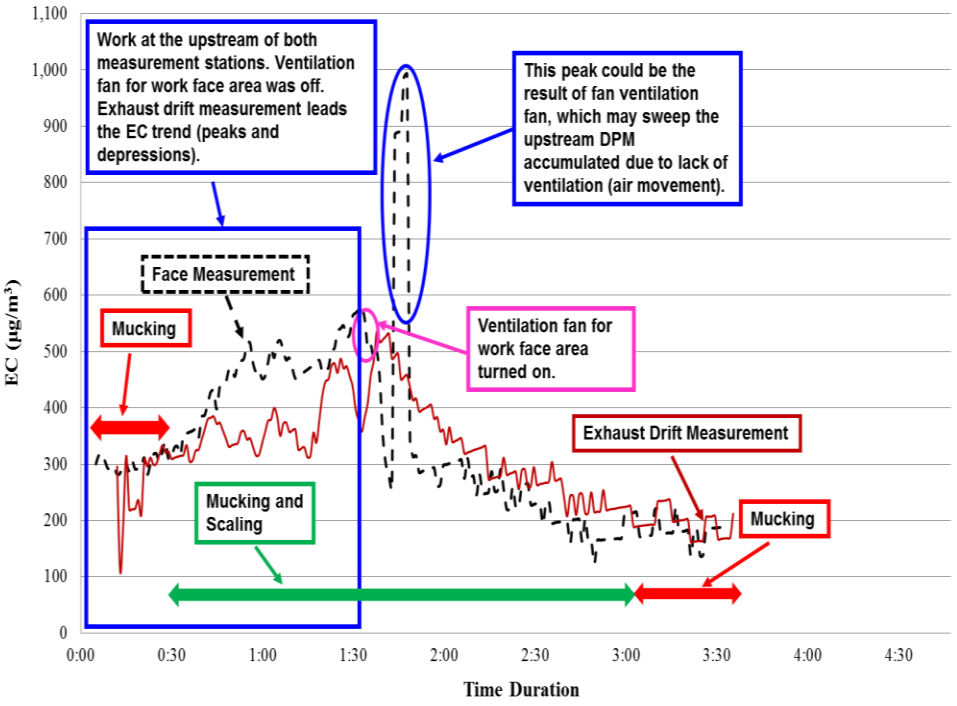

Figure 6.9 Work face and exhaust air drift EC during measurements B5

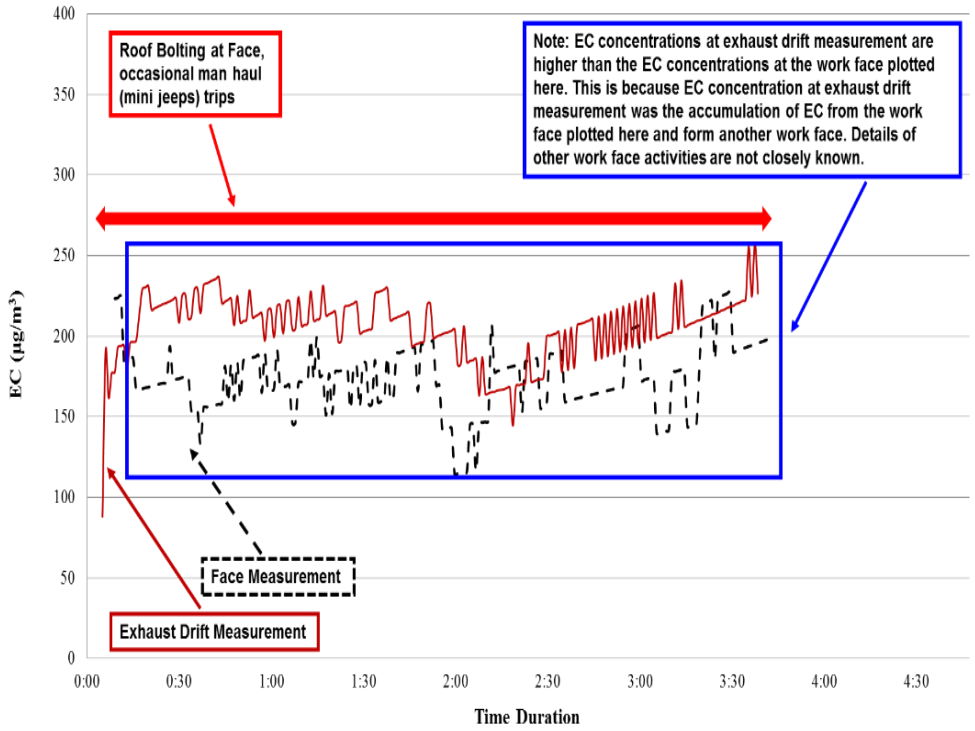

Figure 6.10 Work face and exhaust air drift EC during measurements B6

6.5. INLET AND EXHAUST AIR DRIFT MEASUREMENTS

Figure 6.11 shows a schematic of a generic mine drift with DPM measurement locations and airflow patterns. Arrows in Figure 6.11 represent the direction of the airflow and triangles represent measurement locations. Figure 6.11 shows a combination of ventilation fan and duct system, whereas inlet and exhaust measurement locations are captioned. For easy discussion, all inlet and exhaust air drift measurements are arbitrarily named as A1, A2, A3, and A4.

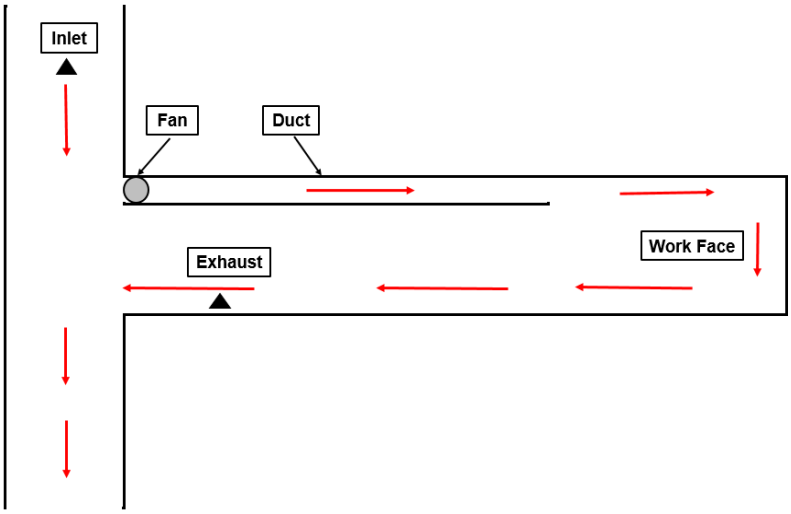

Figure 6.11 Schematic of inlet and exhaust air drift measurements

6.5.1. Measurements A1. Figure 6.12 shows real-time EC profiles of measurements A1. These measurements were conducted simultaneously at the inlet and exhaust air drift locations. Measurements were performed while the work face was active. A 100 kW road grader, a 280 kW CAT FEL, three 298 kW haul trucks and one 186 kW drill machine were in operation during monitoring. Mucking was completed in about two hours while drilling lasted for three hours. A 129 kW scaler was in operation during the last fifteen minute of the monitoring process. Figure 6.12 shows that even at the inlet measurement location high DPM concentrations were observed. This is largely due to another work face that was located further upstream of the inlet measurement location. The inlet measurement location was the upstream for the monitored work face and downstream of other mine working areas (that were not examined). Figure 6.12 shows that the quality of mine air even at work face inlets can be poor at times. In such cases, even minor diesel activity at the face can increase the DPM concentrations to harmful levels. Detail of diesel activities is described in Figure 6.12.

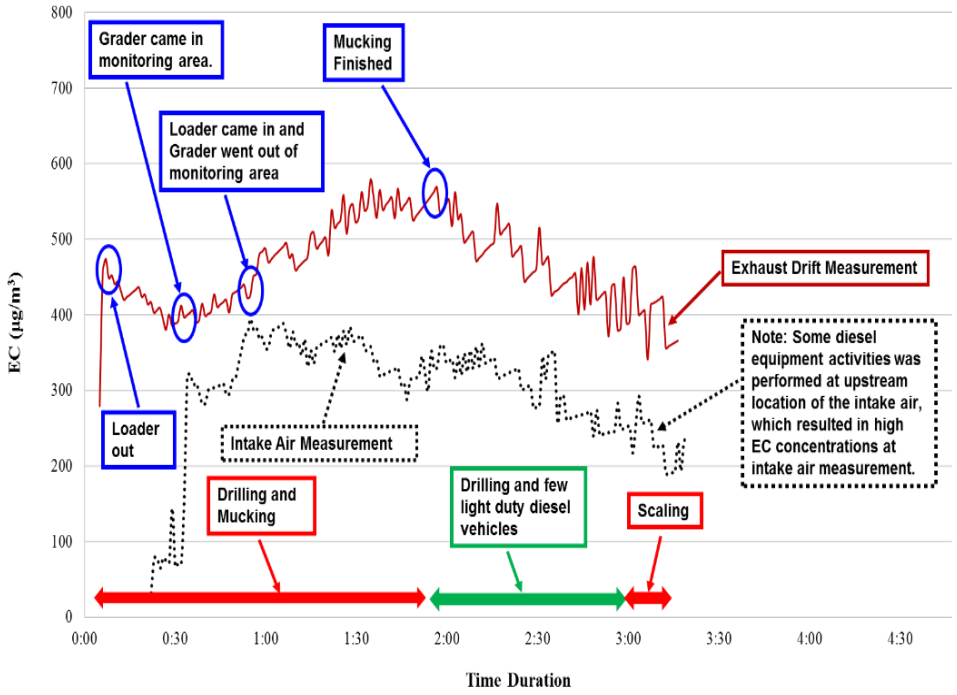

Figure 6.12 Inlet and exhaust air drifts EC during measurements A1

6.5.2. Measurements A2. Figure 6.13 shows the inlet and exhaust air drift DPM concentrations for measurements A2. Monitoring lasted for over five hours, a 186 kW jumbo drill, a 280 kW CAT FEL, three haul trucks each of 298 kW participated in face work activities. Drilling operation finished after one and a half hour. Mucking lasted till the end of monitoring process. It is evident from Figure 6.13 that high DPM concentrations were resulted at exhaust drift monitoring station. The inlet air entering the work face was not particularly clean as consistently showed DPM levels above 100 µg/m^3 of EC. This is due to the presence of diesel equipment activities at other mine locations that were situated further upstream of the inlet air monitoring station. Figure 6.13 shows detail of other diesel activities for measurement A2.

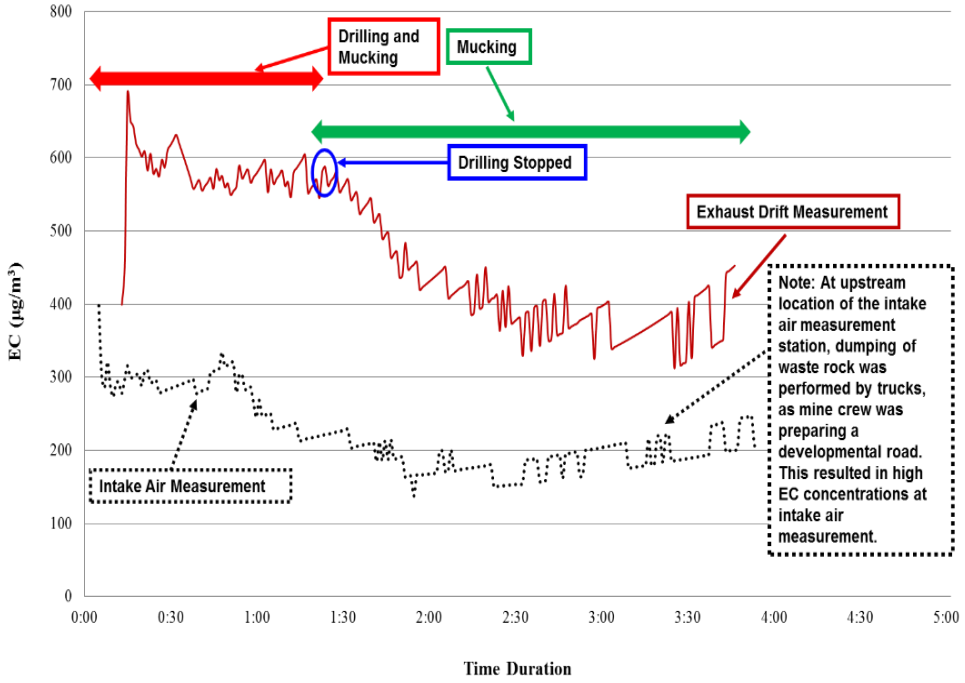

Figure 6.13 Inlet and exhaust air drifts EC during measurements A2

6.5.3. Measurements A3. Figure 6.14 shows inlet and exhaust air drift DPM concentrations for measurements A3. Monitoring period lasted for about four and a half hours. During the first two hours no significant diesel activity was noticed at the work face that was under observation. However at other mine faces, diesel equipment work was in progress that resulted in DPM concentrations at the inlet and exhaust air drift. Mucking started after around two monitoring hours. A 280 kW CAT FEL and two haul trucks each of above 298 kW participated in mucking activity. Mucking lasted for about one and a half hour, afterwards no noticeable diesel activity was performed. Activity detail are shown in Figure 6.14.

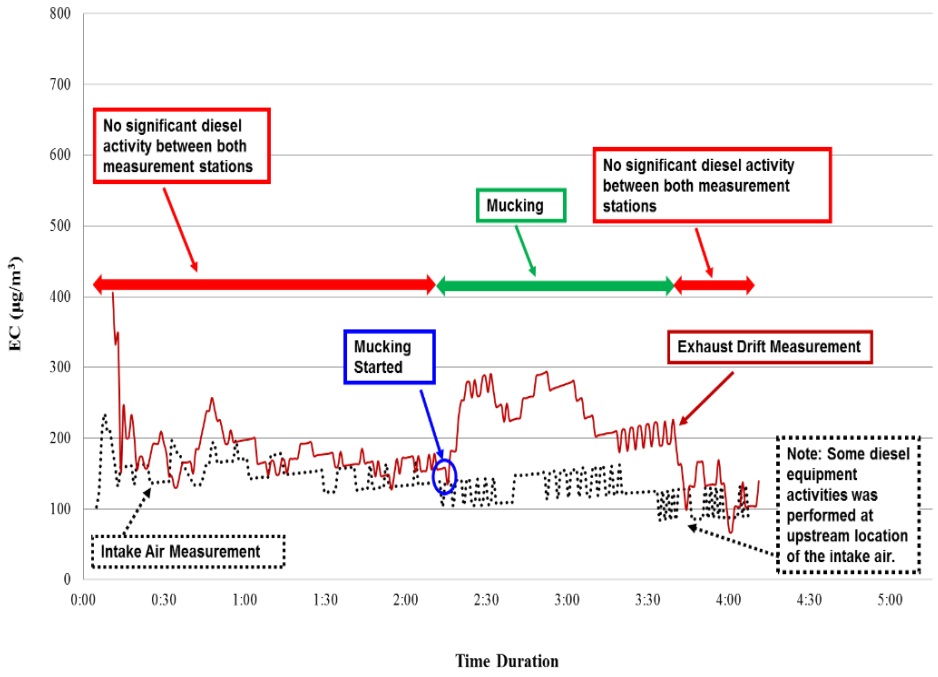

Figure 6.14 Inlet and exhaust air drifts EC during measurements A3

6.5.4. Measurements A4. Figure 6.15 shows the inlet and exhaust air drift measurements A4. Monitoring duration lasted for about five hours and mucking was performed during first three monitoring hours. A 280 kW FEL, four haul trucks each of above 298 kW power were involved in mucking process. No significant face work was recorded after mucking. Some diesel equipment work was in progress at the upstream location of both monitoring stations that caused DPM concentration above 100 µg/m^3 throughout the monitoring duration. Further detail of diesel equipment activities is described in Figure 6.15.

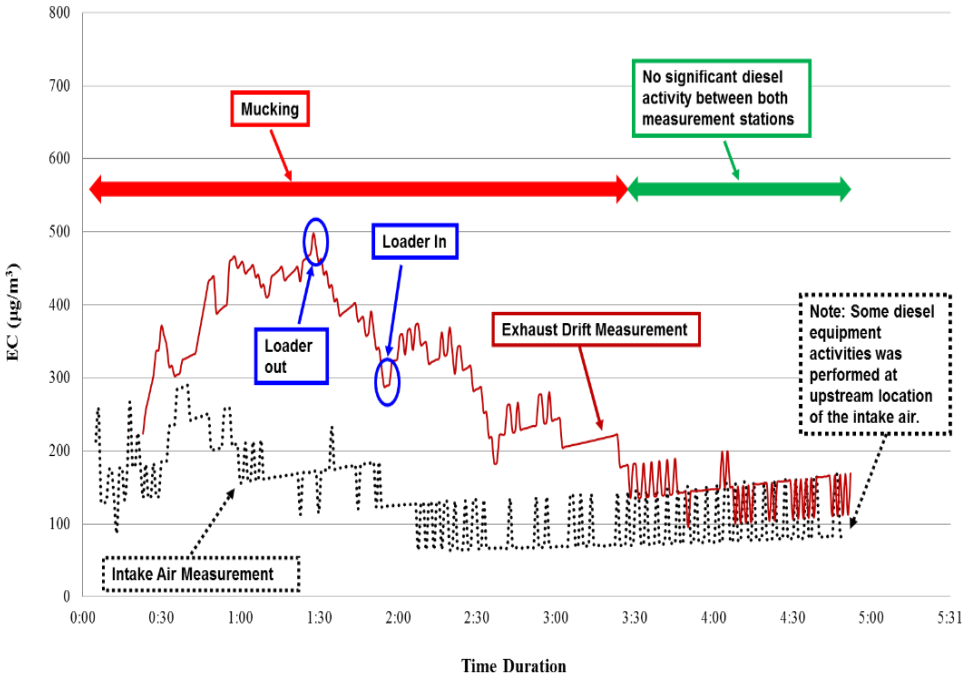

Figure 6.15 Inlet and exhaust air drifts EC during measurements A4

6.6. SUMMARY

Real-time DPM measurements were performed at the work faces, inlet air drifts, and exhaust air drifts of different underground metal mines. High DPM concentrations were observed during individual work face measurements. Simultaneous work face and exhaust air drift measurement plots showed DPM concentrations at these locations. Simultaneous measurements are important to explain variations in DPM levels at different mine locations and help to understanding DPM dilution patterns in mines. The EC concentrations at the work face and exhaust air drift locations were generally quite similar. This is because the air in the work stope that includes both (work face and exhaust air drift) measurement locations is fairly well mixed. In one case (B6) DPM concentrations at exhaust air drift measurement were higher than the work face concentrations. This

happened because the exhaust air drift measurement location captured some DPM from diesel equipment that was operating outside of the work face area. Simultaneous measurements at inlet and exhaust air drifts show the DPM levels that are encountered at these measurement locations. Inlet and exhaust air drift measurements pinpoint the importance of using fresh air for DPM dilution. The EC for all inlet air drift measurements (A1 - A4) was above 100 $\mu g/m^3$. This means that the fresh air used to dilute DPM at the work faces was already heavily polluted by diesel exhaust from other work faces or from fan recirculation. In such situation, even the use of a single diesel-powered equipment can increase DPM concentration to significantly high levels. Therefore, mine operators should try to control DPM recirculation from auxiliary fans, minimize the air leakage from mine doors and stoppings, and design ventilation networks such that the air used for DPM dilutions at the work faces do not contain high pollutants from other mine areas.

7. DPM RECIRCULATION EFFECTS FROM AUXILIARY FAN AND VENTILATION DUCT SYSTEM

7.1. OVERVIEW

Fan recirculation in underground mines is a recognized ventilation issue. In the United States, the use of booster fan in underground coal mines is not allowed due to their tendency to recirculate the polluted air. In non-gassy M/NM underground mines, auxiliary fans are commonly used to push air to work faces. Ventilation requirements for M/NM mines are determined by considering the PI and specific nameplate VR. PI pertains to the DPM concentration and nameplate VR is associated with other gases from the diesel engine exhaust. In non-gassy M/NM mines, recirculation from auxiliary fans is generally overlooked because these mines do not pose a certain threat of forming explosive gas mixture either by fan recirculation or otherwise. However, fan recirculation can have a noticeable impact on the DPM concentrations of M/NM mines, especially at and or near mines' work faces. Although in an underground mine, it is difficult to completely eliminate recirculation from an auxiliary fan, however, recirculation can certainly be controlled. A reasonable control of fan recirculation can improve the quality of mine air considerably in the context of DPM. This Section focuses on the determination of recirculation from auxiliary fan in one of the studied mines. This Section highlights the existence and impact of auxiliary fan recirculation in M/NM mines. In this study a significant increase in DPM concentration level has been observed due to fan recirculation. Based on the study results, suggestions have been made to mine management for control of fan recirculation. The mine management has adopted the suggested modification and changed the location of auxiliary fan as recommended.

7.2. RESEARCH METHODOLOGY AND RESULTS ANALYSIS

Recirculation was measured by installing the Airtec real-time DPM monitors at upstream and downstream locations of the auxiliary fan and ventilation duct system. Figure 7.1 shows the schematic of a generic mine drift, auxiliary fan, and ventilation duct. Arrows in Figure 7.1 show the direction of airflow and triangles represent DPM measurement locations.

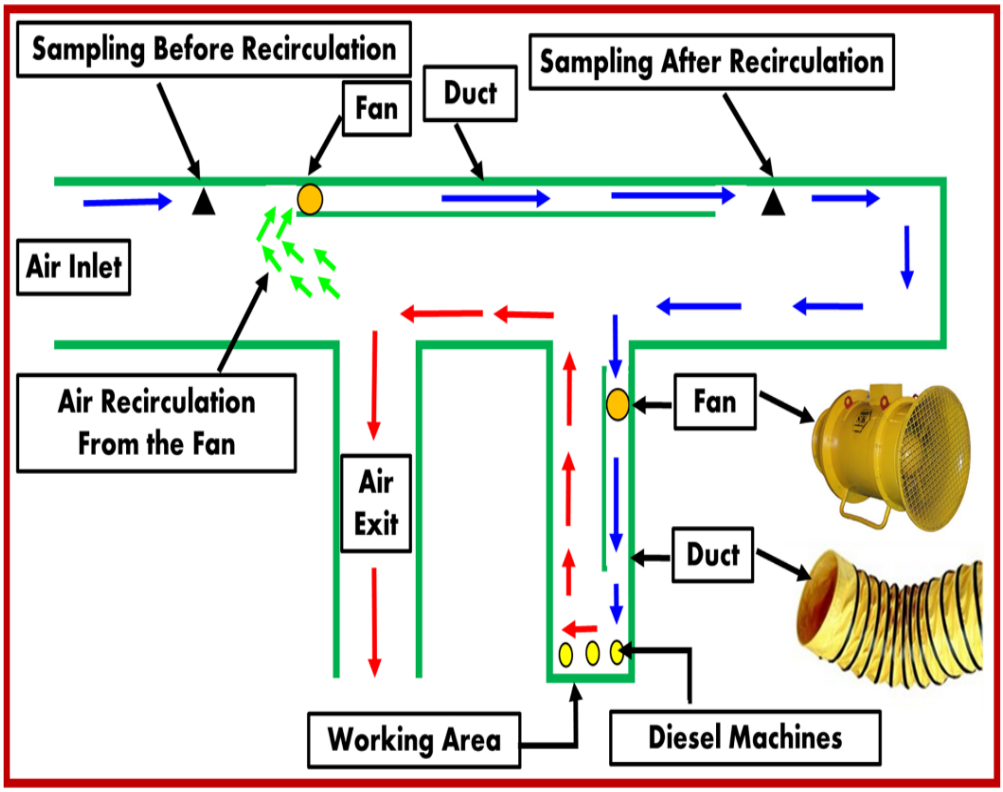

Figure 7.1 Schematic of auxiliary fan and ventilation duct system in a mine drift

Both measurement locations are separated by an auxiliary fan and ventilation duct system, thus any diesel activity between these measurement locations cannot occur. In an ideal case (zero recirculation) scenario, both measurement locations (upstream and

downstream) should show same DPM concentration. All samples were collected under close observation by research team members. The Airtec monitors were regularly checked during sampling and those measurements that encountered any sort of error (for example, flow rate error, clogging of the Airtec filter cassette) were discarded. Detailed logs of diesel equipment activities in the monitoring areas were maintained and discussed. The following sections discuss fan recirculation measurements and for the sake of easy discussion, measurements were arbitrarily named as R1, R2, and R3.

7.3. MEASUREMENT R1

Figure 7.2 shows real-time EC plots of DPM measurements conducted in a mine drift at locations upstream and downstream of the auxiliary fan and ventilation duct system. The measurements set described in Figure 7.2 is termed as R1. A couple of peaks were observed in EC concentrations at the upstream measurement location, due to the movement of some diesel equipment at locations further upstream of the measurement location. A mine door was left open by the mine crew by mistake during the first one and half monitoring hour. Less recirculation was observed due to the opening of a mine door, since the door opening has changed the designed ventilation network of the mine, keeping some other mine areas essentially unventilated. Increase in DPM recirculation was observed after the mine door was closed and ventilation network came back to the normal position. At downstream measurement locations, an increasing DPM concentration trend was observed due to recirculation. Detail of the mine activity during the measurement period is shown in Figure 7.2.

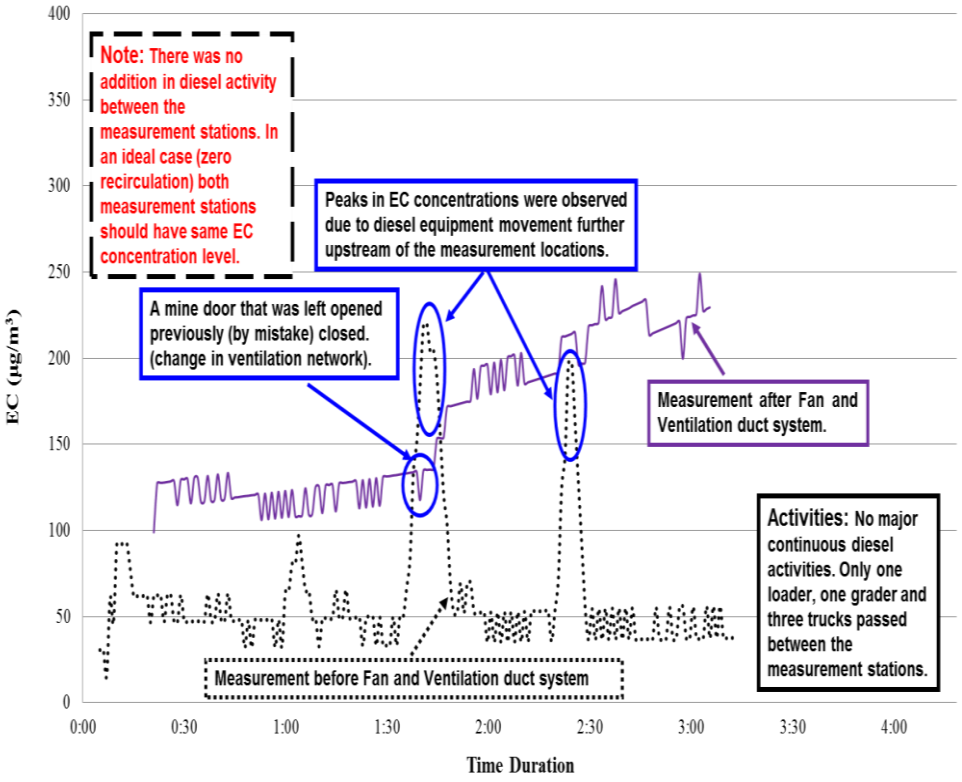

Figure 7.2 EC before and after recirculation for measurements R1

7.4. MEASUREMENT R2

Figure 7.3 shows EC concentration profiles measured at upstream and downstream of the auxiliary fan and ventilation duct system. This set of measurements is named as R2. Figure 7.3 shows details of activities during this measurement. Similar to Figure 7.2 recirculation has seemed to increase DPM concentrations at the downstream measurement location. Increase in the magnitude of DPM recirculation was observed after a jumbo drill passed by the measurement location.

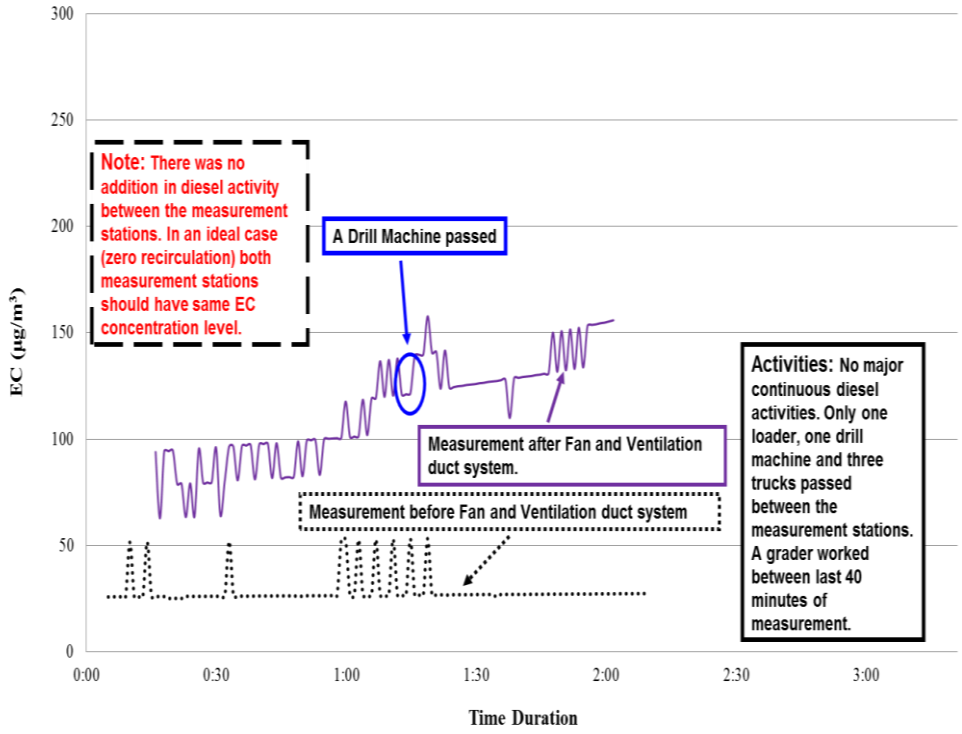

Figure 7.3 EC before and after recirculation for measurements R2

7.5. MEASUREMENT R3

Figure 7.4 shows another DPM recirculation measurement named as R3. Similar to previous recirculation measurements DPM was measured at upstream and downstream locations of the auxiliary fan and ventilation duct system. Figure 7.4 represent DPM recirculation caused by a 280 kW FEL, three 298 kW haul trucks and one 186 kW drill machine that were involved in work face activities. Significant increase in DPM concentrations due to recirculation was observed. It was noticed that relatively high diesel activity can result in elevated DPM recirculation levels.

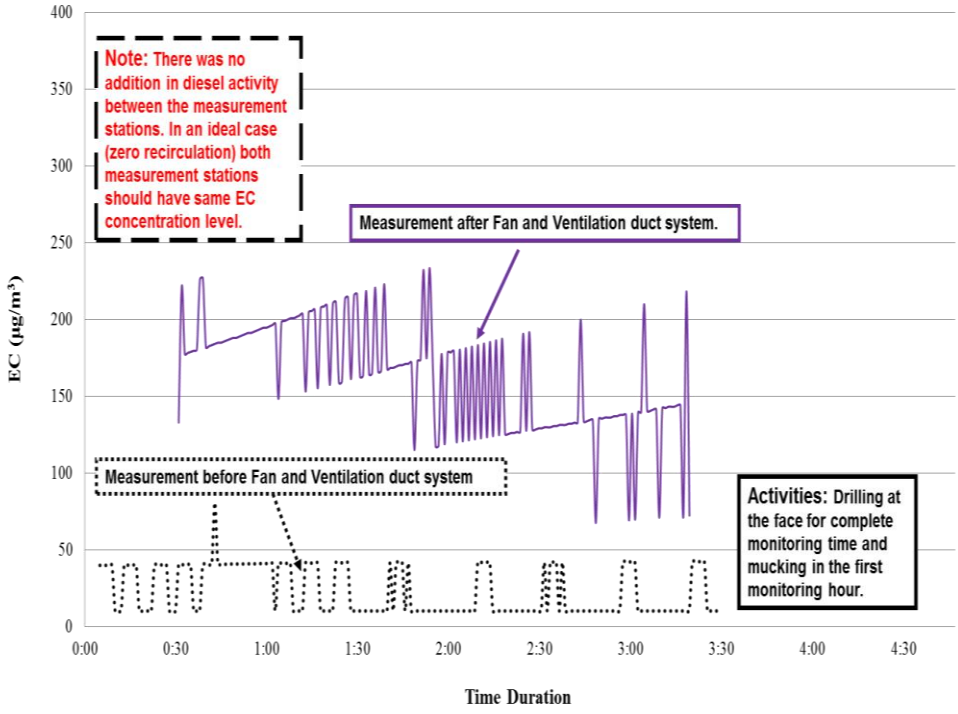

Figure 7.4 EC before and after recirculation for measurements R3

7.6. SUMMARY

Recirculation from an auxiliary fan and ventilation duct system has been examined in a metal mine. Three recirculation measurements were performed on separate days. The Airtec monitors were used to determine real-time EC concentrations at both (upstream and downstream) measurement locations. In an ideal case scenario (zero recirculation) the DPM concentration at both measurement locations should remain same, since there was no addition of any diesel activity in between these locations. Measurement results showed that the fan recirculation can cause a significant increase in DPM concentration. Overall high recirculation was observed in one of the periods that involved high diesel equipment activity. The effect of mobile diesel equipment (haul trucks, road grader, FEL, moving

drill) on recirculation seems to be more pronounced as compared to relatively stationery diesel equipment (face drill, rock bolter, and explosive charger). Based on the results of the DPM recirculation measurements and field observations, a modification in the existing ventilation arrangements has been suggested to the mine management. It was recommended to increase the distance between the exhaust air drift and auxiliary fan from around 10 m (1 to 1.25 times the width of the exhaust air drift) to around 25 m (2.5 to 3 times the width of the exhaust air drift). The mine management has adopted the suggested modification in the ventilation network and changed the location of the auxiliary fan that have caused high DPM recirculation in their mine. In M/NM mines DPM recirculation should be considered seriously and the quality of mine air can be considerably improved by controlling DPM recirculation from auxiliary mine fans.

8. STUDY OF STOPE VENTILATION PARAMETERS USING 2D CFD MODEL

8.1. OVERVIEW

In underground metal and nonmetal mines, diesel operated equipment is the preferred choice. Total airflow requirements of an underground mine depend upon many factors that include mine's total horsepower, types of engines used, and the overall airflow distribution system. DPM is one of the critical constituents in mine air mixture. Controlling DPM concentrations is an important aspect of mine ventilation since human exposure to diesel exhaust has deleterious health effects. Several approaches have been adopted by the mining industry to control and reduce miners' exposure to DPM. One approach focuses on the design and types of diesel engines, another highlights the importance of appropriate ventilation for DPM dilution. Few approaches recommend using exhaust after-treatment devices, whereas some of these approaches encourage the use of alternative fuels, environmental cabs and PPE. Although various methods have been used for DPM reduction in underground mines, there is no single best available option. The best approach to control DPM in mines is the adoption of more than one control strategy and technology (A. D. Bugarski et al., 2011). Even though several approaches have been adopted for controlling DPM in mines, dilution of DPM concentration by ventilation is the most important and widely adopted method. McPherson stated that in any underground facility where personnel are required to enter, the dilution of pollutants by providing sufficient airflows is a main objective of an underground ventilation program (Mc Pherson, 2012).

Numerical simulations using CFD technique have been successfully adopted in mine ventilation related research areas. This include the analysis of mine explosions in

gassy mines, spontaneous combustion of coal, and design and optimization of gob ventilation (Ting Ren & Balusu, 2005; Saki, 2016; L Yuan & Smith, 2007; Liming Yuan & Smith, 2008). CFD simulations have also been utilized to understand mine airflow patterns and gas concentrations in continuous miner operations, as well as during heading development (Hargreaves & Lowndes, 2007; Kollipara, Chugh, & Relangi, 2012; Petrov, 2014; Torno, Toraño, Ulecia, & Allende, 2013). In longwall mining, the intake designs of scrubber and dust control operations were investigated by CFD approach (TX Ren & Balusu, 2008). CFD modelling techniques have now became a recognized tool to understand complex airflows and behavior of various gases and dust particles in three dimensional space. Valuable information required to test initial research concepts and novel ideas can also be achieved by utilizing CFD simulations.

Several studies have used CFD to simulate the behavior of DPM, characterize its dispersion patterns, analyze its propagation, and examined the effect of different ventilation practices on DPM levels in various mining conditions (Thiruvengadam, Zheng, Lan, & Tien, 2016; Thiruvengadam, Zheng, & Tien, 2016; Yi Zheng, Lan, Thiruvengadam, & Tien, 2011; Yi Zheng et al., 2017; Y. Zheng, M. Thiruvengadam, H. Lan, & C. J. Tien, 2015a; Y. Zheng, M. Thiruvengadam, H. Lan, & J. C. Tien, 2015b; Yi Zheng, Thiruvengadama, Lanb, & Tienc, 2015; Y Zheng & Tien, 2008). One CFD study used a two model (particle tracking and species transport) approach to study DPM emissions in three dimensional space. The researchers noted that the computational time and computer memory space requirements are less demanding in species transport model as compared to the particle tracking model. Both models predicted similar distribution pattern in an isolated zone study, however, the species transport model was found to produce results

quickly and conveniently (Thiruvengadam, Zheng, & Tien, 2016). Thus the use of the species transport model is preferred for DPM simulations. A study which simulated DPM dispersion in underground M/NM mines showed DPM distribution patterns and successfully identified DPM affected areas that were above the threshold limit value (Y Zheng & Tien, 2008). Another study used CFD to compare commonly encountered mining operations at the work face inside a single dead-end entry and suggested various good practices for efficient and economic ventilation for different work operations. This study suggested an increase in flow capacities of blower and the exhaust fans from their designed values for better ventilation in the face area (Yi Zheng, Thiruvengadama, et al., 2015), however this particular study did not suggest any particular means to increase air flow quantities. Another study evaluated DPM distribution of loading operation for four auxiliary ventilation systems inside a single dead-end entry and suggested that ventilation conditions play an important role to control DPM and without proper ventilation arrangements high DPM concentrations can accumulate at work faces (Yi Zheng, Thiruvengadam, et al., 2015a). In another study, Zhang et al. (2015) evaluated the effect of four different push-pull ventilation systems on DPM distribution inside a single dead-end entry for a loading operation and showed that CFD can be used to select DPM control measures (Yi Zheng, Thiruvengadam, et al., 2015b). Zheng et al. (2017) used a CFD model to simulate DPM distribution and temperature in sloped dead end entries ventilated with push tube and blower fan system, they recommended avoiding mining towards a face in the upward direction and encouraged mining towards the downward face (effect of dead end plume).This particular study suggested an increase in air flow rates to decrease DPM concentrations at work faces (Yi Zheng et al., 2017). Although this study from Zheng et al.

(2017) suggests that an increase in flow air quantities can reduce DPM concentrations, the study has not evaluated the effect of specific ventilation related parameters on DPM levels.

Even though several studies suggested various DPM distribution patterns and different ventilation arrangements to control DPM at the work faces. However, not a single known study has specifically evaluated the effect of duct inlet air velocity, duct diameter, their optimum combination, appropriate air quantity that is required for proper DPM dilution, and duct advancement on DPM concentrations. This Section primarily focuses on ventilation parameters and evaluates duct inlet velocity, duct diameter, duct advancement, location of DPM sources, and total air quantity required to dilute and remove DPM from the work face of a dead-end mine entry.

8.2. CFD MODELING ENVIRONMENT

A number of steps were involved in order to build a CFD model for this study. The model geometry was constructed utilizing ANSYS design modeler (DM). ANSYS meshing module is used for geometric meshing. Tools available in ANSYS FLUENT CFD program are used for method solution and results analysis. Details about modeling parameters are described in the following sections.

8.2.1. CFD Model Geometry. CFD models were developed for a relatively simple geometry of a typical mine stope. This geometric configuration was selected to better understand the direct effect of ventilation parameters on DPM dilution and its dispersion. The model geometry is created by ANSYS DM platform. A 100 m long and 10 m wide dead-end mine entry was modeled. The air inlet is located at 49 m distance from the dead-end (face) and the DPM source is installed at 3 m distance from the dead-end. Model

geometric dimensions were selected as a representative of a generic metal mine stope. A FEL is used as a DPM source that was represented by a point source in the model geometry. In some simulation cases, two front-end loaders were simulated. Details of simulation cases and the number of DPM sources installed at one or more locations in the mine entry are described case by case in the following section. Figure 8.1 shows a general model geometry, its boundaries and a DPM source.

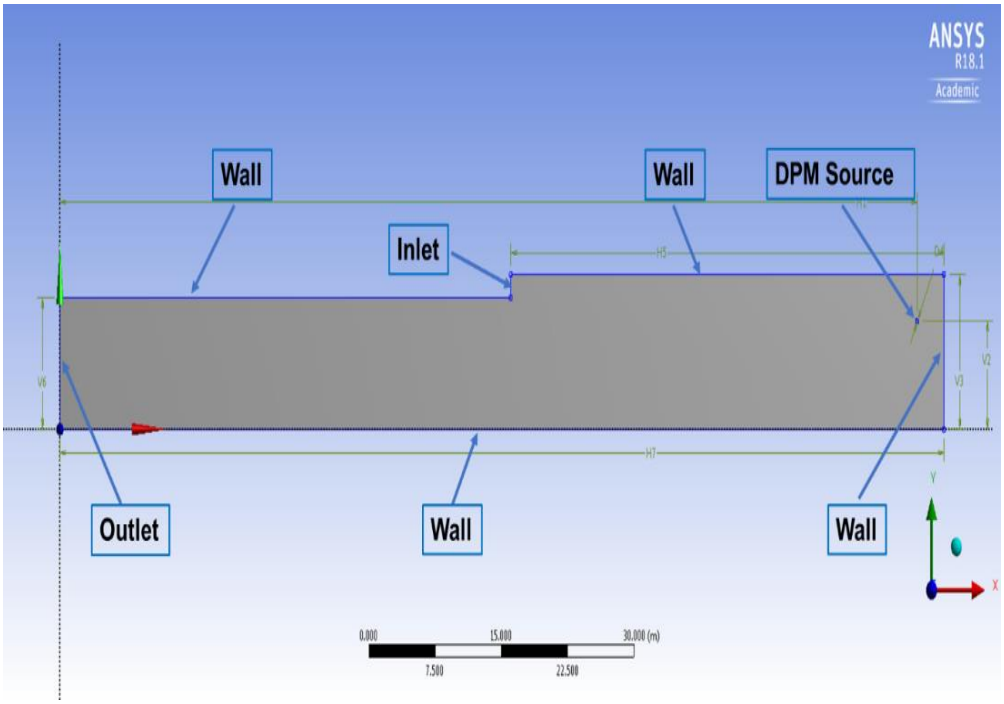

Figure 8.1 Model geometry with boundaries and DPM source

8.2.2. CFD Modeling Cases. Four simulation cases were studied, these cases differ from each other in terms number of DPM sources, their location in the mine entry, and location of duct inlet with respect to the dead-end. Description of simulation cases is provided in the following section.

8.2.2.1. One DPM source (one FEL) at one location (Case 1). This particular simulation case used a 280 kW CAT FEL as a DPM source which is located near the dead-end. Several scenarios that have different combinations of duct diameter, duct inlet velocity, and air quantity were simulated for this case. The simulations results are described in a Section 8.3. A schematic layout for Case 1 is shown in Figure 8.2.

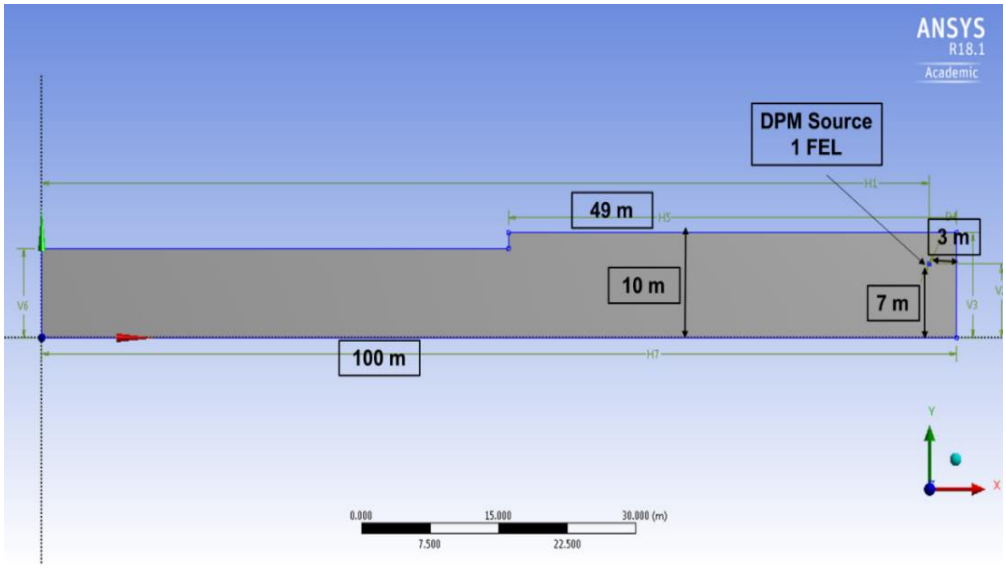

Figure 8.2 Case 1 model configuration

8.2.2.2. Effect of duct advancement on DPM (Case 1A). In this particular case, the inlet of the ventilation duct is moved 50% closer to the DPM source as compared to Case 1. The duct inlet was moved closed to the dead-end and DPM source in order to determine the effect of duct advancement on DPM concentrations. The effect of extending duct inlet with respect to the DPM source is assessed by comparing the simulation results of Case 1 and Case 1A. The geometric configuration of Case 1A is shown in Figure 8.3, whereas a comparison of Case 1 and Case 1A is discussed in Section 8.3.2.

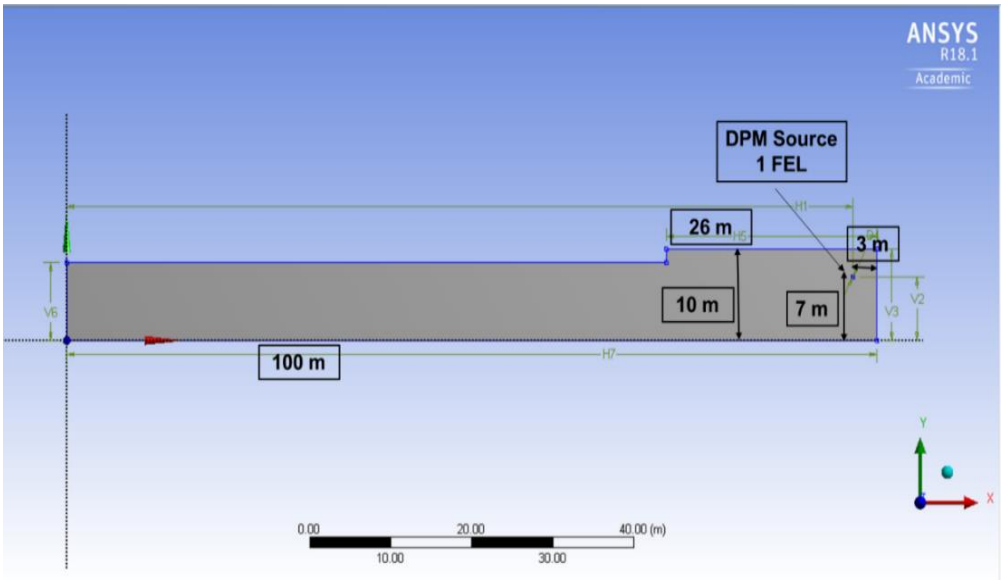

Figure 8.3 Case 1A model configuration

8.2.2.3. One DPM source (two FEL) at one location (Case 2). This case simulates two pieces of CAT FEL each with a power of 280 kW. Both front-end loaders were assumed to work at one location (close proximity), for simplicity, a single point source is used to represent both front-end loaders. The location of the DPM source is similar to the Case 1. Simulation scenarios similar to Case 1 have been performed. Simulation results for Case 2 are described in Section 8.3. A schematic layout for Case 2 is shown in Figure 8.4.

8.2.2.4. Two DPM sources (two FEL) at two locations (Case 3). This particular case has two DPM sources at two different location in the mine entry model. Each location assumes one FEL of 280 kW power, thus a total of two front-end loaders were used for DPM generation. The location of both DPM sources in the model and schematic diagram is shown in Figure 8.5. Several simulation scenarios similar to Case 1, Case 1A and Case

2 were performed for Case 3. Simulation results and their details are described in Section 8.3.2.

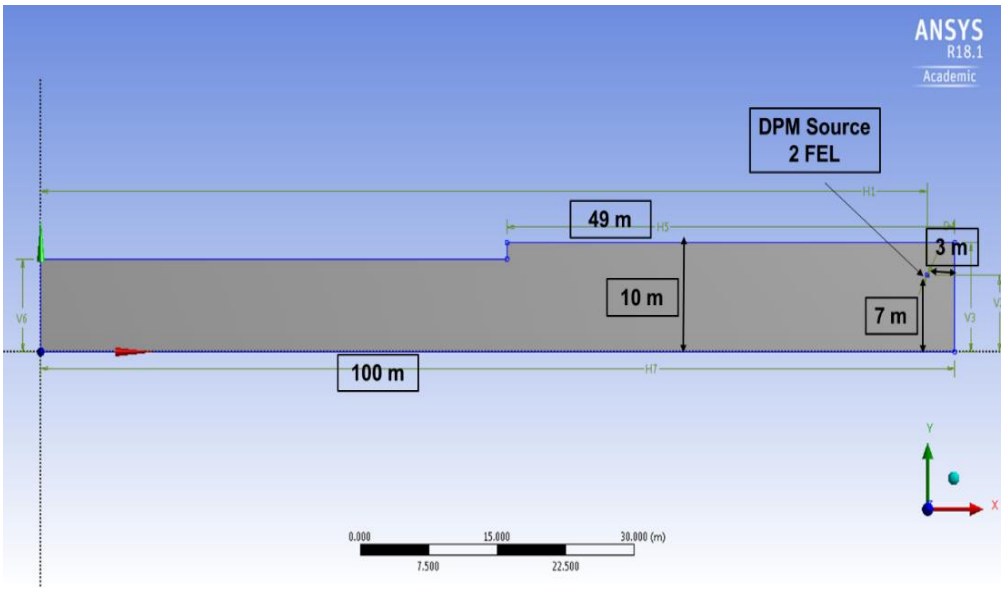

Figure 8.4 Case 2 model configuration

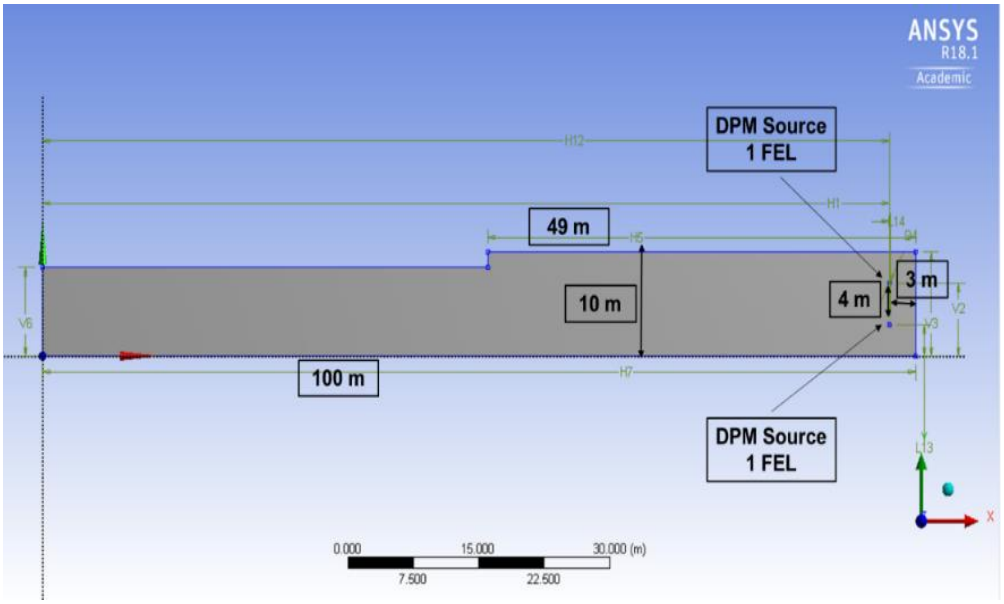

Figure 8.5 Case 3 model configuration

8.2.3. CFD Model Formulation. Different aspects of CFD model formulation are discussed below:

8.2.3.1. Model assumptions. Based on various studies (Thiruvengadam, Zheng, Lan, et al., 2016; Thiruvengadam, Zheng, & Tien, 2016; Yi Zheng et al., 2011; Yi Zheng et al., 2017; Yi Zheng, Thiruvengadam, et al., 2015a; Yi Zheng, Thiruvengadam, et al., 2015b; Yi Zheng, Thiruvengadama, et al., 2015; Y Zheng & Tien, 2008), this particular 2D CFD model was generated under the following assumptions: (1) DPM was considered as a gas; (2) the species transport model was used and the chemical reactions between species were not considered; (3) n-octane vapor (C_8H_{18}) is selected to be the representative of DPM; (4) both air and DPM are considered to be incompressible; (5) fluid flow is considered to be steady and simulations were solved for steady state solution; (6) all DPM sources are fixed at particular locations in the model geometry; (7) all DPM sources have constant DPM emission rate; (8) the fluid flow in the domain is fully turbulent.

8.2.3.2. Model settings. The solver settings are based on the recommendations of FLUENT, previous similar studies, and test run simulations. A 2D model is selected with pressure based solver, whereas velocity formulation was set at absolute. Models are assumed to be steady state, with gravity was turned off. In ANSYS FLUENT model setting options energy equation and specie transport were used, whereas standard k-ε model with standard wall functions was selected. In species transport, two species: DPM (C_8H_{18}) and air were included with no provision for chemical reaction.

8.2.3.3. Solution methods and convergence approach. The numerical solution of governing equations and boundary conditions were conducted using ANSYS FLUENT 18.1. Default pressure velocity coupling scheme with coupled algorithm is used for

simulations. In spatial discretization least square cell based option was used. This scheme is least computationally intensive and it performs well using structured meshes. Pressure was kept at standard, momentum, energy, and species transport were selected as second order upwind. Discretization scheme for turbulent kinetic energy and turbulent dissipation rate were selected as first order upwind. Standard initialization of the solution was used and initialization parameters were computed from the air inlet with reference frame set at relative to cell zone option. Simulations were run until achieving steady state solutions and all solutions were converged. At convergence overall mass flow balances at inlet, outlet, and DPM sources have been determined and found satisfactory for all simulations.

8.2.3.4. Boundary conditions. Since multiple simulation scenarios were covered in this Section, some of the boundary conditions remained constant for all scenarios, whereas some varied. A general summary of adopted boundary conditions is described in the Table 8.1.

Table 8.1 Boundary conditions summary

	Boundary	**Details**
Inlet	Velocity inlet	Normal to boundary, velocity magnitude varies case by case. (10 m/s, 15.5 m/s, 22.4 m/s). DPM mass fraction 0.
Outlet	Pressure outlet	(0 Pa), normal to boundary.
Walls	Walls	Stationery walls, no slip, standard.
DPM Source	Mass flow inlet	Normal to boundary, varies case by case (0.451 kg/s and 0.902 kg/s). DPM mass fraction 0.00093.

8.2.4. Meshing of CFD Model. ANSYS meshing module was used for model mesh generation. Sections of the model geometry were meshed using edge and face sizing controls, mapped face controls and inflation layers option was used for smooth transition wherever applicable. Proximity and curvature option is used for size function, relevance angle and span angle center options were selected to be medium. Faces and edges option was opted for proximity size function sources. Minimum face size and proximity minimum size was chosen to be 0.05 m, whereas default option was selected for minimum size and growth rate. Automatic mesh bases disfeaturing was turned on with default disfeature size. Skewness of 0.9 was achieved by selecting automatic option, whereas inflation option was set at smooth transition. Finally mesh morphing was enabled and pinch tolerance was set at default value. For all CFD models and scenarios, at the selected mesh, there are over 0.74 million nodes. Figure 8.6 shows representative model meshing, Figure 8.7 displays mesh configuration at inlet. Figure 8.8 shows meshing at outlet and model surface body. Figure 8.9 shows meshing setup around DPM point source.

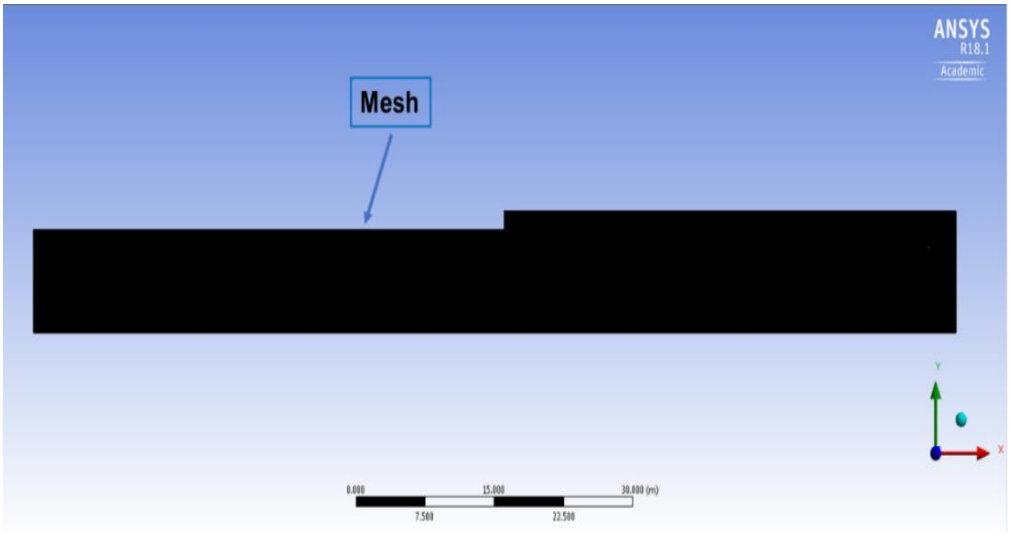

Figure 8.6 Representative model meshing

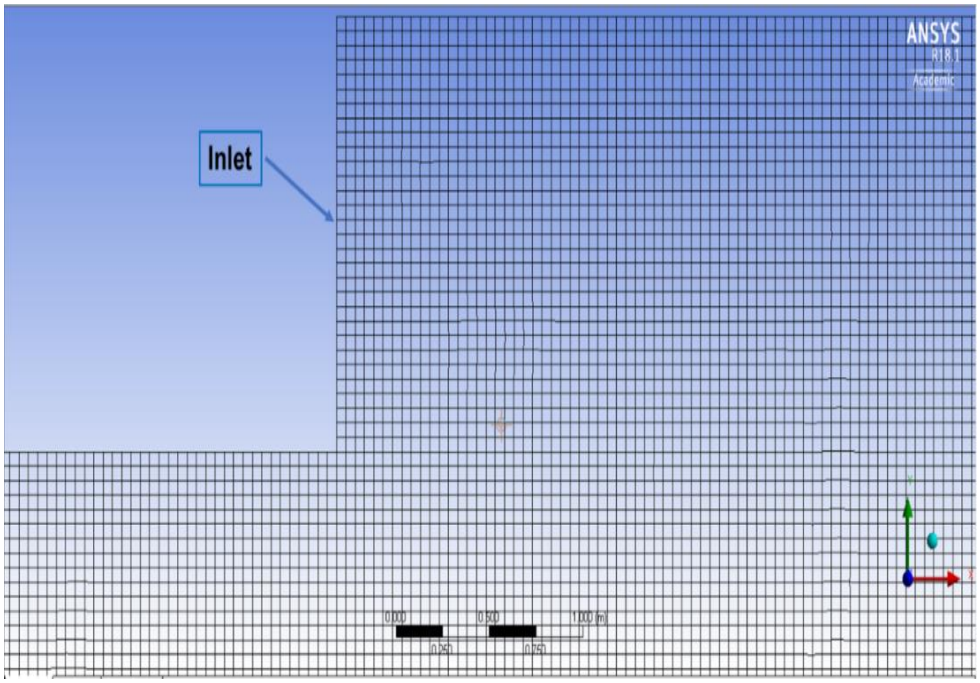

Figure 8.7 Model meshing at inlet

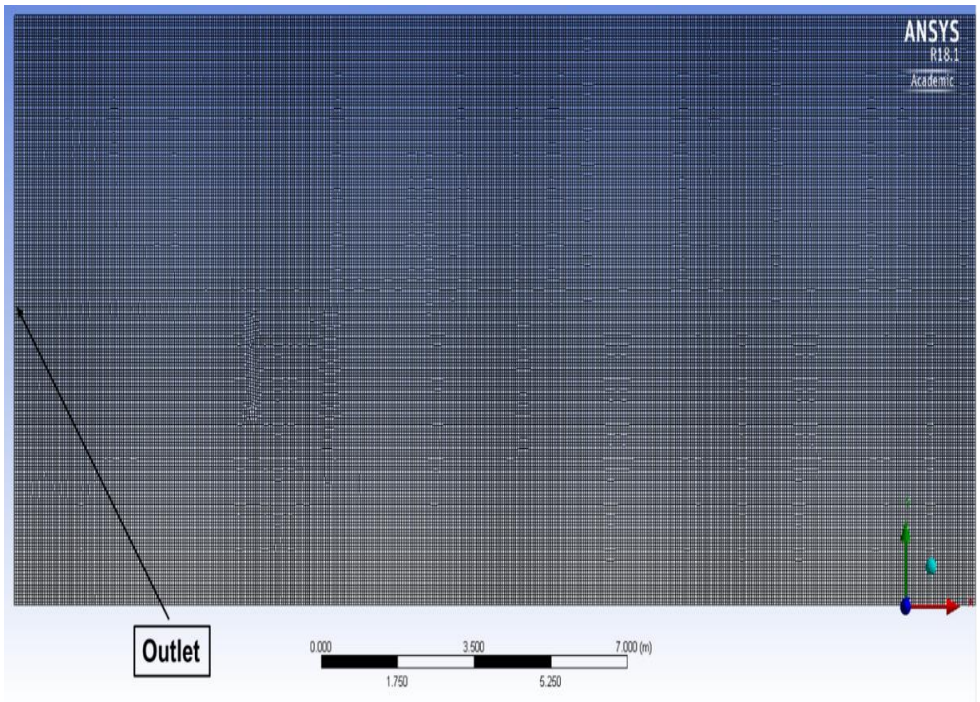

Figure 8.8 Model meshing at outlet and surface body

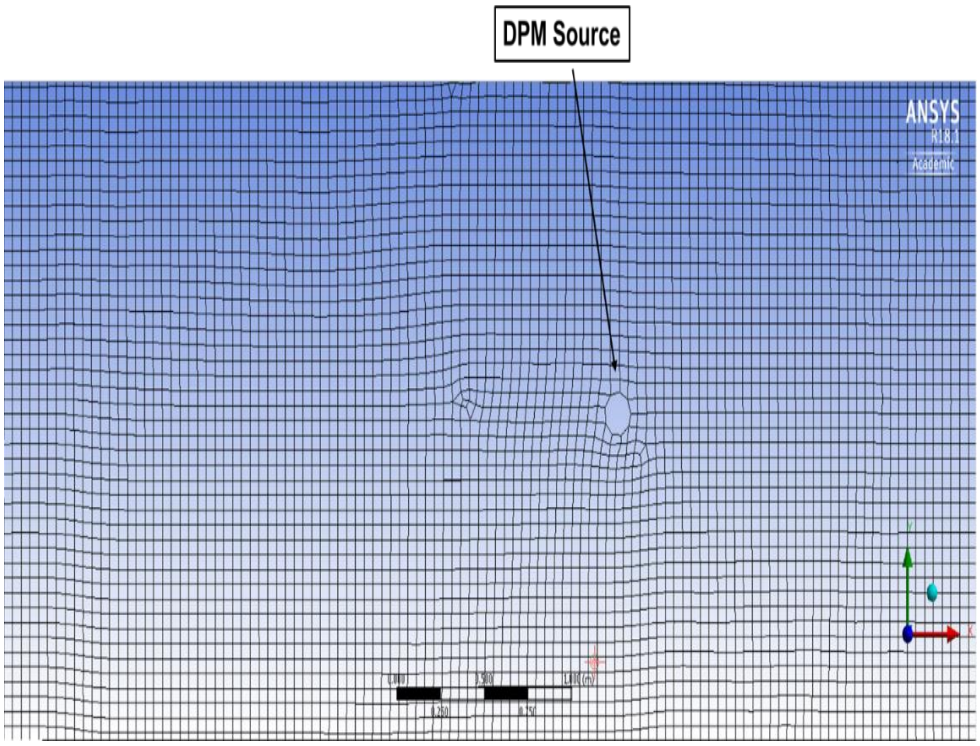

Figure 8.9 Model meshing near DPM source

Study of mesh independence: Meshing effects the results of a CFD model. A CFD model is considered to be independent of mesh size if solution results does not change by decreasing mesh size. A CFD model can be considered reliable only if model solution does not depend upon mesh size. In this particular study a number of different sized meshes were generated and their results were compared. During mesh independence study, a range of minimum face size and proximity minimum size was chosen. The selected sizes were 0.15 m, 0.1 m, 0.075 m, 0.06 m, 0.05 m, 0.04 m, and 0.03 m. In order to check the mesh independence, a simulation case was selected that has constant duct inlet velocity (15.5 m/s), duct diameter (1.5 m), and a DPM source (one FEL). Horizontal velocity (u) profiles were plotted at three 'x' values (0 m, 30 m, and 60 m) for different sized meshes. The number of nodes for different selected meshes ranges from 0.084 million to over 2 million.

It was observed that velocity profiles showed similar trends whenever the mesh contained more than 0.33 million nodes. Thus a base mesh was selected that have 0.74 million nodes. Figure 8.10 shows horizontal velocity profiles that were plotted for different 'x' values (0 m, 30 m and 60 m). In Figure 8.10 fine mesh corresponds to the mesh that has over 1 million nodes, whereas finest mesh contains more than 2 million nodes. It is evident from Figure 8.10 that the velocity profiles follow similar trends for all selected meshes.

Figure 8.11 shows the horizontal velocity contours for the base mesh, whereas similar contours for the finest sized mesh is shown in Figure 8.12. It can be seen from Figure 8.11 and Figure 8.12 that the overall velocity contours for base mesh behave similar to the finest mesh and simulation results were not affected by reduction in mesh size.

Mesh independence is also assessed by plotting the decay in horizontal air velocity against the distance covered in x-direction (longitudinal direction of mine). Decay in horizontal velocity is plotted because the stream of air that flows out of the ventilation duct is similar to a jet stream. Since this air stream has a wall on one side of the duct, therefore it can be viewed as a classic wall jet velocity. Decay in horizontal velocity is plotted against distance covered by the jet in longitudinal direction (x-axis) for the base mesh (0.74 million) and for other two meshes that have 1.1 million (fine mesh), and 2.04 million nodes (finest mesh), respectively. All plots showed similar decay of jet velocity. The 2D solution of wall jet velocity case determined by (Glauert, 1956) suggests similar trends for decay in the jet velocity. This showed that the selected mesh and model input parameters were appropriate and independent of mesh size. Figure 8.13 shows the plot of decay in maximum horizontal velocity versus distance covered in x direction for the base mesh, whereas similar plots of other two mesh sizes are shown in Figure 8.14 and Figure 8.15.

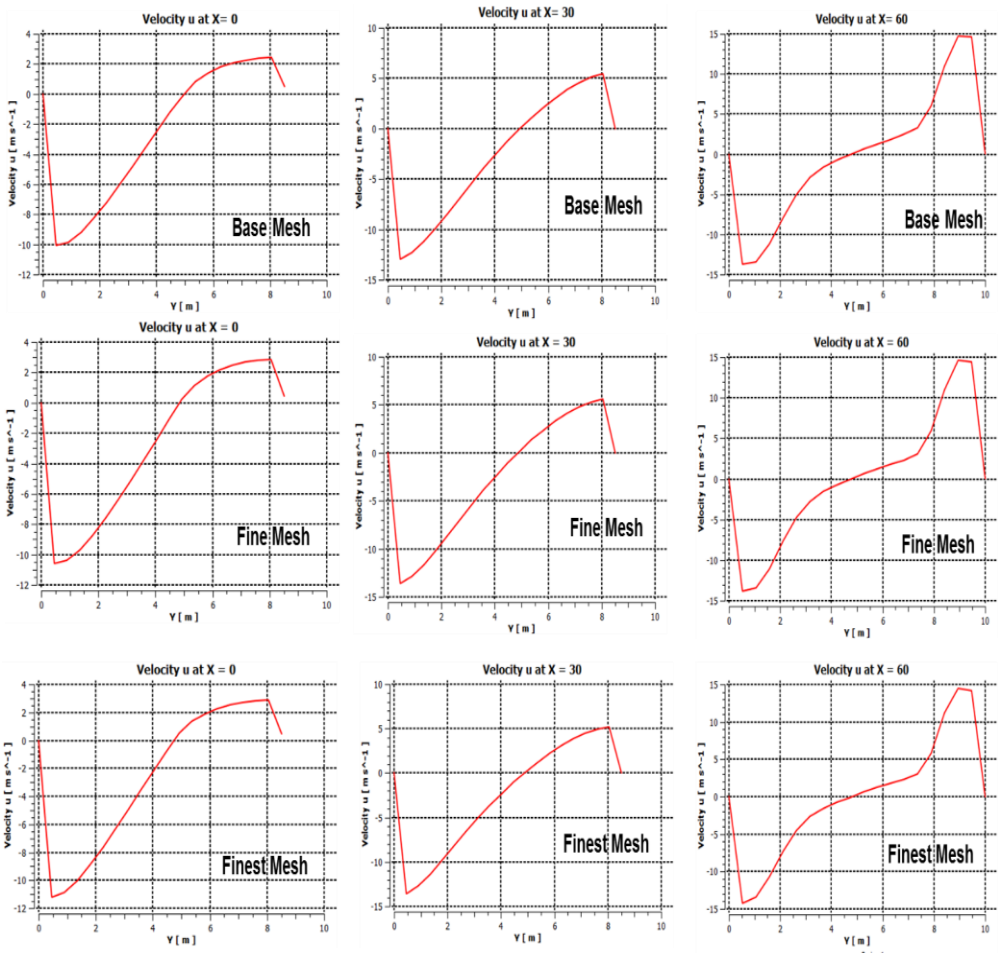

Figure 8.10 Horizontal velocity (u) profiles for base, fine, and finest mesh

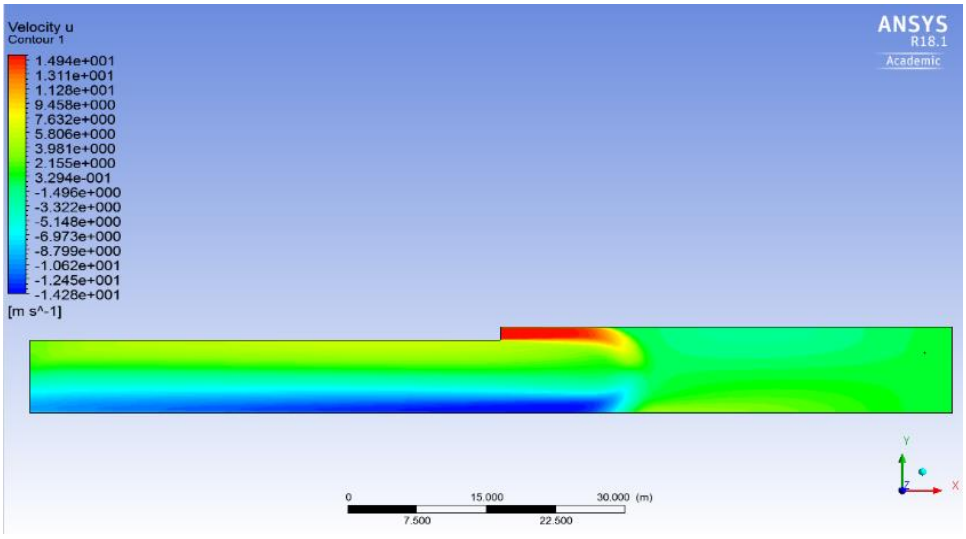

Figure 8.11 Horizontal velocity contours for base mesh (0.74 million nodes)

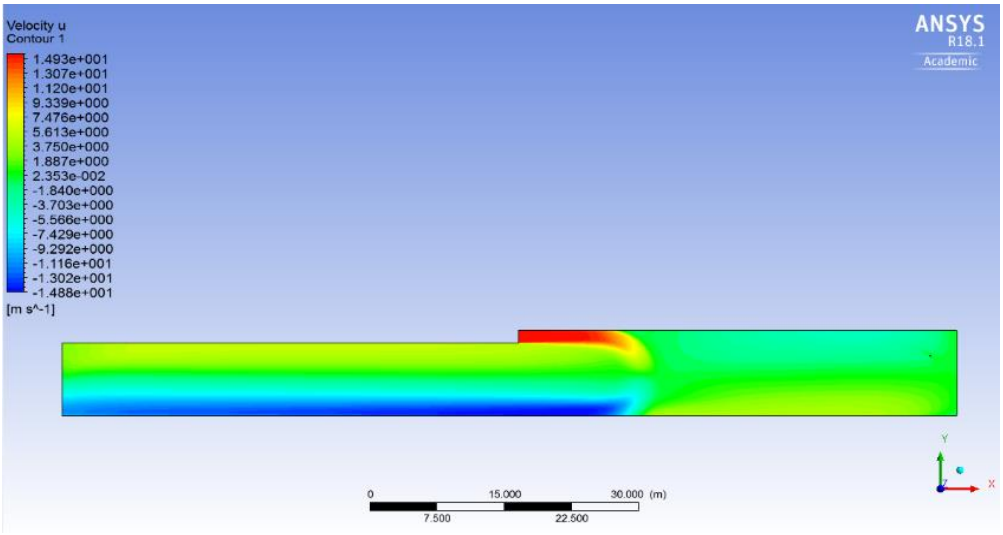

Figure 8.12 Horizontal velocity contours for finest mesh (2.04 million nodes)

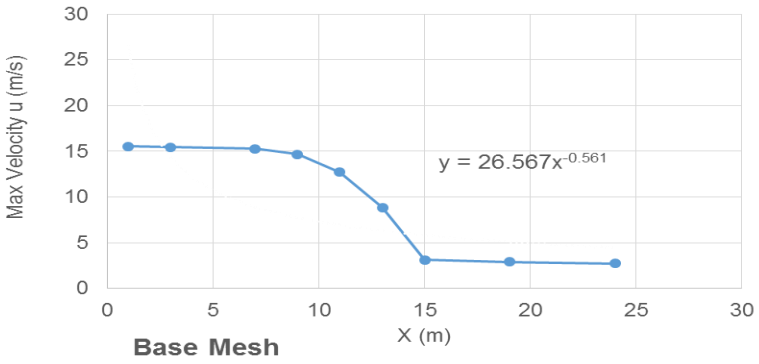

Figure 8.13 Maximum horizontal velocity vs distance in x direction for base mesh

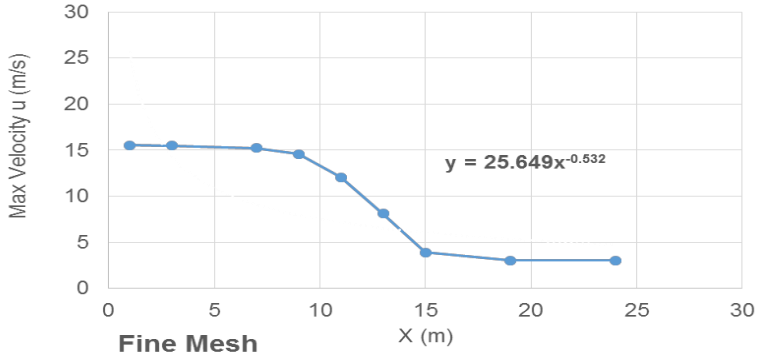

Figure 8.14 Maximum horizontal velocity vs distance in x direction for fine mesh

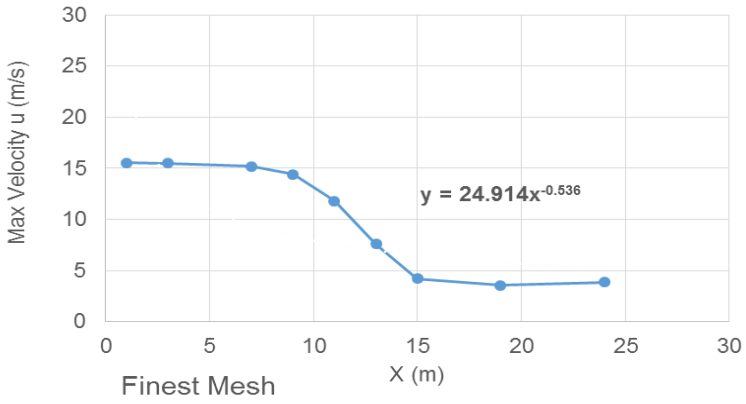

Figure 8.15 Maximum horizontal velocity vs distance in x direction for finest mesh

8.3. RESULTS AND DISCUSSIONS

The effect of ventilation parameters on a mine dead-end entry was evaluated by performing several CFD simulations. Four simulations cases (as described in Section 8.2.2) were studied. Each case comprises seven different combinations of duct inlet air velocity, duct diameter, and the air quantity. For the sake of simplicity in discussion, simulation combinations were arbitrarily named as S1, S2, S3, S4, S5, S6 and S7. The detail of simulation parameters and their names are described in Table 8.2.

Cumulative DPM mass fraction plots are examined for each simulation of all cases. For each studied case in all simulation scenarios, it was noticed that increase in accumulated DPM mass fraction occurred only within 40 m distance from the face (work zone). Figure 8.16 shows some representative plots of accumulative DPM mass fraction for various cases and scenarios. It is evident from Figure 8.16 that DPM concentrations became almost constant after about 40 m distance from the face.

Table 8.2 Simulations parameters combinations

	Duct Diameter (m)	Inlet Air Velocity (m/s)	Air Quantity (m^3/s)
S1	1.5	15.5	23.6
S2	1.5	22.4	33.9
S3	1.5	10.0	15.4
S4	1.85	15.5	28.9
S5	1.25	15.5	19.5
S6	1.25	22.4	28.9
S7	1.85	10.0	19.5

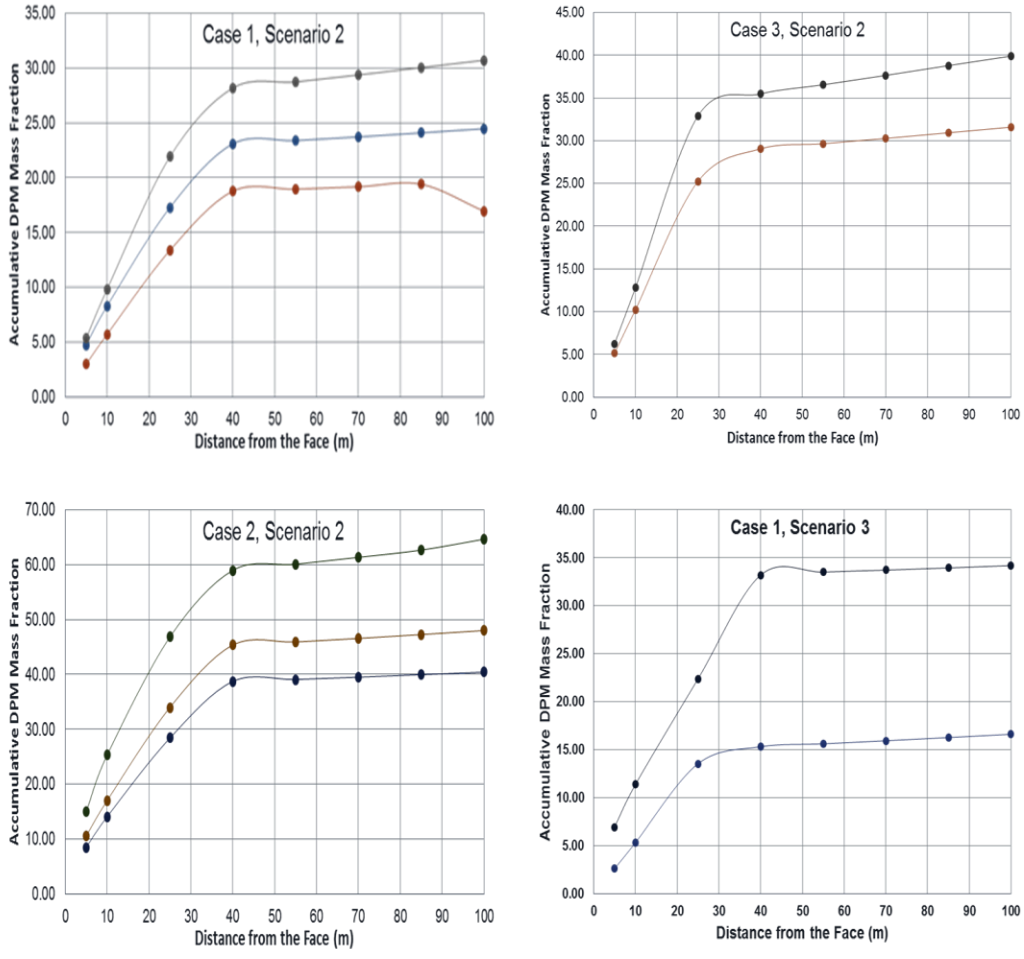

Figure 8.16 Accumulative DPM mass fraction for various scenarios and cases

The rise in cumulative DPM mass fractions for all simulation cases became almost zero after around 40 m distance from the face. This happened because DPM particles seemed to be mixed uniformly with the fresh air stream at around 40 m distance from the face. Since no rise in DPM concentrations after about 40 m distance from the mine face was observed, DPM concentration for Case 1, Case 3 and Case 1A were quantitatively evaluated by computing average DPM concentrations for a 40 m work zone from the face. Since Case 2 and Case 3 simulation results were found similar (discussed in a later Section 8.3.2.2), therefore the average DPM concentrations were not computed for Case 2.

8.3.1. Simulation Scenarios. For each case, simulations were categorized into three scenarios. Each scenario includes simulations that have varying ventilation parameters. Scenario 1 determines the effect of change in inlet air quantity by changing the duct diameter at a constant duct inlet velocity. In scenario 2 the effect of change in air quantity is achieved by changing the duct inlet velocity at a constant duct diameter. Scenario 3 assesses the best combinations of inlet air velocity and the duct diameter at constant air quantity. All three scenarios and their results are discussed in the following section

8.3.1.1. Constant duct inlet velocity (Scenario 1). Constant duct inlet velocity CFD simulations were performed for three different velocities. Duct inlet velocities were divided into three categories; (i) low (10.0 m/s), (ii) intermediate (15.5 m/s) and high (22.4 m/s). For each category of the inlet air velocity, a minimum of two different duct diameters were used. The air quantity in each simulated case was changed by changing the diameter of duct. For each case (Case 1, Case 1A, Case 2 and Case 3), seven simulations were

performed for three different air velocities. The details of simulations were described in Table 8.3.

Figure 8.17 shows concentration plots of accumulative DPM mass fractions versus distance from the face for simulations that have 10.0 m/s inlet air velocity. Figure 8.17 shows that for a constant duct velocity, large duct diameter and large quantity produces high accumulative DPM mass fraction. Figure 8.18 shows the work zone's average DPM concentrations for scenario 1 for Case 1, Case 1A and Case 3 at 10 m/s inlet air velocity. Figure 8.18 shows that the average DPM concentrations were increased with increasing duct diameter at a constant velocity. Thus an increase in air quantity achieved by increasing the duct diameter has increased the DPM concentrations in all cases.

Table 8.3 Constant inlet air velocity simulation combinations

	Inlet Air Velocity (m/s)	**Duct Diameter (m)**	**Air Quantity (m^3/s)**
1	10.0	1.85	19.5
		1.5	15.4
2	15.5	1.25	19.5
		1.5	23.6
		1.85	28.9
3	22.4	1.25	28.9
		1.5	33.9

Figure 8.19 shows Case 1 plots of accumulative DPM mass fraction versus distance from the work face at 15.5 m/s duct inlet velocity. Figure 8.20 shows average DPM concentrations at the work zone for Case 1, Case 1A, and Case 3. Plots from Figure 8.19 and Figure 8.21 show that at a fixed duct inlet velocity, large duct diameter and higher air quantity resulted in high DPM in the area. This showed that for a constant inlet velocity, less duct inlet diameter dilutes DPM more efficiently.

Figure 8.21 represents accumulative DPM mass fraction profiles of Case 1 that are plotted against distance from the work face at 22.4 m/s inlet air velocity. Figure 8.22 shows average DPM concentrations at work zone for Case 1, Case 1A, and Case 3. The trends of all plots in Figure 8.21 and Figure 8.22 were similar to other constant velocity simulations that high DPM concentrations were observed with bigger duct diameter and large air quantities.

It is evident from scenario 1 simulations that for a constant duct inlet velocity, less duct inlet diameter results less DPM concentrations and a better quality of air. This means, although an increase in duct diameter increases the quantity of mine air, however, it does not improve mine air quality, rather it is counterproductive. Apparently it seem peculiar, as a ventilation engineer may assume that an increased air quantity will always improve the quality of the mine air. Simulation results from all cases (Case 1, Case 1A, Case 2 and Case 3) suggest that an increase in air quantity by enlarging duct diameter did not reduce DPM concentrations in a mine entry. Since Case 1A, Case 2, and Case 3 have shown trends that are very similar to Case 1, thus accumulative DPM mass fraction plots for these cases are not included in this Section.

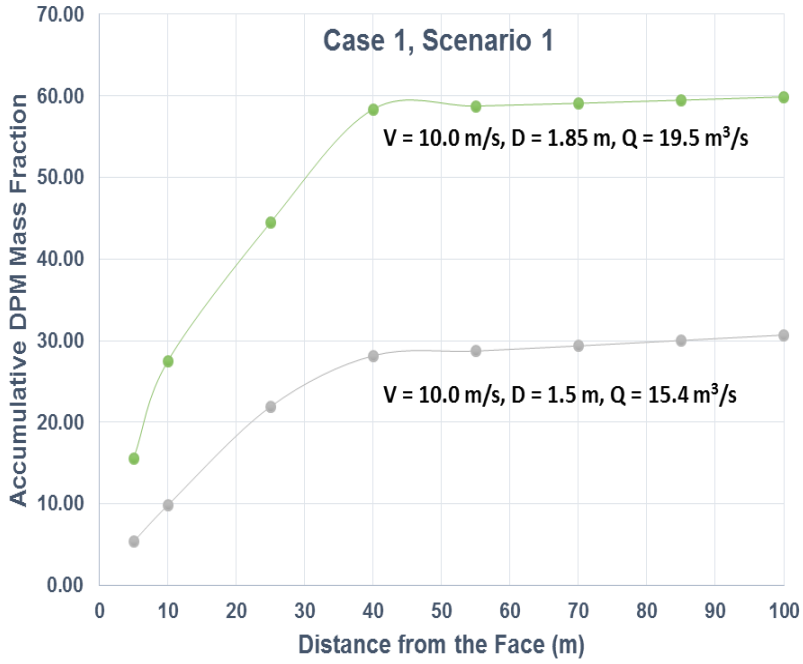

Figure 8.17 Accumulative DPM mass fraction versus face distance (10.0 m/s)

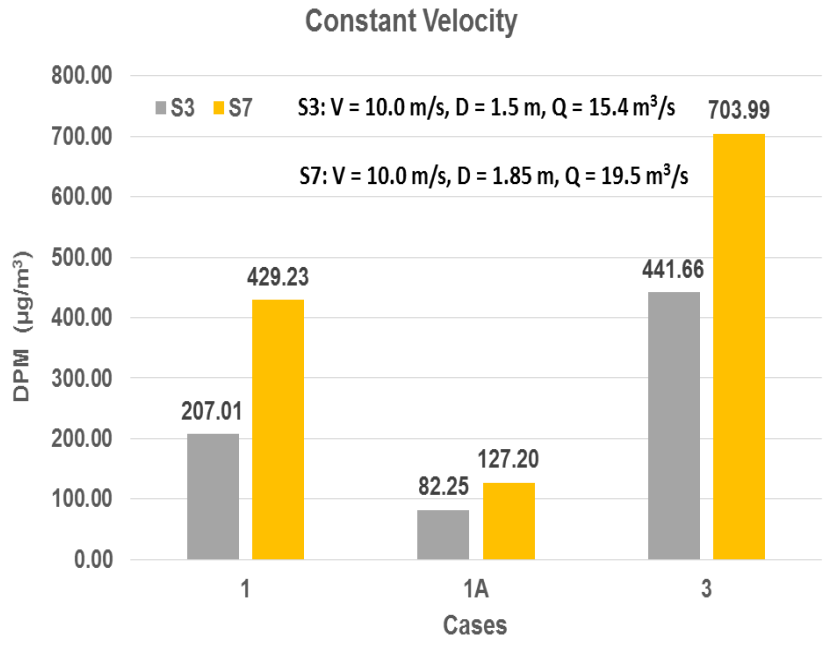

Figure 8.18 Average DPM for Case 1, Case 1A and Case 3 (10.0 m/s)

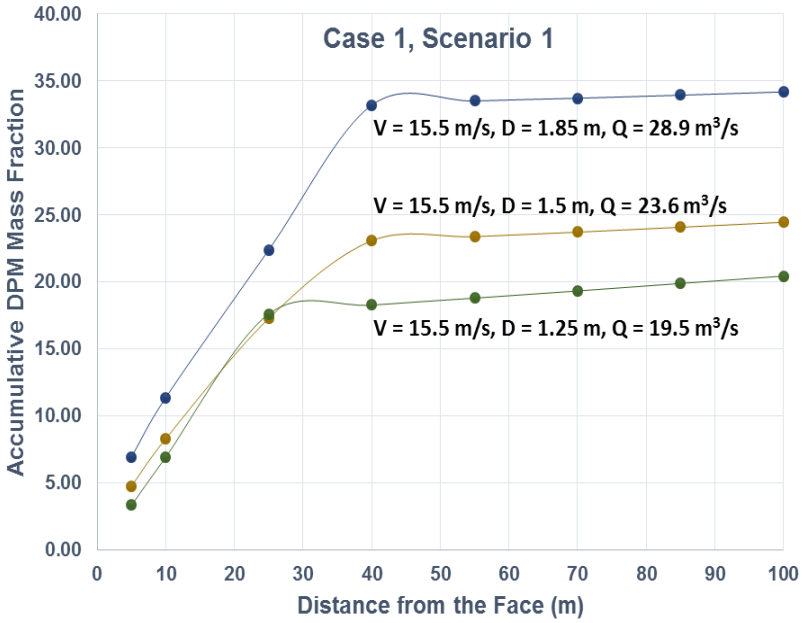

Figure 8.19 Accumulative DPM mass fraction versus face distance (15.5 m/s)

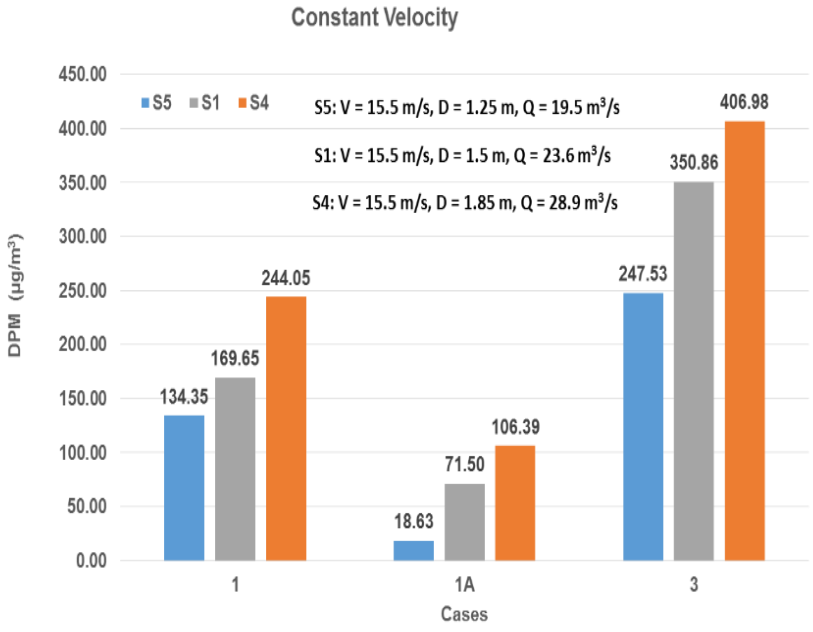

Figure 8.20 Average DPM for Case 1, Case 1A and Case 3 (15.5 m/s)

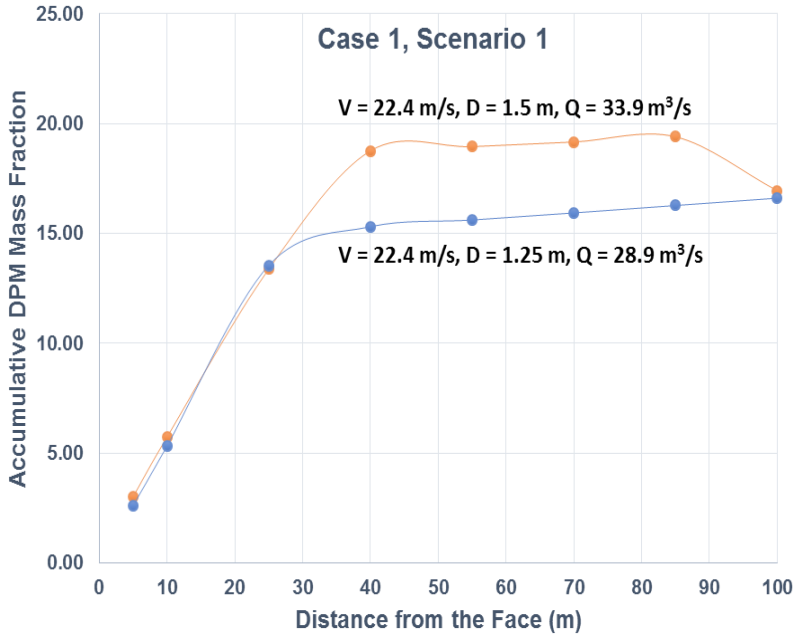

Figure 8.21 Accumulative DPM mass fraction versus face distance (22.4 m/s)

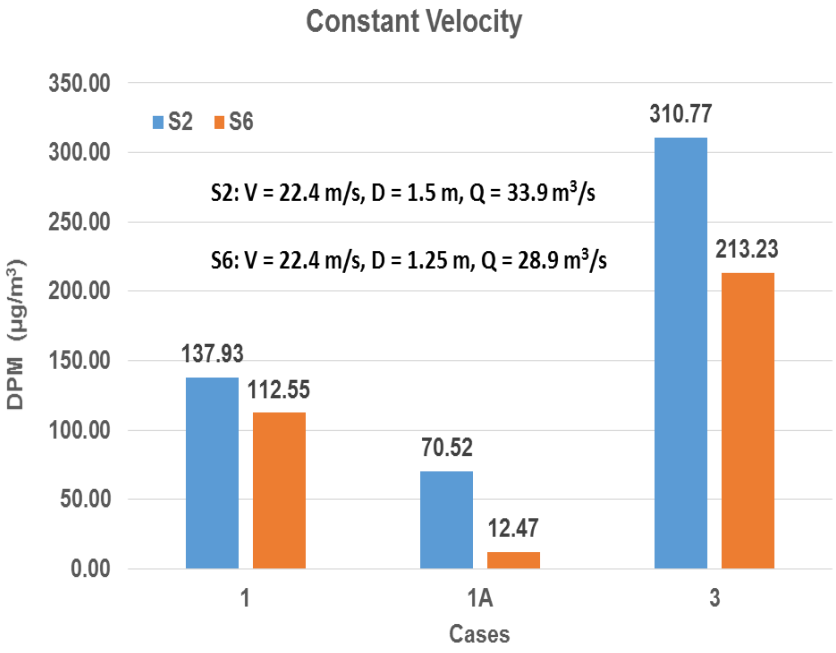

Figure 8.22 Average DPM for Case 1, Case 1A and Case 3 (22.4 m/s)

8.3.1.2. Constant duct inlet diameter (Scenario 2). The effect of change in the quantity of air by changing duct inlet velocity is determined in another set of CFD simulations. Three sizes of ventilation ducts were selected, the diameter of selected ducts were 1.25 m, 1.5 m, and 1.85 m. A minimum of two different velocities were simulated for each sized duct. All combinations of air velocities and duct diameters resulted in total of seven simulations. Detail of simulation combinations are presented in Table 8.4.

Table 8.4 Constant duct inlet diameter simulation combinations

	Duct Diameter (m)	**Inlet Air Velocity (m/s)**	**Air Quantity (m^3/s)**
1	1.25	15.5	19.5
		22.4	28.9
2	1.5	10.0	15.4
		15.5	23.6
		22.4	33.9
3	1.85	10.0	19.5
		15.52	28.9

The relationship between accumulative DPM mass fraction and distance from the face for 1.25 m diameter duct for Case 1 is shown in Figure 8.24. Average DPM concentrations for work zone with 1.25 m diameter duct were computed. Figure 8.25 shows the average computed DPM concentrations for Case 1, Case 1A, and Case 3. Results from Figure 8.23 and Figure 8.24 showed that an increase in air quantity that is achieved by increasing duct inlet velocity removes DPM efficiently. Thus high duct inlet velocity results in less DPM concentrations and a better quality of mine air.

Constant velocity simulation results for 1.5 m diameter duct were plotted. Figure 8.25 shows the accumulative DPM mass fraction plots for Case 1 and Figure 8.26 shows the average DPM concentrations for Case 1, Case 1A, and Case 3. Figure 8.25 and Figure 8.26 results show that for a fixed duct diameter, higher velocity reduced DPM concentrations more efficiently as lowest DPM was observed when the duct inlet velocity was maximum.

Figure 8.27 and Figure 8.28 present constant velocity results from 1.85 m duct diameter. Figure 8.27 shows accumulative DPM mass fraction plotted against distance from the face. Figure 8.28 shows work zone average DPM concentrations for Case 1, Case-1A, and Case 3. Similar to other constant duct diameter cases, higher velocity and higher quantity produced better quality mine air.

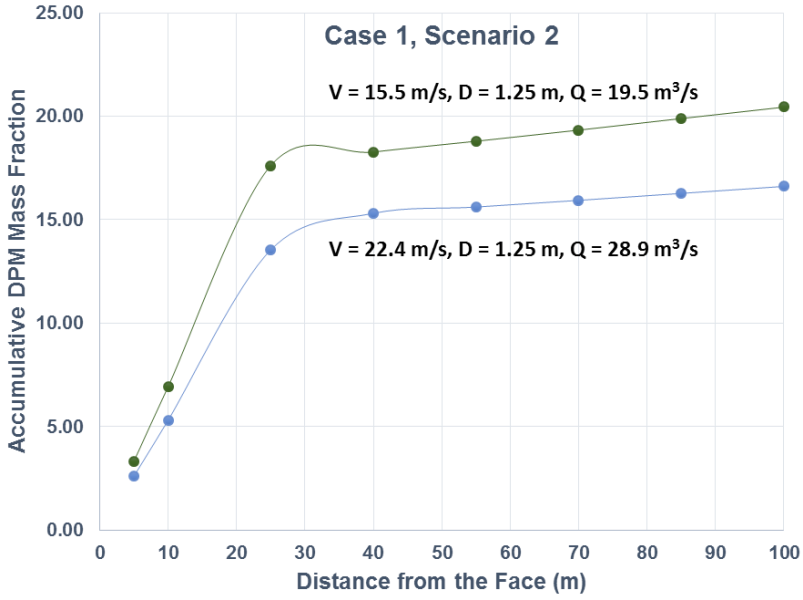

Figure 8.23 Accumulative DPM mass fraction versus face distance (1.25 m)

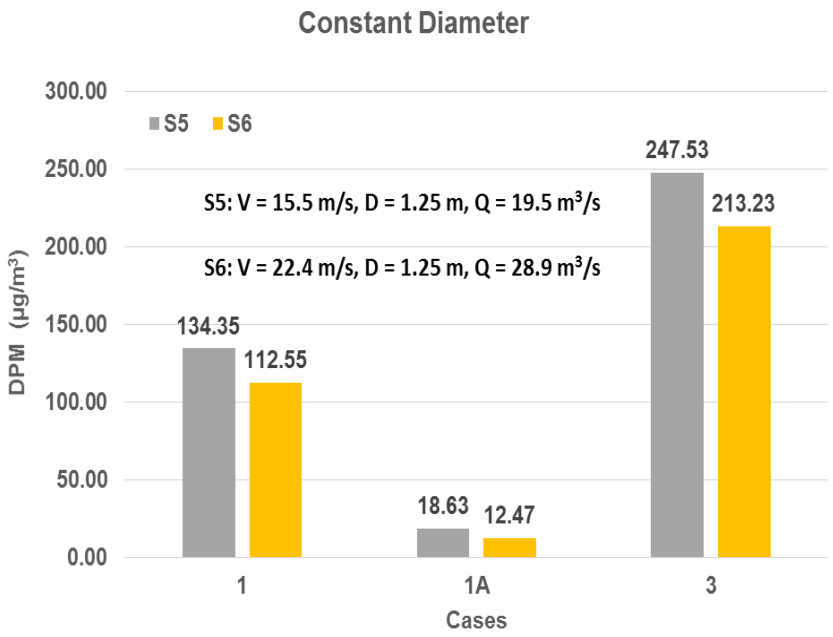

Figure 8.24 Average DPM for Case 1, Case 1A and Case 3 (1.25 m)

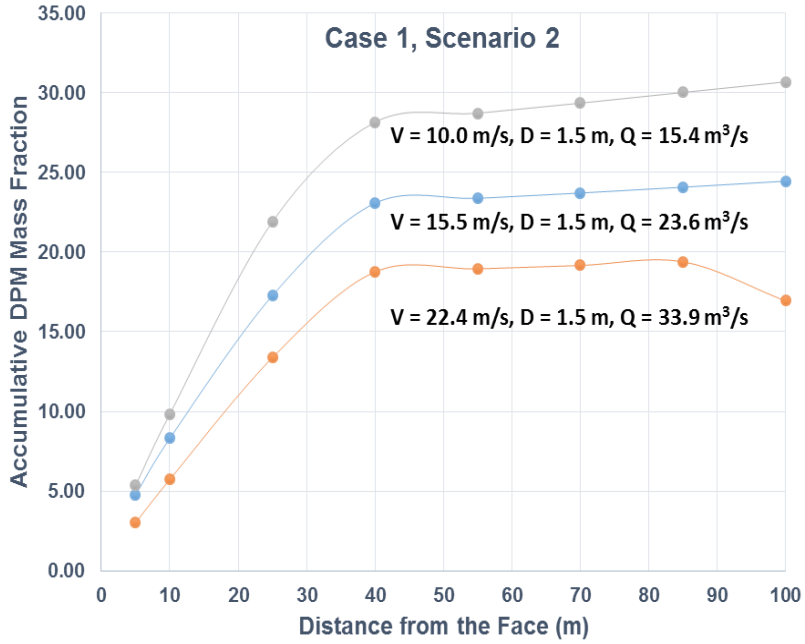

Figure 8.25 Accumulative DPM mass fraction versus face distance (1.5 m)

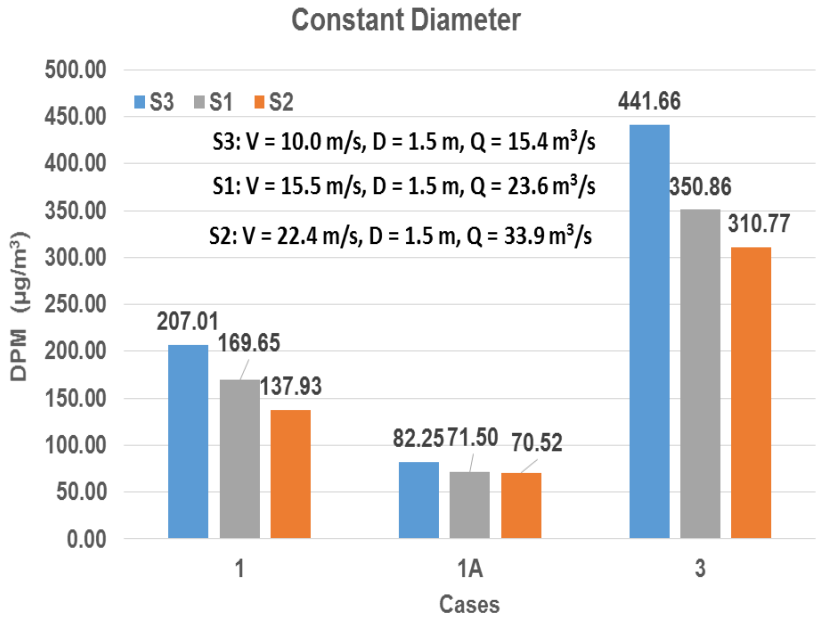

Figure 8.26 Average DPM for Case 1, Case 1A and Case 3 (1.5 m)

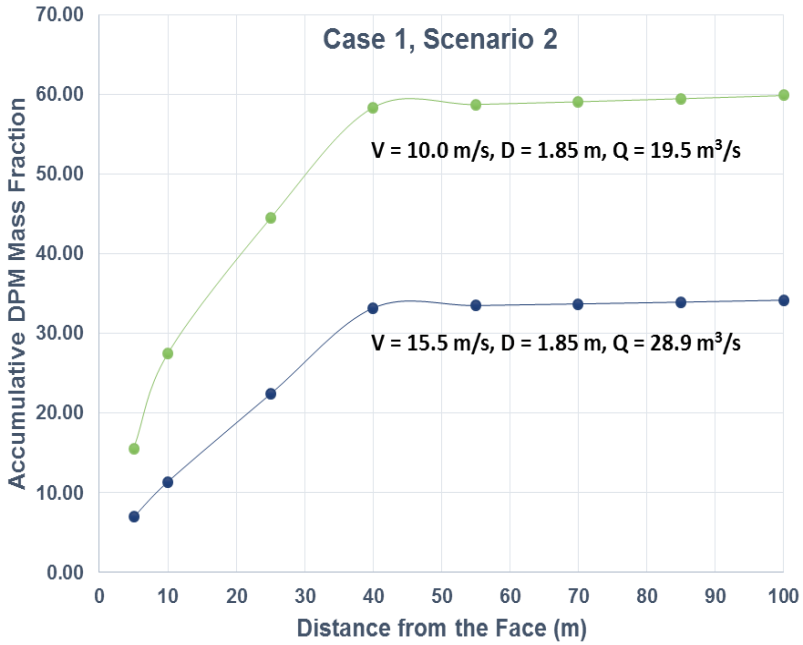

Figure 8.27 Accumulative DPM mass fraction versus face distance (1.85 m)

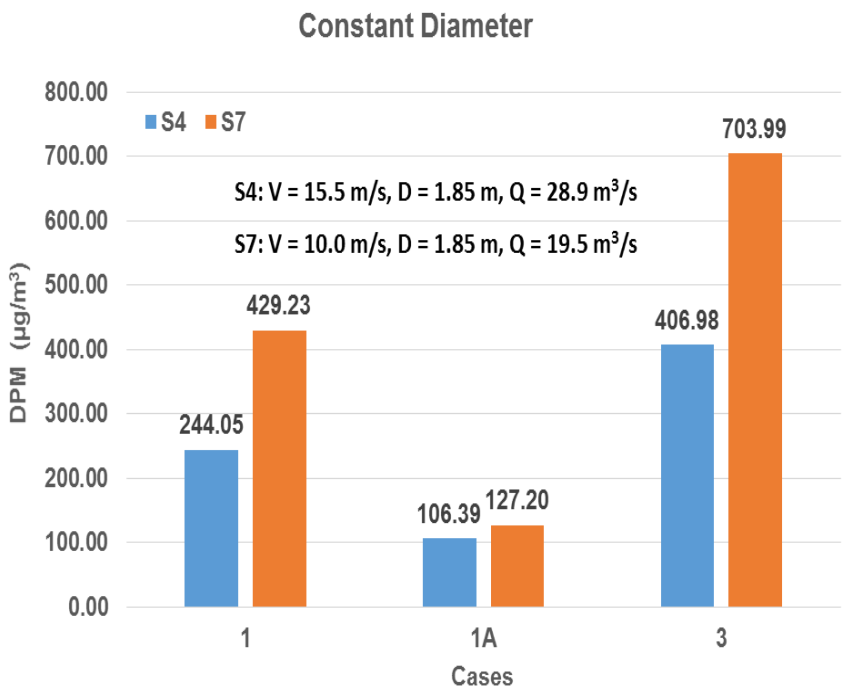

Figure 8.28 Average DPM for Case 1, Case 1A and Case 3 (1.85 m)

It was noticed from all constant duct diameter plots that for a fixed duct diameter, best quality mine air is achieved with high duct inlet air velocity. Results indicate that best dilution of DPM concentrations was achieved, if increase in air quantity is achieved by increasing duct inlet velocity. This trend is opposite to what was observed in constant duct inlet velocity scenario where higher air quantities leaves high DPM levels. Thus we conclude that an approach in which higher flow rates are achieved by enlarging duct diameter without increasing duct inlet velocity is counterproductive and increases DPM at work areas. A comparison of scenario 1 and scenario 2 results showed that an increase in air quantity is beneficial only, if that is achieved by increasing the duct inlet velocity. Scenario 2 plots of accumulative DPM mass fraction for Case 1A, Case 2 and Case 3 showed trend very similar to Case 1, therefore these plots are not included in this Section.

8.3.1.3. Constant inlet air quantity (Scenario 3). Constant air quantity cases were simulated for two distinct air quantities. Constant quantity is achieved by changing the duct diameter and duct inlet air velocity simultaneously. Two values of air quantities (19.5 m^3/s and 28.9 m^3/s) were selected for simulations. For each value of a constant quantity, two combinations of duct inlet velocity and diameter were used. A total number of four simulations were performed for each case. The details of simulated cases are described in Table 8.5.

Table 8.5 Constant inlet air quantity simulation combinations

	Air Quantity (m^3/s)	**Inlet Air Velocity (m/s)**	**Duct Diameter (m)**
1	19.5	10.0	1.85
		15.5	1.25
2	28.9	15.5	1.85
		22.4	1.25

Figure 8.29 shows the accumulative DPM mass fraction and Figure 8.30 shows the average DPM concentrations at work zone for air quantity of 19.5 m^3/s. Figure 8.29 contains mass fraction plots for Case 1, whereas Figure 8.30 contains average DPM concentrations for Case 1, Case 1A and Case 3. For a fixed air quantity, high DPM is observed when duct inlet velocity was low and duct diameter was large, whereas high inlet velocity and low duct diameter resulted in low DPM concentrations.

Figure 8.31 shows accumulative DPM mass fraction plotted against distance from the face. Figure 8.32 presents work zone's average DPM concentrations for Case 1, Case

1A and Case 3. Both Figure 8.31 and Figure 8.32 were plotted for constant inlet air quantity (28.9 m^3/s). Results showed that low DPM is observed with high inlet velocity. This trend is similar to what has been observed for air quantity of 19.5 m^3/s that higher velocity results better air quality. Accumulative DPM mass fraction plots for other Case 1A, Case 2, and Case 3 have shown similar trends, therefore these plots are not included in this Section.

8.3.2. Comparison of Simulation Cases. Comparisons of different simulations cases are discusses below:

8.3.2.1. Comparison of Case 1 and Case 1A. Results from all seven simulations for Case 1 and Case 1A are compared. Figure 8.33 shows a comparison of both cases (Case 1 and Case 1A). The accumulative DPM mass fractions are significantly reduced by advancing ventilation duct towards the DPM source. It is evident from Figure 8.33 that advancement of the duct inlet has reduced DPM concentrations to a great extent. In some simulations the reduction was up to 80%, whereas some results showed 50% reduction in DPM. Comparison results showed that DPM in a mine dead-end entry can be efficiently reduced by advancing the duct inlet close to the dead-end and DPM source. Although, in a mine entry, DPM concentrations can be effectively reduced by advancing ventilation duct, but practically ventilation duct advancement has certain limitations. Since moving ventilation duct too close to the dead-end can eventually result in duct damage during the next round blasting. However temporary arrangements can be made to extend ventilation duct during diesel equipment operation if needed.

8.3.2.2. Comparison of Case 2 and Case 3. Case 2 and Case 3 use the same number of DPM source. However these DPM sources are located at different positions in a mine entry. Simulation results for both cases were compared in order to determine the

effect of DPM source location with respect to the duct inlet and the dead-end. Figure 8.34 shows the comparison of seven simulations for both cases. It is evident from Figure 8.34 that both (Case 2 and Case 3) have produced similar levels of DPM. The location of the DPM source with respect to the position of duct inlet does not seemed to affect DPM concentrations as both cases produced similar levels of DPM, even though they are located at different mine positions.

8.3.2.3. Comparison of Case 1, Case 1A and Case 3A. Average DPM concentrations were compared for all simulation combinations (Table 8.2). Figure 8.35 shows the average DPM concentration for all simulations of Case 1, Case 1A and Case 3. Average DPM concentration is computed for work zone from the face. As evident from Figure 8.34 that highest average DPM concentrations were observed for Case 3 simulations that have two front-end loaders. Lowest DPM is seen for Case 1A that have ventilation duct installed closest to the work face and DPM source. Among all simulations for studied cases, simulation S7 resulted in worst mine air quality. Simulation S7 represents a combination of biggest duct diameter (1.85 m) and the lowest duct inlet velocity (10.0 m/s). Simulation S6 represents the best combination of inlet air velocity and duct diameter that has overall lowest average DPM concentrations. However, simulation S5 seems to be the optimum combination as it requires almost 33% less quantity of air as compared to simulation S6 and still produces comparable results. The results showed that flooding dead-end mine entry with a huge air quantity does not guarantee better ventilation and hence better DPM dilution. Thus a ventilation engineer should consider all design parameters.

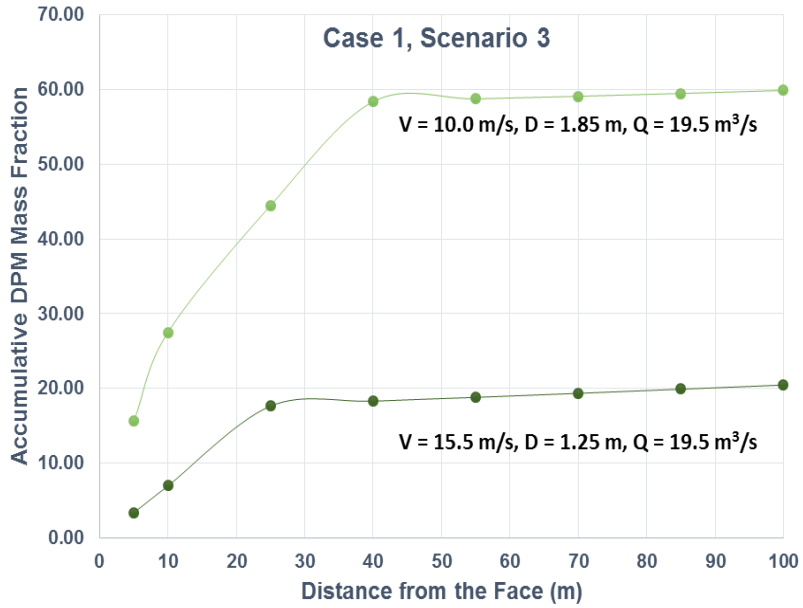

Figure 8.29 Accumulative DPM mass fraction versus face distance (19.5 m^3/s)

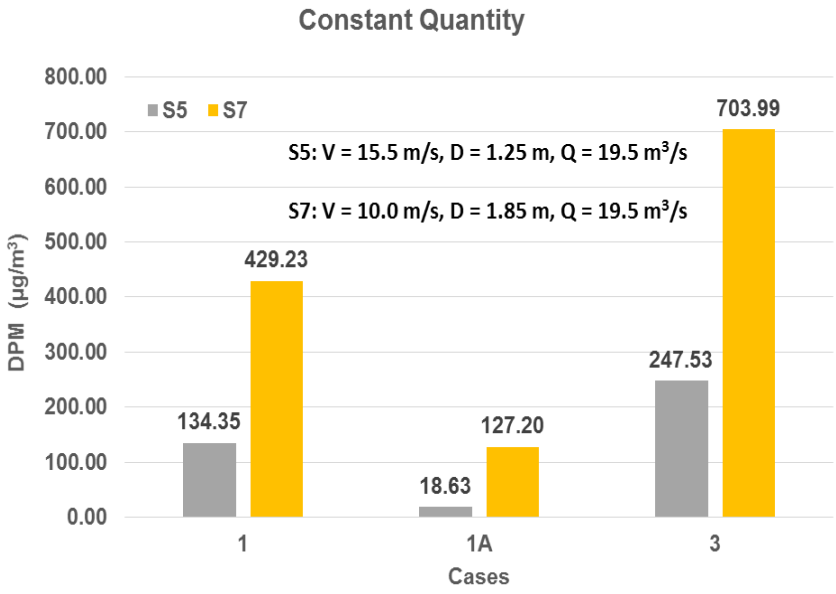

Figure 8.30 Average DPM for Case 1, Case 1A and Case 3 (19.5 m^3/s)

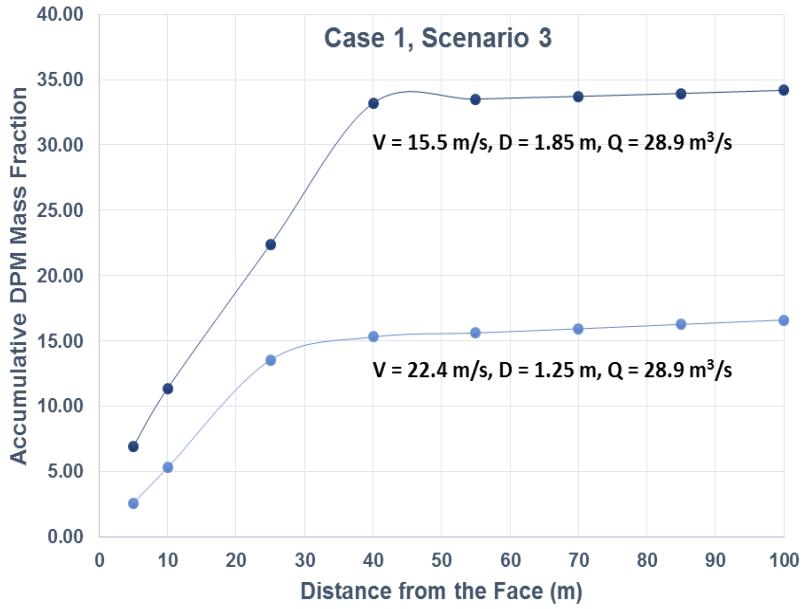

Figure 8.31 Accumulative DPM mass fraction versus face distance (28.9 m^3/s)

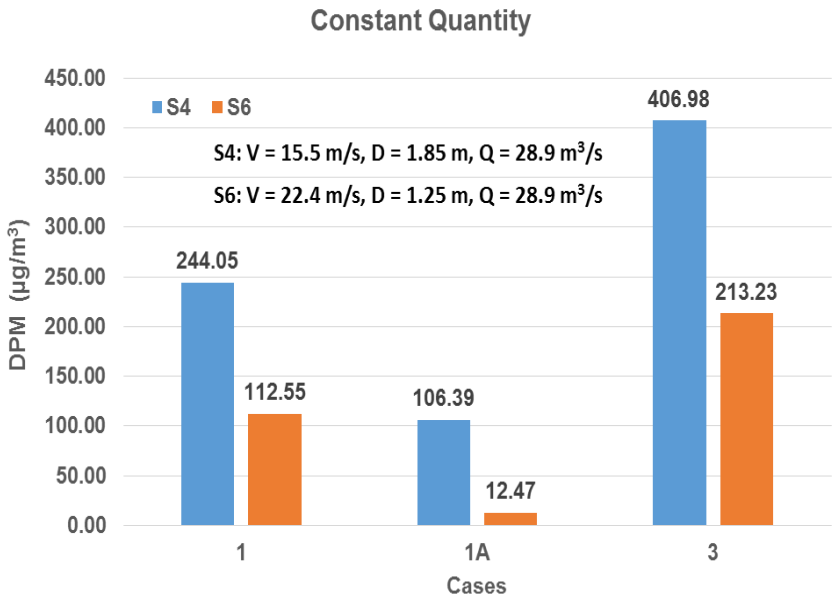

Figure 8.32 Average DPM for Case 1, Case 1A and Case 3 (28.9 m^3/s)

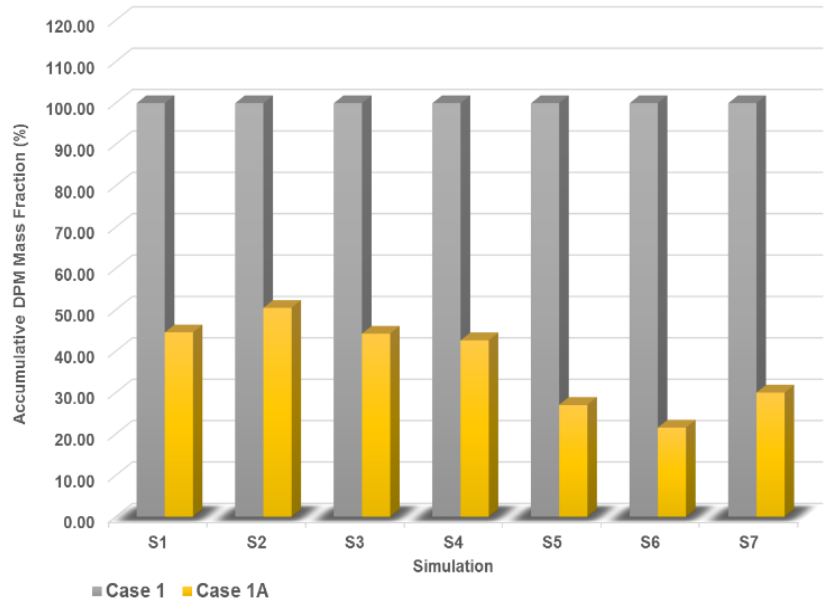

Figure 8.33 Simulations comparison for Case 1 and Case 1A

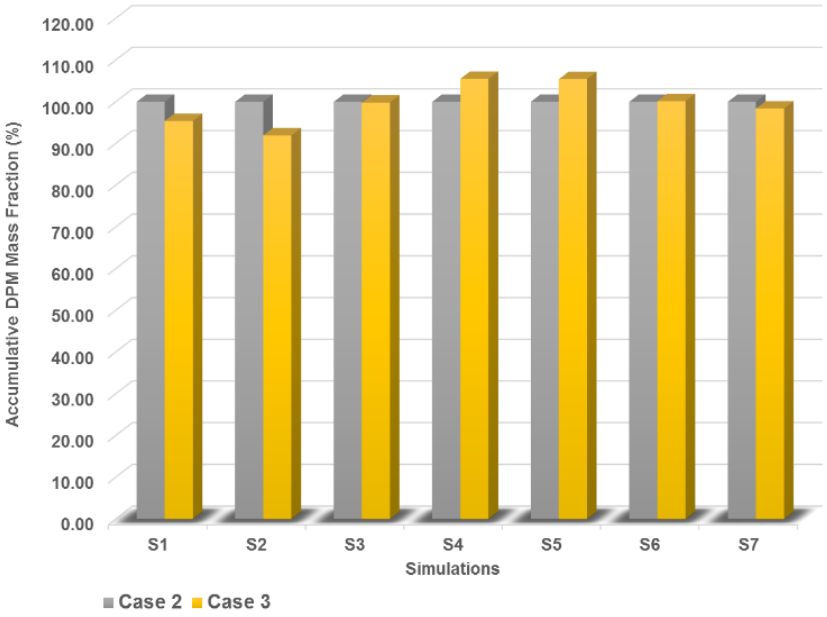

Figure 8.34 Simulations comparison for Case 2 and Case 3

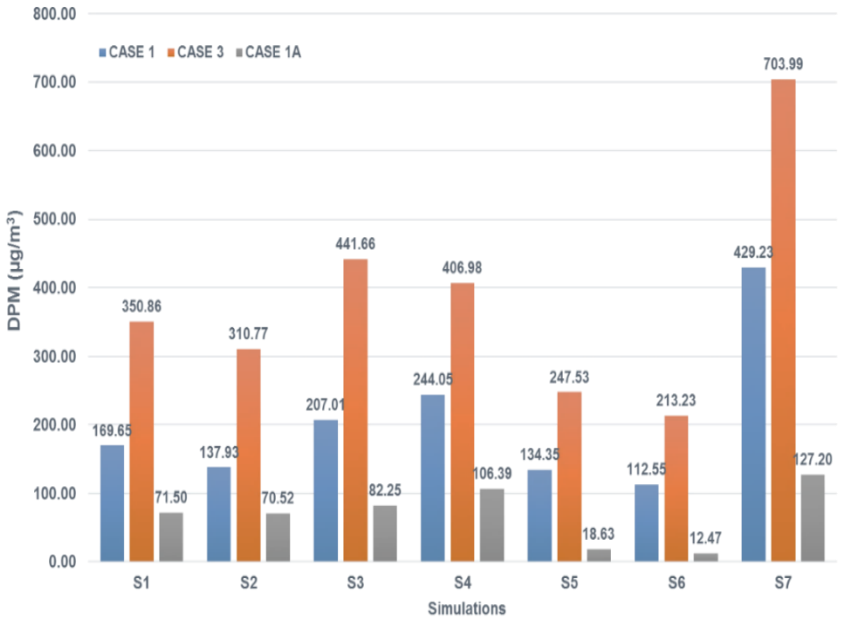

Figure 8.35 Average DPM for Case 1, Case 1A and Case 3

8.4. SUMMARY

Dilution of DPM by ventilation is the most commonly adopted DPM control method. Numerous studies have successfully used CFD to study several mine ventilation related issues. CFD has been used by a number of researchers to simulate the behavior of DPM in mines. A CFD study recommends an increase in air flow rates to decreasing DPM concentrations at work faces (Yi Zheng et al., 2017), however, this study has not specifically evaluated the effect of change in duct diameter, duct inlet velocity, duct positioning with respect to the dead-end on the DPM levels. This Section determined the role of ventilation related parameters on DPM in a dead-end mine entry. The effect of duct diameter, duct inlet velocity, the optimum combination of duct diameter and velocity, and location of duct inlet with respect to dead-end and DPM source is examined. A total of four cases were simulated that differ in terms of the number of DPM sources, their location in

the mine entry, or the position of duct inlet with respect to the dead-end and DPM source. A total of seven combinations of different duct inlet velocity and diameter were simulated for each case. Simulations were divided into three scenarios: (i) constant dust diameter; (ii) constant duct velocity; (iii) constant air quantity. Simulations results showed that an increase in duct diameter at variable volumetric flow rates is counterproductive as it increases DPM concentrations in the mine entry. However, an increase in duct inlet velocity resulted in best quality mine air. Lowest DPM is observed in simulations that have highest duct inlet velocity and lowest duct diameter. The effect of duct inlet advancement is examined by advancing duct closer to the DPM source. It was found that the DPM concentrations can be drastically reduced by advancing duct inlet position. Reduction in DPM as much as 80% is observed. The location of DPM source in mine entry is studied by changing the locations of DPM sources and it was found that the DPM concentration does not depend upon the location of DPM source in mine entry. Finally, average DPM concentrations were computed for different simulated cases and both the best and the optimum combination of duct inlet velocity, duct diameter and air quantity is suggested for examined conditions.

9. FLIR AIRTEC GOOD WORK PRACTICES AND RECOMMENTATIONS

9.1. OVERVIEW

In this research the FLIR Airtec real-time DPM monitor has been extensively used in several underground metal mines in the United States over a period of one year. The FLIR Airtec monitor has been tested in high dust up to 4 mg/m^3 and DPM up to 700 $\mu g/m^3$ concentrations. The relative humidity of the studied mines ranges from 60% to 90% during monitoring periods. The performance of the Airtec was found satisfactory under those hostile work environments. After using the Airtec monitor for a long period in underground mines and conducting laboratory test on the monitor, several good work practices have been identified. These suggested practices can help to eliminate some errors/problems that may occur while using the Airtec monitor in underground mines and while interpreting its results. The following sections delineates work practices identified from laboratory tests and field experiences.

9.2. LABORATORY TESTS

The FLIR Airtec contains two filter cassettes: (i) a pre-filter which is used to separate the sub-micron sized particles from larger sized particles that are present in the mine atmospheres; and (ii) an EC accumulation filter cassette (DPM cassette). Figure 9.1 shows a pre-filter cassette and Figure 9.2 shows the DPM cassettes.

Figure 9.1 Pre-filter cassettes of the Airtec monitor

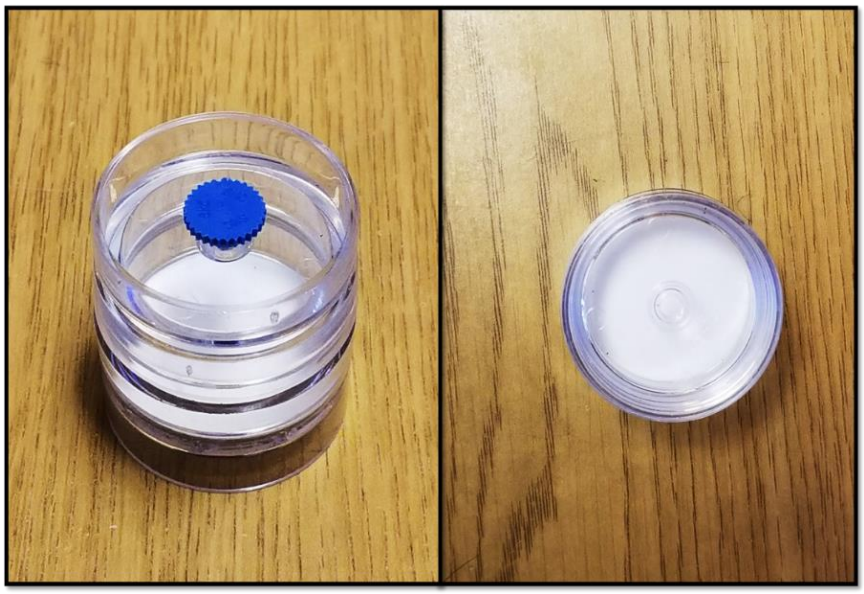

Figure 9.2 DPM cassette of the Airtec monitor

The flow rate of the FLIR Airtec monitor was tested in the laboratory by installing both types of filter cassettes each with different contamination levels. Both types of filter cassettes were randomly chosen from a large set of available cassettes. Three cassettes of

each contamination level and type were used to test the flow rates. Pre-filter cassettes are enclosed in a plastic case in such a way that their level of contamination cannot be gauged by any means. Therefore, the contamination levels for pre-filter cassette were established based on the number of hours these cassettes were used in mines during DPM monitoring process. The contamination levels for both types of cassettes are described in the following section.

For laboratory testing, three levels of contamination were established for the pre-filter cassettes: (a) absolutely clean (new cassette); (b) moderately contaminated (used for less than 10 hours); (c) highly contaminated (used for 10 to 20 hours). These levels actually represent the concentrations of particles on the pre-filter. Since pre-filter cassettes were used in similar mining conditions, greater usage does correspond directly to more particle accumulation on the pre-filter cassette. Figure 9.3 shows one of the tested pre-filter cassettes.

Figure 9.3 Airtec tested pre-filter cassette

Based on visual observation and the usage of DPM cassettes, three levels of contamination were established for DPM cassettes: (a) absolutely clean; (b) moderately contaminated; (c) highly contaminated. An absolutely clean cassette represents a new cassette, intermediate contamination level represents a filter cassette about half way through its life, whereas a highly contaminated level represents maximum possible concentration on the cassette (just before alarm sign appears on the Airtec monitor). Figure 9.4 shows moderately contaminated DPM cassettes, while Figure 9.5 shows highly contaminated DPM cassettes. The description of flow rate test and their results are given in Table 9.1.

Table 9.1 Airtec flow rates test results

	DPM Cassette	**Pre-filter Cassette**	**Remarks**
1	Absolutely clean	Absolutely clean	No issue in flow rate was found, constant and consistent flow rates were observed.
		Moderately contaminated	
		Highly contaminated	
2	Moderately contaminated	Absolutely clean	No issue in flow rate was found, constant and consistent flow rates were observed.
		Moderately contaminated	
		Highly contaminated	
3	Highly contaminated	Absolutely clean	Slightly increase (within allowable limit) in flow rate was observed. Although flow rate remained constant and consistent but it was slightly on the higher side.
		Highly contaminated	

Figure 9.4 Moderately contaminated DPM cassettes

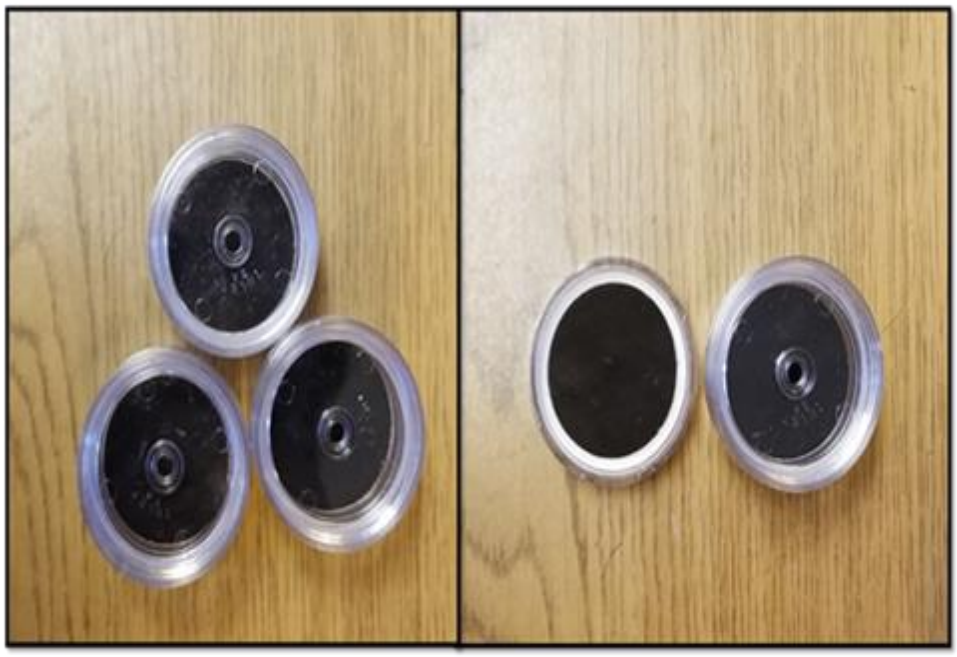

Figure 9.5 Highly contaminated DPM cassettes

As described in the Table 9.1, the contamination level of pre-filter cassette did not affect flow rates of the Airtec monitor. In spite of this, it is recommended to change the

pre-filter cassette after using it with two DPM cassettes. However, depending upon the concentrations of the DPM and other particles in the monitoring area, one pre-filter cassette can be used with three DPM cassettes as prescribed by the manufacturer.

Table 9.1 shows that, the flow rate of the Airtec is not affected by clean or moderately contaminated DPM cassette, whereas highly contaminated DPM cassette has increased the flow rate (although still within allowable limit) of the monitor. The increase in flowrate of the Airtec with even a highly contaminated DPM cassette is negligible and within allowable limits. One possible reason for the increase in the Airtec flow rate with highly contaminated DPM cassette is that high DPM particles accumulation on a cassette may cause some wear and tear of the filter of DPM cassette and open up the filter pores. Another reason could be the interaction of biodiesel exhaust with the material of DPM cassette filter that partially loosen the pores of filter and cause slight increase in the Airtec's flow rate. However, since the mechanism was not established, it is recommended to use clean/new DPM cassette especially if DPM measurements are to be performed for longer durations or in mine areas that have very high DPM concentrations.

9.3. FIELD OBSERVATIONS

1. In this research, a correlation between TWA EC by the Airtec and the NIOSH 5040 has been established for high-percent biodiesel exhaust measurements. A slight trend of overestimation was observed while measuring TWA EC by the Airtec monitor for EC concentrations below 200 $\mu g/m^3$. The proposed relationship is recommended for correcting TWA EC by the Airtec monitor for EC below 200 $\mu g/m^3$ with biodiesel fueled equipment.

2. The flowrate of the Airtec monitor should be checked before and after its use so as to maintain it at 1.7 ± 5% liters per minute. Although the flow rate of the pump used in Airtec monitor was highly consistent and no issues were observed with the pump flow rate. The flow rate of the Airtec is a critical parameter and any change in the flow rate would cause serious experimental error. In case the flow rate is not equal to 1.7 ± 5% liters per minute, the user should use a mathematical relation described by Noll et al. (2013) to back calculate the actual EC concentration (James Noll et al., 2013).
3. The monitor's battery should be fully charged before a full day usage. In this study, the Airtec was run for up to 10 hours and no specific issues were observed with either the battery or the monitors' performance. However, the Airtec monitors were fully charged before every measurement day
4. The Airtec provides TWA concentrations based upon eight hour work shift calculations. If the measurement duration is other than the presumed eight hours, the TWA values provided by the Airtec monitor should be converted to the respective duration.
5. The Airtec is sensitive to sudden and sharp temperature changes and requires around 2 to 5 minutes to adjust sudden and sharp changes in temperatures. Sudden and sharp change in temperature can cause the Airtec to read negative or zero EC values. Therefore, a miner should be careful while moving the Airtec from the exhaust air drift to the fresh air drift that may have significant temperature difference (especially in winter). This particular assessment is based on observation only.

6. High air humidity (90%) seems to have no effect on the performance of the Airtec. However, any direct and prolonged contact of water with the Airtec can destroy the monitor's ability to determine DPM. It is therefore recommended to avoid any direct water contact with the Airtec. If the Airtec is used in conditions that have water sprays coming from the rock surfaces or otherwise, a protective water proof covering should be used around the monitor.
7. The Airtec monitor shows a warning sign when the DPM filter cassette requires replacement. Although the warning signal serves primarily as an initial warning, the cassette may work well for further measurements (measurement duration depends upon the EC concentration in the air). However, in order to avoid erroneous measurements, it is best to change the DPM filter cassette right after a warning sign is observed.
8. Data acquisition software provided by the manufacturer allows real-time data to be downloaded from the Airtec monitor. The transfer monitor requires only a single cable and the provided data acquisition software.

10. CONCLUSIONS AND RECOMMENDATIONS

10.1. SUMMARY

The standard DPM monitoring method termed NIOSH 5040 method involves a time-lag in determining DPM and is unable to detect DPM transients during DPM measurement. Limitations of the NIOSH 5040 method exist because it is a shift-average based DPM measurement method and requires a remotely located commercial laboratory for DPM sampling analysis. Real-time DPM monitors avoid the issue of lag-time and are capable of rapidly quantifying a changing mining environment. Real-time DPM monitoring is important to understand the changes in DPM concentrations due to variable diesel equipment activities.

Biodiesel is often used in the mining industry, instead of regular petroleum diesel due to its lower DPM emission. Existing real-time DPM monitors had not been calibrated for high-percent biodiesel exhaust prior to this research. This research shows current real-time DPM monitor can be used to determine DPM exhaust from high-percent biodiesel albeit with a correction factor necessary for accurate results. Extensive DPM sampling has been conducted in several underground metal mines that use high-percent biodiesel. The FLIR Airtec real-time DPM monitor was tested against the standard NIOSH 5040 DPM sampling method under a variety of mining conditions in several underground metal mines. A correlation is proposed for the Airtec monitor that applies when the TWA EC concentrations determined by the Airtec monitor remain below 200 $\mu g/m^3$. The proposed equation can be used for accurate determination of biodiesel exhaust by the Airtec monitor.

A series of real-time DPM area monitoring at the work faces and in exhaust air drifts have been conducted. During work face and exhaust air drift measurements, wide variations in DPM profiles have been observed, including decreasing, increasing, essentially constant, and seemingly random. The highest DPM concentrations were observed at work faces. Multiple diesel-powered equipment resulted in overall higher DPM levels at work faces and in exhaust air drifts. Work face and exhaust air drift DPM measurements provide significant data base regarding transient DPM levels in underground metal mines. The collected data provides a basis for likely to be encountered DPM concentrations in similar mining operations. This study has also been able to relate DPM transient levels with diesel equipment activities in mines by carefully logging activities during all of the extensive real-time monitoring. No research work has been reported to date, to the author's knowledge, that has comprehensively studied real-time DPM concentrations in active underground metal mines.

The frequency distribution patterns of DPM concentrations encountered in underground mines' work faces and exhaust air drifts were also studied. It was observed that DPM concentrations at work faces and exhaust air drifts are not normally distributed. Although some DPM frequency distributions did not fit an obvious pattern, many individual work face and exhaust air drift measurements followed either lognormal or Weibull distribution. Combined work face concentration results are best represented by a Weibull distribution, whereas exhaust air drift measurements more closely followed a lognormal distribution pattern.

Simultaneous DPM measurement results from the work faces, inlet air drifts, and exhaust air drifts were analyzed. Simultaneous measurement plots helped to understand the

variations in DPM levels and DPM dilution patterns at different mine locations. DPM recirculation from auxiliary fan and ventilation duct system was evident and clearly leads to an increase in the DPM concentration at the work face. A modification in auxiliary fan location was suggested to the mine management to reduce DPM recirculation. The mine management has adopted the suggested modification and DPM recirculation was reduced.

A 2D CFD model was developed to study the role of stope ventilation related parameters including duct diameter, duct inlet velocity, air quantity, and the location and number of DPM sources in a dead-end mine entry. Higher duct inlet velocities were found to dilute and disperse DPM efficiently. It was observed that the advancement of duct close to DPM source and dead-end of the mine entry can reduce DPM concentrations drastically. Finally, based on field observations, experience, and laboratory tests good work practices for using the FLIR Airtec real-time DPM monitor has been suggested.

10.2. CONCLUSIONS

A comprehensive literature review provided valuable insight into real-time DPM monitoring methods and the Unites States DPM regulations. A detailed review of real-time DPM monitoring in underground mines was conducted and led to identification of the need to correlate the Airtec monitor with the standard NIOSH 5040 method for high-percent biodiesel exhaust determinations. No previous study had linked the Airtec with the NIOSH 5040 method for high-percent biodiesel exhaust determination. The following specific conclusions are drawn from the original body of work presented in this dissertation:

1. A detailed comparison of the Airtec and the NIOSH 5040 method showed that the Airtec usually overestimates the EC concentrations when EC is less than

200 µg/m^3. A correlation is proposed, and a strong correlation with a high value of correlation coefficient (R^2 = 0.92) is obtained. The proposed equation can be used for accurate estimation of EC concentration by the Airtec monitor when used under similar mining conditions. The correlation equation was validated by an independent set of samples and its prediction capability was found to be satisfactory. The correlation equation is given below:

$$EC\ (5040) = 0.885 \times EC\ (Airtec) \qquad \text{Eq. 1}$$

2. Results indicated no correction is required for the Airtec when TWA EC concentration exceeds 200 µg/m^3. This research showed that with the proposed correction, the Airtec has excellent potential to be used as an accurate alternative to the NIOSH 5040 method for assessing EC in similar underground mines.
3. The bias in the Airtec measurements for EC concentrations below 200 µg/m^3 is hypothesized to be due to the presence of some non-absorbing aerosols in high-percent biodiesel fuel mixture. The impact of the non-absorbing particles in biodiesel exhaust would be reduced as EC accumulates on the DPM filter cassette, leading to an EC prediction without any bias at high (> 200 µg/m^3) EC concentration.
4. This study showed that the work face and exhaust air drift DPM concentration trends of any active mine are highly variable, as all kinds (increasing, decreasing, essentially constant, and random) of DPM concentration profiles were observed. Mine work faces contain the overall highest levels of DPM, since most of the diesel-powered equipment (jumbo drill, bolter, front-end

loader etc.) usually operates at or near the work faces. Exhaust air drifts that are located near the work faces (0 m to 700 m) contain overall high DPM levels, however these DPM concentrations are usually lower than the concentrations at work faces.

5. The introduction of DPM frequency distribution models for work face and exhaust air drift concentrations offers a means to quantify likely DPM exposure. The frequency distribution of discrete DPM concentration measurements at work faces and exhaust air drifts is not normally distributed. Although some variations were observed, the measurements were generally represented by either lognormal or Weibull distribution. A Weibull distribution is the best representative of a combined work face DPM concentration results, whereas lognormal distribution is the best representation of the combined exhaust air drift DPM concentrations. The combined (work face and exhaust air drift) DPM concentrations can be represented by either lognormal or Weibull distribution. However, lognormal distribution captures the peak in the data more effectively.
6. The frequency distributions predict the most likely EC concentrations at the work face and in exhaust air drift to be 339 $\mu g/m^3$ and 287 $\mu g/m^3$, respectively.
7. The frequency distribution patterns developed in this research can be used to predict the likelihood of DPM levels to which a miner who works at active mining zones without an environmental cab and a respirator is exposed. Research results showed that the chances of having area EC concentrations above 150 $\mu g/m^3$ at work faces and in exhaust air drifts are over 75%. This means a miner who visits work faces or exhaust air drifts (situated near active

work face) has a 75% chance of exposure to areas that have EC concentration above 150 µg/m^3.

8. This study showed that the mine air area sampling is important to ensure better quality of mine air. In order to better understand the mine air environment, DPM area sampling is necessary along with personal DPM sampling. Mine authorities should also conducted the DPM area sampling relatively frequently.
9. The present results provide justification for DPM STEL given the observed high levels over many short and significantly long periods. DPM STEL measurements and its regulatory implementation may be adopted by MSHA in future.
10. Simultaneous real-time PM measurements at work faces and in exhaust air drifts are shown to be useful to understand the DPM dilution patterns in a mine drift. This study showed that for work faces and exhaust air drifts often have similar DPM concentrations if the mine air is uniformly mixed. However, in some instances, an exhaust air drift that is situated near the work face can capture DPM from more than one work area and exhibit quite high DPM.
11. This research also highlights the importance of ensuring clean air for DPM dilution at the work faces, because even a single diesel-powered equipment can cause high DPM at work faces if the mine air being supplied is already polluted from other work areas.
12. The present results also show that recirculation from auxiliary fan can causes significant increase in DPM concentrations. In particular, mobile diesel equipment (haul trucks, road grader, FEL) has a more pronounced effect on

DPM recirculation as compared to relatively stationery diesel equipment (face drill, rock bolter, and explosive charger). In M/NM mines DPM recirculation should be considered seriously. The quality of mine air can be considerably improved by controlling DPM recirculation from auxiliary mine fans.

13. A 2D CFD model was used to study the role of stope ventilation parameters on DPM dilution in a dead-end mine entry. CFD model suggested that increase in air quantity by enlarging duct diameter is counterproductive and increases DPM concentrations, whereas an increase in air quantity achieved by increasing the duct inlet velocity results low DPM and best quality of mine air. The CFD results showed that the best combination for DPM dilution in a dead-end mine entry is achieved by using maximum possible duct inlet velocity with smallest duct diameter.
14. This study showed that DPM concentrations in a dead-end mine entry can be decreased up to 80% by advancing the duct inlet position near the entry's dead-end and DPM source. Although movement of ventilation duct too close to the dead-end can result in its damage during next round blast. However if hostile DPM levels prevail, temporary arrangements should be made to extend ventilation duct during diesel equipment operation.
15. During this research, the Airtec monitor was extensively used in different mining conditions. The Airtec's performance was found highly satisfactory. Further recommendations and good work practices about the Airtec monitor and its use are discussed in detail in Section 9.

10.3. PHD RESEARCH SCHOLARLY CONTRIBUTIONS

All the stated research objective that are described in Section 1.3 are successfully achieved within the scope of this research. Key contributions from this research are discussed below:

- This research is the first successful effort to correlate the FLIR Airtec DPM monitor with the standard NIOSH 5040 method for high-percent biodiesel exhaust determinations. As a result of this research, the mining industry now has access to a real-time monitor that can be used in underground mines for accurate determination of DPM in high-percent biodiesel exhaust.
- This is a first comprehensive study that has specifically examined DPM levels at a variety of active underground mine work faces and exhaust air drifts under various mining conditions. It represents a significant body of data detailing about transient DPM concentrations at mine work faces and exhaust air drifts, as well as its relationship to diesel equipment activity. The information about transient DPM levels can help to understand and interpret commonly encountered DPM levels in conventional underground metal mines.
- This research constitutes a pioneering method for utilizing frequency distribution models to quantify work face and exhaust air drift DPM levels. The DPM frequency distribution models identified as a part of this research enables determination of probable DPM exposure at key locations in underground mines.
- This study highlights the imperative of DPM area sampling to understand and control mine DPM concentration effectively. Frequent DPM area sampling is essential to evaluate the quality of mine air.

- This research also indicates merits of introducing STEL for DPM exposures. STEL determinations of DPM can help in reducing miners' overall DPM exposure.
- This research is apparently a first attempt to determine recirculation of DPM from an auxiliary ventilation fan. This research showed that recirculation can cause significant increase in DPM levels, therefore special attention should be given to control the recirculation from auxiliary fans in underground metal mines.
- This research has exclusively evaluated stope ventilation parameters in a dead-end mine entry and suggested best and optimum stope ventilation practices.
- This research has provided a generic modelling approach that can be used in any underground mine to evaluate the dispersion of gases, fine, and ultrafine particles present in the mine air.

10.4. SITE SPECIFIC CONTRIBUTIONS

Real-time and shift-average based DPM area sampling conducted at underground metal mines during this research has resulted both long and short term modifications in the existing mining practices and its structure. Site specific contributions resulting from this research are as follows:

1. The mine management has decided to construct a new ventilation shaft from the surface. The approximate depth of the shaft is 347 m, as of now, over 72 m shaft has been excavated and its expected completion date is in the first quarter of year 2018. The forecasted cost of shaft construction is around 22 million US dollars.
2. A battery operated load-haul dump was purchased for mucking out the excavated material from highly concentrated DPM areas of mines. However, some problems

were encountered while using battery-powered load-haul dump. One of the main problems was relatively short battery life (work time after one complete recharge), as the battery often died before finishing mucking from one entire heading. Even though mining equipment manufacturing companies are trying to improve battery life of such heavy duty mining equipment, it appears that it will take a while before sufficient improvements can be made. Therefore, unless markedly improved compatible battery-operated equipment become available, diesel-operated equipment will remain a preferred choice of large mining operations.

3. The mine management has decided to lower the threshold limit values of the exhaust gasses especially NO_x, CO as high DPM levels were observed at previously set threshold limit values of exhaust gasses. Threshold limit value is important as miners' must suspend their work and evacuate the area until concentration of pollutants reduces to a certain allowable value. Implementation of stringent threshold values impacted mine production and prompted the mine management to be more expeditious in ventilation projects. These adopted changes show the necessity of designating DPM threshold limit value, short term exposure limit, and mine area sampling. All of which become possible only with real-time DPM monitors.
4. After the initial findings of this research, the mine management started scheduling mining operations in areas of limited ventilation such that, only one diesel equipment was allowed to operate at a time. This has pushed the mine engineers to develop new work faces and expand mine boundaries sooner.

5. The mine management has excavated a drift to alter the stope ventilation scheme from a dead-end drift ventilation to similar to U-tube (mine air enter from one drift and exit from another) ventilation. As high DPM concentration were observed at work faces and in exhaust air drifts with dead-end drift ventilations system.
6. After identifying highly concentrated DPM areas in underground mines, the mine management has implemented a rule that required all miners to wear respirators during their stay at high DPM areas.
7. Auxiliary ventilation fans were moved to other mine locations in order to control the DPM recirculation from the fan.

10.5. RECOMMENDATIONS FOR FUTURE WORK

Based on the field measurements and numerical simulation results of this study, some promising suggestions for future research has been made. The following section enlist few future research recommendations:

1. The effect of high-percent biodiesel exhaust on the Airtec's DPM cassette can be studied in a controlled environment in order to examine the suggested hypothesis or explore the exact reason of positive bias in Airtec monitor's measurements for low (< 200 $\mu g/m^3$) EC concentration in high-percent biodiesel exhaust.
2. DPM transient levels provides sufficient evident of varying DPM concentrations at work faces and in exhaust air drifts. It is quite possible that the personal TWA DPM exposure of a miner may remain below PEL even though he is exposed to very high levels of DPM concentration for short durations. High level of DPM may harm miners' health even when their PEL remain within allowable limit. The health

effects of miners' short term exposure to very high DPM levels have are not known specifically. Researchers who work in the health sector may find real-time DPM data generated during this research useful and explore harmful health effects of short term high level DPM exposures. This may allow them to define a short term exposure limit for DPM.

3. Results of DPM frequency distribution models that are formulated in this research can be combined with health studies data in order to explore the probable harmful effect of DPM exposure to those miners' health who visit areas of high DPM concentrations without proper protection.
4. There is a need to establish a relationship between DPM concentrations of mine area sampling and miners' personal exposure sampling.
5. Airtec DPM monitor can be rigorously tested to determine miners' DPM STEL in active underground mines.
6. The effect of the power of auxiliary fan and its location (with respect to the exhaust air drift) on DPM recirculation can be studied by numerical simulation approaches.
7. Stope ventilation parameters can be examined by using a 2D and 3D unsteady models and by changing stope geometry
8. Field correlation between NO_x, CO with DPM concentration (either EC or TC) can be investigated for high-percent biodiesel exhaust.

BIBLIOGRAPHY

ACGIH, J. (1998). American Conference of Governmental Industrial Hygienists. *Industrial Ventilation: A Manual of Recommended Practice*.

ADS Gillies, B. Belle, H.W Wu, & Khan, M. (2014). Comparison of Diesel Particulate Matter Ambient Monitoring Practices in Underground Mines in Australia, the United States and South Africa. *10th International Mine Ventilation Congress* 277.

Ålander, T. J., Leskinen, A. P., Raunemaa, T. M., & Rantanen, L. (2004). Characterization of diesel particles: effects of fuel reformulation, exhaust aftertreatment, and engine operation on particle carbon composition and volatility. *Environmental science & technology, 38*(9), 2707-2714.

Ames, R. G., Attfield, M., Hankinson, J., Hearl, F., & Reger, R. (1982). Acute Respiratory Effects of Exposure to Diesel Emissions in Coal Miners 1–4. *American Review of Respiratory Disease, 125*(1), 39-42.

Anon. (2001). Federal Register. In MSHA (Ed.), (Vol. 66).

Arnott, W., Arnold, I., Mousset-Jones, P., Kins, K., & Shaff, S. (2008). Real-time Measurements of Diesel EC and TC in a Nevada Gold Mine With Photoacoustic and Dusttrak Instruments: Comparison With NIOSH 5040 Filter Results.

Arnott, W., Moosmüller, H., Sheridan, P., Ogren, J., Raspet, R., Slaton, W., . . . Collett, J. (2003). Photoacoustic and filter-based ambient aerosol light absorption measurements: Instrument comparisons and the role of relative humidity. *Journal of Geophysical Research: Atmospheres, 108*(D1).

Attfield, M. D., Schleiff, P. L., Lubin, J. H., Blair, A., Stewart, P. A., Vermeulen, R., . . . Silverman, D. T. (2012). The diesel exhaust in miners study: a cohort mortality study with emphasis on lung cancer. *Journal of the National Cancer Institute, 104*(11), 869-883.

Birch, M., & Cary, R. (1996). Elemental carbon-based method for monitoring occupational exposures to particulate diesel exhaust. *Aerosol Science and Technology, 25*(3), 221-241.

Birch, M. E. (1998). Analysis of carbonaceous aerosols: interlaboratory comparison. *Analyst, 123*(5), 851-857.

Birch, M. E. (2002). Occupational monitoring of particulate diesel exhaust by NIOSH method 5040. *Applied occupational and environmental hygiene, 17*(6), 400-405.

Birch, M. E., & Cary, R. A. (1996). Elemental carbon-based method for occupational monitoring of particulate diesel exhaust: methodology and exposure issues. *Analyst, 121*(9), 1183-1190.

Birch, M. E., & Noll, J. D. (2004). Submicrometer elemental carbon as a selective measure of diesel particulate matter in coal mines. *Journal of Environmental Monitoring, 6*(10), 799-806.

Biswas, S., Hu, S., Verma, V., Herner, J. D., Robertson, W. H., Ayala, A., & Sioutas, C. (2008). Physical properties of particulate matter (PM) from late model heavy-duty diesel vehicles operating with advanced PM and NOx emission control technologies. *Atmospheric Environment, 42*(22), 5622-5634.

Bond, T. C., Anderson, T. L., & Campbell, D. (1999). Calibration and intercomparison of filter-based measurements of visible light absorption by aerosols. *Aerosol Science & Technology, 30*(6), 582-600.

Borak, J., Sirianni, G., Cohen, H., Chemerynski, S., & Wheeler, R. (2003). Comparison of NIOSH 5040 method versus Aethalometer™ to monitor diesel particulate in school buses and at work sites. *Aiha Journal, 64*(2), 260-268.

Bugarski, A., Janisko, S., & Cauda, E. (2011). Diesel aerosols and gases in underground mines: guide to exposure assessment and control. Department of Health and Human Services, Centers for Disease Control and Prevention. *National Institute for Occupational Safety and Health, Office of Mine Safety and Health Research, Pittsburgh and Spokane*.

Bugarski, A. D., Cauda, E. G., Janisko, S. J., Hummer, J. A., & Patts, L. D. (2010). Aerosols emitted in underground mine air by diesel engine fueled with biodiesel. *Journal of the Air & Waste Management Association, 60*(2), 237-244.

Bugarski, A. D., Cauda, E. G., Janisko, S. J., Mischler, S. E., & Noll, J. D. (2011). *Diesel Aerosols and Gases in Underground Mines: Guide to Exposure Assessment and Control*: Department of Health and Human Services, Public Health Service, Center for Disease Control and Prevention, National Institute for Occupational Safety and Health, Office of Mine Safety and Health Research.

Bugarski, A. D., Janisko, S. J., Cauda, E. G., Noll, J. D., & Mischler, S. E. (2012). *Controlling exposure to diesel emissions in underground mines*: SME.

Bugarski, A. D., Schnakenberg, J., George H, Hummer, J. A., Cauda, E., Janisko, S. J., & Patts, L. D. (2009). Effects of diesel exhaust aftertreatment devices on concentrations and size distribution of aerosols in underground mine air. *Environmental science & technology, 43*(17), 6737-6743.

Cancer, I. A. f. R. o. (2011). Agents classified by the IARC Monographs. *IARC Monographs on the Evaluation of Carcinogenic Risks to Humans: IARC*.

Cancer, I. A. f. R. o. (2012). IARC: diesel engine exhaust carcinogenic; [cited 2012 Jun 23]. *Availabe from: http://www. iarc. fr/en/media-centre/pr/2012/pdfs/pr213_E. pdf*.

Cantrel, B. K., Rubow, K. L., & Watts, W. F. (1993). *Pollutant levels in underground coal mines using diesel equipment.* Paper presented at the the 6 th US Mine Ventilation Symposium, Salt Lake City, UT, USA, 06/21-23/93.

Cantrell, B. (1987). *Source Apportionment Analysis Applied to Mine Dust Aerosols: Coal Dust and Diesel Emissions Aerosol Measurement.* Paper presented at the Proc. of the 3rd Mine Ventilation Symp., Soc. Min. Eng., Littleton, CO.

Cantrell, B. K., & Watts Jr, W. F. (1997). Diesel exhaust aerosol: Review of occupational exposure. *Applied occupational and environmental hygiene, 12*(12), 1019-1027.

Cantrell, B. K., Williams, K., Watts, W., & Jankowski, R. (1993). Mine aerosol measurement. *Aerosol measurement: principles, techniques, and applications. Van Nostrand*, 591-611.

Chow, J. C., Engelbrecht, J. P., Freeman, N. C., Hashim, J. H., Jantunen, M., Michaud, J.-P., . . . Wilson, W. E. (2002). Chapter one: exposure measurements. *Chemosphere, 49*(9), 873-901.

Coen, M. C., Weingartner, E., Apituley, A., Ceburnis, D., Fierz-Schmidhauser, R., Flentje, H., . . . Petzold, A. (2010). Minimizing light absorption measurement artifacts of the Aethalometer: evaluation of five correction algorithms. *Atmospheric Measurement Techniques, 3*(2), 457-474.

Cohen, H., Borak, J., Hall, T., Sirianni, G., & Chemerynski, S. (2002). Exposure of miners to diesel exhaust particulates in underground nonmetal mines. *AIHA Journal, 63*(5), 651-658.

Control, C. f. D. (1988). NIOSH recommendations for occupational safety and health standards 1988. *MMWR. Morbidity and mortality weekly report, 37*, 1.

Du, H., & Yu, F. (2006). Role of the binary H 2 SO 4–H 2 O homogeneous nucleation in the formation of volatile nanoparticles in the vehicular exhaust. *Atmospheric Environment, 40*(39), 7579-7588.

EPA. (2001, 2001). *Nonroad diesel emission standards*. Washington.

EPA. (2002). *Health assessment document for diesel engine exhaust*: National Center for Environmental Assessment.

Gaillard, S., McCullough, E., & Sarver, E. (2016). Area monitoring and spot-checking for diesel particulate matter in an underground mine. *Mining Engineering, 68*(12).

Gamble, J., Jones, W., Hudak, J., & Merchant, J. (1978). *Acute changes in pulmonary function in salt miners.* Paper presented at the Proceedings of an American Council of Governmental Industrial Hygienist Topical Symposium: Industrial Hygiene for Mining and Tunneling.

Gillies, A. (2011). Real-time diesel particulate matter ambient monitoring in underground mines. *Journal of Coal Science and Engineering (China), 17*(3), 225-231.

Gillies, A., & Wu, H. (2008). Evaluation of a first mine real-time diesel particulate matter (DPM) monitor. *Australian Coal Association Research Program Grant C, 15028*.

Gillies, S., & Wu, H. W. (2008). Underground atmosphere real time personal respirable dust and diesel particulate matter direct monitoring.

Glauert, M. (1956). The wall jet. *Journal of Fluid Mechanics, 1*(6), 625-643.

Grenier, M. (1998). The evaluation of three diesel particulate matter sampling and analysis methods at a high sulphide ore mining operation. *The Diesel Emissions Evaluation Program (DEEP) Technical Committee*.

Griffith J. F., a. K. J. R. (2012). Pilot Study-Protection factor of closed cab equipment for diesel particulate matter in an underground mine. *14th US North American Mine Ventilation Symposium, Utah*.

Guo, G., Xu, N., Laing, P. M., Hammerle, R. H., & Maricq, M. M. (2003). *Performance of a catalyzed diesel particulate filter system during soot accumulation and regeneration* (0148-7191). Retrieved from

Haney, R. (1990). Diesel particulate exposures in underground mines.

Haney, R. A., Saseen, G. P., & Waytulonis, R. W. (1997). An overview of diesel particulate exposures and control technology in the US mining industry. *Applied occupational and environmental hygiene, 12*(12), 1013-1018.

Hargreaves, D., & Lowndes, I. (2007). The computational modeling of the ventilation flows within a rapid development drivage. *Tunnelling and underground space technology, 22*(2), 150-160.

Heywood, J. B. (1988). *Internal combustion engine fundamentals* (Vol. 930): Mcgraw-hill New York.

ICRP, & Protection, I. C. o. R. (1994). *ICRP Publication 66: Human Respiratory Tract Model for Radiological Protection*: Elsevier Health Sciences.

Janisko, S., & Noll, J. (2008). *Near real time monitoring of diesel particulate matter in underground mines.* Paper presented at the Proceedings of the 12th US/North American Mine Ventilation Symposium.

Janisko, S., & Noll, J. (2010). *Field evaluation of diesel particulate matter using portable elemental carbon monitors.* Paper presented at the Proceedings of the 13th US/North American Mine Ventilation Symposium.

Jarvis, N., Birchall, A., James, A., Bailey, M., & Dorrian, M. (1996). LUDEP 2.0: Personal computer program for calculating internal doses using the ICRP Publication 66 respiratory tract model. *NRPB-SR287*.

Joy, G., Mcwilliams, L., MISCHLER, S., PAGE, S., TUCHMAN, D., VOLKWEIN, J., & WINSON, R. (2006). Laboratory and Field Performance of a Continuously Measuring Personal Respirable Dust Monitor.

Kahn, G., Orris, P., & Weeks, J. (1988). Acute overexposure to diesel exhaust: report of 13 cases. *American journal of industrial medicine, 13*(3), 405-406.

Keith, F., and Larry, T. (2011). Technical Notes, Airtec Technology. In FLIR (Ed.).

Khan, M. U., & Gillies, S. (2015a). *Realtime diesel particulate matter monitoring in U.S. underground mines.* Paper presented at the 2015 SME Annual Conference and Expo and CMA 117th National Western Mining Conference - Mining: Navigating the Global Waters.

Khan, M. U., & Gillies, S. (2015b). Real-time monitoring of DPM, airborne Dust and correlating Elemental Carbon measured by two methods in underground mines in USA. *15th North American Mine Ventilation Symposium, Blacksburg, VA.*

Kittelson, D., Pipho, M., Ambs, J., & Siegla, D. (1986). *Particle concentrations in a diesel cylinder: Comparison of theory and experiment*. Retrieved from

Kittelson, D., Watts, W., Johnson, J., Remerowki, M., Ische, E., Oberdörster, G., . . . Kim, E. (2004). On-road exposure to highway aerosols. 1. Aerosol and gas measurements. *Inhalation Toxicology, 16*(sup1), 31-39.

Kittelson, D. B. (1998). Engines and nanoparticles: a review. *Journal of aerosol science, 29*(5), 575-588.

Kollipara, V. K., Chugh, Y. P., & Relangi, D. D. (2012). *A CFD analysis of airflow patterns in face area for continuous miner making a right turn cut.* Paper presented at the 2012 SME Annual Meeting & Exhibit (preprint).

Konstandopoulos, A. G., & Papaioannou, E. (2008). Update on the science and technology of diesel particulate filters. *KONA Powder and Particle Journal, 26*(0), 36-65.

Lack, D. A., Cappa, C. D., Covert, D. S., Baynard, T., Massoli, P., Sierau, B., . . . Ravishankara, A. (2008). Bias in filter-based aerosol light absorption measurements due to organic aerosol loading: Evidence from ambient measurements. *Aerosol Science and Technology, 42*(12), 1033-1041.

LaRosa, L. E., Buckley, T. J., & Wallace, L. A. (2002). Real-time indoor and outdoor measurements of black carbon in an occupied house: an examination of sources. *Journal of the Air & Waste Management Association, 52*(1), 41-49.

Leidel, N. A., Busch, K., & Lynch, J. (1977). The inadequacy of general air (area) monitoring for measuring employee exposures. *Technical Appendix C in Occupational Exposure Sampling Strategy Manual, NIOSH Publication*(77-173), 75-77.

Lloyd, A. C., & Cackette, T. A. (2001). Diesel engines: environmental impact and control. *Journal of the Air & Waste Management Association, 51*(6), 809-847.

Mathis, U., Mohr, M., Kaegi, R., Bertola, A., & Boulouchos, K. (2005). Influence of diesel engine combustion parameters on primary soot particle diameter. *Environmental science & technology, 39*(6), 1887-1892.

Mc Pherson, M. J. (2012). *Subsurface ventilation and environmental engineering*: Springer Science & Business Media.

McCartney, T., & Cantrell, B. (1992). *A cost-effective personal diesel exhaust aerosol sampler*. Paper presented at the Diesels in underground mines: Measurement and control of particulate emissions (Information circular 9324), Proceedings of the Bureau of Mines information and technology transfer seminar, Minneapolis, MN, September.

McDonald, J. D., Zielinska, B., Sagebiel, J. C., & McDaniel, M. R. (2002). Characterization of fine particle material in ambient air and personal samples from an underground mine. *Aerosol Science & Technology, 36*(11), 1033-1044.

McDonald, J. D., Zielinska, B., Sagebiel, J. C., McDaniel, M. R., & Mousset-Jones, P. (2003). Source apportionment of airborne fine particulate matter in an underground mine. *Journal of the Air & Waste Management Association, 53*(4), 386-395.

McKinnon, D. (1999). Diesel Emission Control Strategies Available to the Underground Mining Industry.

Mody, V., & Jakhete, R. (1987). Dust control handbook for minerals processing.

MSHA. (2003). Diesel Particulate Matter Exposure of Underground Metal and Nonmetal Miners.

MSHA. (2014). 30 CFR Part 72 Diesel Particulate Matter Exposure of Coal Miners. *Fed. Regist*.

Noll, J., Bugarski, A., Patts, L., Mischler, S., & McWilliams, L. (2007). Relationship between elemental carbon, total carbon, and diesel particulate matter in several underground metal/non-metal mines. *Environmental science & technology, 41*(3), 710-716.

Noll, J., Gilles, S., Wu, H. W., & Rubinstein, E. (2015). The relationship between elemental carbon and diesel particulate matter in underground metal/nonmetal mines in the United States and coal mines in Australia. *Journal of occupational and environmental hygiene, 12*(3), 205-211.

Noll, J., & Janisko, S. (2007). *Using laser absorption techniques to monitor diesel particulate matter exposure in underground stone mines.* Paper presented at the Optics East 2007.

Noll, J., & Janisko, S. (2013). Evaluation of a Wearable Monitor for Measuring Real-Time Diesel Particulate Matter Concentrations in Several Underground Mines. *Journal of occupational and environmental hygiene, 10*(12), 716-722.

Noll, J., Janisko, S., & Mischler, S. E. (2013). Real-time diesel particulate monitor for underground mines. *Analytical Methods, 5*(12), 2954-2963.

Noll, J., Patts, L., & Grau, R. (2008). *The effects of ventilation controls and environmental cabs on diesel particulate matter concentrations in some limestone mines.* Paper presented at the Proceedings of the 12th US/North American Mine Ventilation Symposium.

Noll, J., Volkwein, J., Janisko, S., & Patts, L. (2013). Portable instruments for measuring tailpipe diesel particulate in underground mines. *Mining Engineering, 65*(10), 42.

Noll, J. D., Timko, R. J., McWilliams, L., Hall, P., & Haney, R. (2005). Sampling results of the improved SKC diesel particulate matter cassette. *Journal of occupational and environmental hygiene, 2*(1), 29-37.

Oanh, N. T. K., Thiansathit, W., Bond, T. C., Subramanian, R., Winijkul, E., & Paw-armart, I. (2010). Compositional characterization of PM 2.5 emitted from in-use diesel vehicles. *Atmospheric Environment, 44*(1), 15-22.

Panel, N. R. C. D. I. S. C. H. E. (1981). *Health effects of exposure to diesel exhaust: the report of the Health Effects Panel of the Diesel Impacts Study Committee, National Research Council*: Natl Academy Pr.

Petrov, T. P. (2014). Development of Industry Oriented CFD Code for Analysis/Design of Face Ventilation Systems.

Pietikäinen, M., Oravisjärvi, K., Rautio, A., Voutilainen, A., Ruuskanen, J., & Keiski, R. L. (2009). Exposure assessment of particulates of diesel and natural gas fuelled buses in silico. *Science of the total environment, 408*(1), 163-168.

Pronk, A., Coble, J., & Stewart, P. A. (2009). Occupational exposure to diesel engine exhaust: a literature review. *Journal of exposure science and environmental epidemiology, 19*(5), 443-457.

Ramachandran, G., & Watts, W. F. (2003). Statistical comparison of diesel particulate matter measurement methods. *AIHA Journal, 64*(3), 329-337.

Reger, R., Hancock, J., Hankinson, J., Hearl, F., & Merchant, J. (1982). Coal miners exposed to diesel exhaust emissions. *Annals of Occupational Hygiene, 26*(8), 799-815.

Ren, T., & Balusu, R. (2005). CFD modelling of goaf gas migration to improve the control of spontaneous combustion in longwalls.

Ren, T., & Balusu, R. (2008). Innovative CFD modeling to improve dust control in longwalls. *University of Wollongong and the Australiasian Institute of Mining and Metallurgy*, 137-142.

Ris, C. (2007). US EPA health assessment for diesel engine exhaust: a review. *Inhalation Toxicology, 19*(sup1), 229-239.

Safety, M. (2001a). Health Administration (MSHA)(2005). 30 CFR Part 57 Diesel Particulate Matter Exposure of Underground Metal and Nonmetal Miners; Final Rule. *Fed. Reg, 70*(107), 32868.

Safety, M. (2001b). Health Administration, 30 CFR Part 72 Diesel Particulate Matter Exposure of Coal Miners; Proposed Rule. *Fed. Regist, 68*.

Safety, M. (2005a). Health Administration.(June 6, 2005) 30 CFR Part 57 Diesel Particulate Matter Exposure of Underground Metal and Nonmetal Miners; Final Rule. *Fed. Reg, 70*(107), 32868.

Safety, M. (2005b). Health Administration.(June 6, 2005) 30 CFR Part 57 Diesel Particulate Matter Exposure of Underground Metal and Nonmetal Miners; Final Rule *Fed. Reg* (Vol. 70, pp. 32868).

Safety, M. (2008). Health administration, US department of labor. 30 CFR parts 7 and 75 refuge alternatives for underground coal mines final rule. *Natl. Arch. Rec. Adm, 82*, 18-20.

Saki, S. A. (2016). *Gob ventilation borehole design and performance optimization for longwall coal mining using computational fluid dynamics*: Colorado School of Mines.

Schnakenberg, G. H., & Bugarski, A. D. (2002). *Review of technology available to the underground mining industry for control of diesel emissions*: US Department of Health and Human Services, Public Health Service, Centers for Disease Control and Prevention, National Institute for Occupational Safety and Health, Pittsburgh Research Laboratory.

Scott, D. F., Grayson, R. L., & Metz, E. A. (2004). Disease and illness in US mining, 1983–2001. *Journal of occupational and environmental medicine, 46*(12), 1272-1277.

Shah, S. D., Cocker, D. R., Johnson, K. C., Lee, J. M., Soriano, B. L., & Miller, J. W. (2007). Reduction of particulate matter emissions from diesel backup generators equipped with four different exhaust aftertreatment devices. *Environmental science & technology*, *41*(14), 5070-5076.

Silverman, D. T., Samanic, C. M., Lubin, J. H., Blair, A. E., Stewart, P. A., Vermeulen, R., . . . Travis, W. D. (2012). The diesel exhaust in miners study: a nested case–control study of lung cancer and diesel exhaust. *Journal of the National Cancer Institute*.

Skillas, G., Qian, Z., Baltensperger, U., Matter, U., & Burtscher, H. (2000). The influence of additives on the size distribution and composition of particles produced by diesel engines. *Combustion science and Technology, 154*(1), 259-273.

Spencer, E. (2009). *Assessment of Equipment Operators' Noise Exposure in Western Underground Gold and Silver Mines.* Paper presented at the 2009 SME Annual Meeting and Exhibit.

Stephenson, D. J., Spear, T., & Lutte, M. (2006). Comparison of sampling methods to measure exposure to diesel particulate matter in an underground metal mine. *Mining Engineering*, *58*(8), 39-42, 44-45.

Takiff, L., & Aiken, G. (2010). *A real-time, wearable elemental carbon monitor for use in underground mines.* Paper presented at the Proc. 13th United States/North American Mine Ventilation Symposium, Hardcastle & McKinnon (eds).

Thiruvengadam, M., Zheng, Y., Lan, H., & Tien, J. C. (2016). A diesel particulate matter dispersion study inside a single dead end entry using dynamic mesh model. *International Journal of Mining and Mineral Engineering, 7*(3), 210-223.

Thiruvengadam, M., Zheng, Y., & Tien, J. C. (2016). DPM simulation in an underground entry: Comparison between particle and species models. *International Journal of Mining Science and Technology*, *26*(3), 487-494.

Tomko, D., Stackpole, R., Findlay, C., & Pomroy, W. (2010). Metal/nonmetal diesel particulate matter rule.

Torno, S., Toraño, J., Ulecia, M., & Allende, C. (2013). Conventional and numerical models of blasting gas behaviour in auxiliary ventilation of mining headings. *Tunnelling and underground space technology*, *34*, 73-81.

Turcotte, K. B., Edwardson, E., & Laflamme, G. (1998). Evaluation of Existing Diesel Particulate Matter Sampling and Analysis Methods at a High Sulphide Ore Mine.

Voutilainen, A., Kaipio, J. P., Pekkanen, J., Timonen, K. L., & Ruuskanen, J. (2004). Theoretical analysis of the influence of aerosol size distribution and physical activity on particle deposition pattern in human lungs. *Scandinavian journal of work, environment & health*, 73-79.

Walsh, M. P. (1998). *Global trends in diesel emissions control-a 1998 update* (0148-7191). Retrieved from

Walsh, M. P. (1999). *Global trends in diesel emissions control-A 1999 update*. Retrieved from

Warner, J. R., Johnson, J. H., Bagley, S. T., & Huynh, C. T. (2003). *Effects of a catalyzed particulate filter on emissions from a diesel engine: Chemical characterization data and particulate emissions measured with thermal optical and gravimetric methods* (0148-7191). Retrieved from

Watts, W., & Ramachandran, G. (2000). Diesel Particulate Matter Sampling Methods–Statistical Comparison. *Report of Investigation submitted to the Diesel Emissions Evaluation Program (DEEP) Technical Committee*.

Wu, H., & Gillies, A. (2008). *Developments in real time personal diesel particulate monitoring in mines.* Paper presented at the Proceedings, 12 th US Mine Ventilation Symposium.

Wu, H. W., Gillies, A., Volkwein, J., & Noll, J. (2009). *Real-time DPM ambient monitoring in underground mines.* Paper presented at the Proceedings, Ninth International Mine Ventilation Congress, Oxford and IBH New Delhi, Editor, DC Panigrahi.

Yuan, L., & Smith, A. (2007). Computational fluid dynamics modeling of spontaneous heating in longwall gob areas. *transactions-society for mining metallurgy and exploration incorporated, 322*, 37.

Yuan, L., & Smith, A. C. (2008). Numerical study on effects of coal properties on spontaneous heating in longwall gob areas. *Fuel, 87*(15), 3409-3419.

Zheng, Y., Lan, H., Thiruvengadam, M., & Tien, J. C. (2011). DPM dissipation experiment at MST's experimental mine and comparison with CFD simulation. *Journal of Coal Science and Engineering (China), 17*(3), 285-289.

Zheng, Y., Lan, H., Thiruvengadam, M., Tien, J. C., & Li, Y. (2017). Effect of single dead end entry inclination on DPM plume dispersion. *International Journal of Mining Science and Technology, 27*(3), 401-406.

Zheng, Y., Thiruvengadam, M., Lan, H., & Tien, C. J. (2015a). Effect of auxiliary ventilations on diesel particulate matter dispersion inside a dead-end entry. *International Journal of Mining Science and Technology, 25*(6), 927-932.

Zheng, Y., Thiruvengadam, M., Lan, H., & Tien, J. C. (2015b). Design of push–pull system to control diesel particular matter inside a dead-end entry. *International journal of coal science & technology, 2*(3), 237-244.

Zheng, Y., Thiruvengadama, M., Lanb, H., & Tienc, J. C. (2015). *Simulation of DPM Dispersion for Different Mining Operations Inside a Dead-end Entry*. Paper presented at the Proceedings of the 15th US/North American mine ventilation symposium. Blacksburg, VA (USA).

Zheng, Y., & Tien, J. C. (2008). *DPM dispersion study using CFD for underground metal/nonmetal mines*. Paper presented at the Proceedings of the 12th US/North America mine ventilation symposium, Reno.

Zielinska, B., Sagebiel, J., McDonald, J., Rogers, C., Fujita, E., Mousset-Jones, P., & Woodrow, J. (2002). Measuring diesel emissions exposure in underground mines: a feasibility study. *Research directions to improve estimates of human exposure and risk from diesel exhaust. Health Effects Institute Diesel Epidemiology Working Group, Boston, MA*, 181-232.

VITA

Muhammad Usman Khan hails from Lahore, Pakistan. In 2008, he received his B.Sc. Mining Engineering with Honors from the University of Engineering & Technology (UET), Lahore, Pakistan. He worked as a Junior Tunnel Engineer from 2009 to 2010 at Neelum Jhelum HydroElectric Project (NJHEP) in Muzaffarabad, Azad Jammu & Kashmir. In 2010, he joined the Department of Mining Engineering at UET Lahore as a Lecturer. Alongside his teaching responsibilities, he successfully finished his M.Sc. in Mining Engineering from UET Lahore in 2012. Excellent performance as a lecturer earned him a quick promotion to Assistant Professor.

In 2013, he started his PhD in Mining Engineering at the Missouri University of Science & Technology (S&T), Rolla, USA. He worked as a Teaching Fellow at Saudi Mining Polytechnic (a project of Mining & Nuclear Engineering Department of Missouri S&T) in Arar, Saudi Arabia for almost one year. In 2015, he did a summer internship at an underground metal mine in the United States. During his PhD at Missouri S&T, he remained Graduate Research Assistant as well as he served as a Graduate Teaching Assistant for multiple courses. He was awarded the Outstanding Graduate Teaching Award in 2016. In May 2017, he got a certificate in Engineering Management from Missouri S&T. He received his PhD Mining Engineering from Missouri S&T in December 2017.